

https://dspace.org/

Modelling the impact of climate variability and land-use changes in the Upper Crocodile River Basin, South Africa

Fynn, Byron Melvin

2022
https://hdl.handle.net/10539/33849

Downloaded from a DSpace repository. https://dspace.org/

UNIVERSITY OF THE WITWATERSRAND, JOHANNESBURG

Modelling the impact of climate variability and land-use changes in the Upper Crocodile River Basin, South Africa

---

Byron Melvin Fynn

1463456

Submitted in partial fulfilment of the requirements for the degree of Master of Science in Hydrogeology

Supervisor: Professor Tamiru Abiye

School of Geosciences, Faculty of Science, University of the Witwatersrand, P.O. Box Wits 2050, Johannesburg, South Africa

February 2022

PLAGIARISM DECLARATION

I, Byron Melvin Fynn, hereby declare that this research report titled *'Modelling the impact of climate variability and land-use changes in the Upper Crocodile River Basin, South Africa'* is my own, unaided work. It is being submitted to the Degree of Master of Science in Hydrogeology to the University of the Witwatersrand, Johannesburg. It has not been submitted before for any degree or examination to any other University. Information obtained from sources has been indicated and acknowledged by detailed and complete referencing.

Date: February 2022

Signed: …….

ABSTRACT

Improved understanding of the impacts of climate and land-use changes on water resources in the semi-arid conditions of South Africa is necessary to ensure their sustainability. In this study, the Soil and Water Assessment Tool (SWAT) was applied to the highly urbanised Upper Crocodile River Basin (UCRB) to evaluate the individual and combined effects of climate and land-use changes on streamflow. The SWAT model was calibrated against six discharge stations from 1998 to 2010 and validated from 2010 to 2016. Successful results regarding the coefficient of determination (R^2), percentage bias (PBIAS), and Nash-Sutcliffe efficiency equation (NSE) objective functions against four discharge stations for the calibration and validation periods proved that streamflow predictions were reliable for analysis under climate and land-use changes. The climate change scenarios, reflecting a 1.5 °C temperature increase, and a 20% precipitation decrease, were shown to reduce the antecedent moisture condition of the UCRB. The 5% urban expansion land-use scenario revealed that increasing urbanisation enhanced the imperviousness of the basin. Moreover, in the worst-case scenario, incorporating the climate and land-use changes resulted in a 14% average streamflow decrease in the UCRB. Consequently, the UCRB's predicted climate and human activity changes suggest water availability and quality decreases. Surface water quality will be aggravated as there is less natural water for the dilution of effluent loadings, and groundwater quality may be exacerbated by its connection with surface water in the basin. Therefore, enhanced integrated water management strategies, above those currently considered, is required to ensure the efficient use and sustainability of the UCRB's water resources.

ACKNOWLEDGEMENTS

First and foremost, I would like to thank my supervisor, Professor Tamiru Abiye, for his patience and understanding as this research took much longer than previously anticipated. In addition, a big thank you to Prof. Tamiru Abiye for his guidance and for the opportunity to participate in his hydrogeological programme, which has given me invaluable knowledge that has contributed significantly to this study. I am forever grateful.

My sincere gratitude goes out to Dr Khahliso Leketa, for the advice and knowledge he imparted to me regarding my study area, which greatly contributed to this research.

Thank you to the National Research Foundation (NRF) and United Way South Africa for funding this research. Their financial assistance helped considerably towards the completion of this study.

Thank you to the Department of Water and Sanitation and the South African Weather Service for making relevant data available to me, which enabled the completion of this project.

To my mother, father, and brother, thank you for the love, motivation, and encouragement you have shown me during stressful and hard situations. Without you all, this research would not have been possible.

TABLE OF CONTENTS

PLAGIARISM DECLARATION i

ABSTRACT ii

ACKNOWLEDGEMENTS iii

TABLE OF CONTENTS iv

LIST OF FIGURES vi

LIST OF TABLES x

CHAPTER 1: INTRODUCTION 1

1.1 Background 1

1.2 Aims and Objectives 5

1.2.1 Aim 5

1.2.2 Research Objectives 5

CHAPTER 2: LITERATURE REVIEW 6

2.1 Assessing the influence of climate and human activity changes on basin hydrology 6

2.2 Hydrological Modelling 8

2.3 Soil and Water Assessment Tool (SWAT) description 10

2.4 Description of Study Area 12

2.5 Climate Setting 13

2.6 Geological Setting 14

2.7 Hydrogeological Setting 16

CHAPTER 3: METHODOLOGY 18

3.1 Watershed Delineation 19

3.2 Create Hydrological Response Units 22

3.3 Edit SWAT 28

3.4 Run SWAT 32

3.5 Calibration 34

3.6 Validation 39
CHAPTER 4: RESULTS 40
4.1 Initial Model 40
4.2 Calibration 45
4.2.1 Parameter Sensitivity 45
4.2.2 Calibrated Parameters 47
4.2.3 Model Performance 48
4.3 Validation 54
4.4 Climate Change Scenarios 60
4.4.1 Precipitation Change Scenarios 61
4.4.2 Temperature Change Scenarios 63
4.5 Land-use Change Scenarios 66
4.6 Worst-case Scenario 68
4.7 Comparative Analysis 71
CHAPTER5: DISCUSSION 73
CHAPTER 6: CONCLUSION, CHALLENGES, AND RECOMMENDATIONS 80
6.1 Conclusion 80
6.2 Challenges 81
6.3 Recommendations 82
REFERENCES 84
APPENDIX A: METHODOLOGY 98
APPENDIX B: RESULTS 101

LIST OF FIGURES

Figure 1.1: Locality map of the Upper Crocodile River Basin, its water resources, and urban developments 4
Figure 2.1: Quaternary catchments, stream networks, and reservoirs within the UCRB 13
Figure 2.2: The monthly average rainfall, and maximum and minimum temperatures for the Buffelspoort II AGR and Pretoria University Proefplaas weather stations from 1980 to 2020 14
Figure 2.3: Geological Map and Stratigraphic Legend of the UCRB 17
Figure 3.1: Flow diagram showing the methodology used to generate results for the UCRB SWAT model 18
Figure 3.2: The DEM and River map involved in producing the stream network for the UCRB 20
Figure 3.3: The delineated watershed of the UCRB including its inlets, outlets, reservoirs, and sub-basins 21
Figure 3.4: Location of point sources in relation to the stream network of the UCRB 22
Figure 3.5: The SANLC 2018 land-use/land cover classes operating over the UCRB in 2018 24
Figure 3.6: The HSWD topsoil names and locations in the UCRB 25
Figure 3.7: The locations of the weather stations, reservoirs, and wastewater treatment plants within the UCRB 29
Figure 3.8: The positions of the discharge stations used for accuracy analysis in context of the UCRB's river network 33
Figure 4.1a-f: Regression graphs showing the linear relationships between the measured and simulated streamflow in each of the sub-basins used for analysis (1998-2016) 41
Figure 4.2: The initial model results in sub-basin 3 compared to the observed data at discharge station A2H019 (1998-2016) 42
Figure 4.3: The hydrograph showing the differences in streamflow from the simulations in sub-basin 13 compared to the measured streamflow at recording station A2H083 (1998-2016) 43
Figure 4.4: The initial model streamflow simulations in sub-basin 19 compared to the observed streamflow at the A2H012 discharge station from 1998 to 2016 43

Figure 4.5: The variations in monthly streamflow between the initial simulations in sub-basin 26 and the recorded discharge at the A2H044 station (1998-2016) 44
Figure 4.6: The streamflow hydrograph showing the discrepancies between the measured data at the A2H045 discharge station and SWAT's initial simulations in sub-basin 29 (1998-2016) 44
Figure 4.7: Streamflow hydrograph showing the differences between streamflow simulations in sub-basin 104 compared to those measured at the A2H034 recording station (1998-2016) 45
Figure 4.8a-f: The recession graphs showing the linear relationship between simulated and recorded streamflow for the period of calibration (1998-2010) 49
Figure 4.9: The calibration hydrograph at discharge station A2H019 from 1998 to 2010 51
Figure 4.10: The simulated and observed streamflow hydrograph for discharge station A2H083 during the calibration period (1998-2010) 51
Figure 4.11: The simulated and measured streamflow at the A2H012 discharge station for the calibration period (1998-2010) 52
Figure 4.12: The SWAT simulated and recorded streamflow at the A2H044 discharge station for the calibration period (1998-2010) 52
Figure 4.13: The observed vs simulated streamflow at the UCRB's A2H045 gauging station for the 13-year calibration period 53
Figure 4.14: The hydrograph comparing the SWAT simulated vs recorded streamflow at the A2H034 discharge station (1998-2010) 53
Figure 4.15: The SWAT simulated and recorded streamflow at the A2H019 discharge station for the validation period (2010-2016) 55
Figure 4.16: The hydrograph comparing the SWAT simulated vs recorded streamflow at the A2H083 discharge station (2010-2016) 56
Figure 4.17: The validation hydrograph showing the SWAT simulated vs recorded streamflow at the A2H012 discharge station (2010-2016) 56
Figure 4.18: The validation hydrograph for discharge station A2H044 from 2010 to 2016 .. 57
Figure 4.19: The simulated and observed streamflow hydrograph for discharge station A2H045 during the validation period (2010-2016) 57
Figure 4.20: The observed vs simulated streamflow at the UCRB's A2H034 gauging station for the 6-year validation period 58
Figure 4.21a-f: The recession graphs showing the linear relationship between simulated and recorded streamflow for the validation period (2010-2016) 59

Figure 4.22: The annual average temperatures (a) and precipitations (b) experienced over the UCRB from 1980 to 2020 60
Figure 4.23: Hydrograph showing the change in streamflow in sub-basin 3 from an increase and decrease of 20% in precipitation over the UCRB from 1998 to 2016..... 61
Figure 4.24: Streamflow hydrograph showing the response of sub-basin 13 to increases and decreases in precipitation by 20% (1998-2016) 62
Figure 4.25: The changes in streamflow from the current simulation in sub-basin 19 due to increases and decreases in rainfall by 20% (1998-2016) 62
Figure 4.26: Hydrograph of sub-basin 26 indicating the change in streamflow due to a 20% change in precipitation from 1998 to 2016..... 63
Figure 4.27: The changes in streamflow from the current simulation in sub-basin 3 due to increases and decreases in temperature by 1.5 °C (1998-2016) 64
Figure 4.28: Hydrograph of sub-basin 13 indicating the change in streamflow due to a 1.5 °C change in temperature from 1998 to 2016..... 64
Figure 4.29: Hydrograph showing the change in streamflow in sub-basin 19 from an increase and decrease of 1.5 °C in temperature over the UCRB from 1998 to 2016..... 65
Figure 4.30: Streamflow hydrograph showing the response of sub-basin 26 to increases and decreases in temperature by 1.5 °C (1998-2016)..... 65
Figure 4.31: The streamflow influence of a 5% increase in urbanisation compared to the current simulation in sub-basin 3(1998-2016)..... 66
Figure 4.32: Hydrograph showing the effects of a 5% increase in urbanisation on streamflow in sub-basin 13 from 1998 to 2016 67
Figure 4.33: Streamflow hydrograph indicating the influence of the urbanisation land-use scenario on UCRB streamflow in sub-basin 19 (1998-2016)..... 67
Figure 4.34: Streamflow hydrograph showing the response of sub-basin 26 to a 5% increase in urbanisation (1998-2016) 68
Figure 4.35: The streamflow influence of the worst-case scenario in comparison to the current simulation in sub-basin 3 (1998-2016)..... 69
Figure 4.36: Hydrograph of sub-basin 13 indicating the change in streamflow due to the worst-case scenario from 1998 to 2016..... 69
Figure 4.37: Hydrograph showing the change in streamflow in sub-basin 19 due to the worst-case scenario from 1998 to 2016 70
Figure 4.38: Streamflow hydrograph showing the response of sub-basin 26 to the worst-case climate and land-use change scenario (1998-2016)..... 70

Figure A.1: The 8863 HRUs generated for the UCRB during the Create HRUs stage of model development 100
Figure B.1: The sensitivity analysis graph showing the sensitivities of the different parameters considered for SWATCUP calibration 101
Figure B.2: The sensitivity analysis graph of the 13 parameters used to achieve the best results during model calibration 102
Figure B.3: Scatter plots showing the parameter values used for calibration versus the NSE result obtained 103
Figure B.4: The land-use update table used to define the land-use scenario implemented for analysis 105
Figure B.5: The change in the land-uses of the UCRB showing the land-uses before (left) and after (right) scenario development 106

LIST OF TABLES

Table 3.1: Description and sources of data used in delineating the watershed of the UCRB . 21
Table 3.2: SWAT codes and their description used in the land-use look up table 23
Table 3.3: Description of the different soil hydrological groups and their infiltration rate (adapted from Neitsch et al. 2011) 26
Table 3.4: The physical attributes of the UCRB's reservoirs used in SWAT model development 30
Table 3.5: The attributes of the target release approach used to describe the outflow from the UCRB's reservoirs 31
Table 3.6: The locations and effluent loadings from wastewater treatment plants within the UCRB 32
Table 3.7: The attributes of the stream discharge stations used to assess the precision of streamflow simulations in the UCRB 33
Table 3.8: The performance criteria for the objective functions used to analyse the accuracy of UCRB simulation (adapted from Moriasi et al., 2015) 38
Table 4.1: The initial SWAT model simulation results evaluated in comparison to stream discharges recorded in the UCRB from 1998 to 2016 40
Table 4.2: Parameters considered for sensitivity analysis in SWATCUP 46
Table 4.3: The sensitivity ranking, p-value- and t-stat value of the different parameters considered for calibration 46
Table 4.4: Sensitivity ranking of the parameters used in calibration, including their identifiers, maximum, minimum, and fitted values that achieved the best calibration result . 47
Table 4.5: The calibration results showing the accuracy of simulation compared to recorded data using appropriate model performance indicators 48
Table 4.6: The validation results in each sub-basin showing the accuracy of simulation against recorded streamflow using objective functions 54
Table 4.7: The change in streamflow due to climate and land-use changes and their combined effects in comparison to the current simulation in each sub-basin 71
Table A.1: The Land-use lookup table showing the 73 SANLC 2018 land-use classes associated using SWAT codes 98
Table A.2: The soil look-up table used in SWAT HRU creation where SOIL_ID is the raster image shape identifier and SNAM is the soil name located in the usersoil table 99

CHAPTER 1: INTRODUCTION

1.1 Background

The rise in surface temperatures between 1.4 °C and 5.8 °C, accompanied by a ±20% variability in precipitation as predicted by the Intergovernmental Panel on Climate Change (IPCC) for 2100 relative to 1990 (IPCC, 2001), may be detrimental to the future sustainability of water resources. Climate change is regarded as one of the critical factors surrounding the changing distribution and decreased availability of water resources (Kundzewicz *et al.*, 2008) due to its alteration of soil moisture availability, evaporation, precipitation, and flow-routing time (Prowse *et al.*, 2006). As such, the rapid increase in surface temperatures since 1970, surpassing any 50-year interval over the previous two millennia (IPCC, 2021), may aggravate the current state of global water resources. However, the IPCC's present and projected climate changes are attributed to global warming and its related increases in atmospheric greenhouse gas emissions (IPCC, 2007), owing to recent changes in human activity (IPCC, 2001), which is driven by economic and population growth (IPCC, 2014; 2021). Therefore, understanding the relationship between anthropogenic activities and climate is essential for quantifying and predicting climate changes, and thus, its potential impact on water resources.

Human activities contribute to climate change as they play a vital role in the change of hydrological circulation (Kuchment, 2004) and influence hydro-climatic variables such as precipitation, temperature, and precipitation extremes (Ahn and Merwade, 2014). In turn, Dale (1997) noted that climate change and human activities are interrelated as climate change could alter the politics, social attitudes, and affluence governing the choice of anthropogenic activities. As water resources are central to the predicted impacts of climate change (IPCC, 2007), streamflow is regarded as one of the most crucial resultants for water resources management (Dey and Mishra, 2017). Given that human activities and climate variability impact streamflow (Zhang *et al.*, 2011), the effects of both climate change and anthropogenic activities on stream discharge need to be delineated to strengthen the strategies for the adaptive management of water resources.

Climate change causes considerable impacts on streamflow and water resources by altering the hydrological cycle (Legesse *et al.*, 2010). In addition, anthropogenic activities influence streamflow variability due to the construction of water retention structures such as dams (Ye *et al.*, 2013), urbanisation (Rose and Peters, 2001), and induced land-use changes (Li *et al.*,

2009). Dams place significant controls on the downstream flow of water. In contrast, urbanisation increases peak stream discharge by enhancing surface run-off and reducing the lag-time between rainfall and run-off (Dey and Mishra, 2017). Land-use changes are critical determinates of water supply through a landscape (Fisher and Mustard, 2004) and alter catchment hydrology by modifying soil properties, surface roughness, interception, infiltration, evapotranspiration, groundwater recharge, and flood frequency (Brath *et al.*, 2006; Baker and Miller, 2013). As such, assessing the impacts of human activities on hydrological components remains an essential step for ensuring water resources sustainability (Gyamfi *et al.*, 2016), particularly for countries vulnerable to climate change impacts.

South Africa is a country deemed at risk to the projected effects of climate change (Kusangaya *et al.*, 2014). Climate change predictions for South Africa indicate that the country will continue to warm at a rate significantly higher than the 0.15 °C per decade observed over the 20th Century (Engelbrecht *et al.*, 2015). This warming is expected to result in temperature rises of 5 to 8 °C over the interior by the end of the 21st century, with reduced increases occurring over coastal regions (IPCC, 2007). Moreover, it is envisaged that the country will suffer from reduced rainfall in the future (ASSAf, 2017), which is increasingly worrying given that South Africa already receives annual average precipitation of approximately 490 mm, which is less than half of the global average (WWF-SA, 2016). In addition, South Africa's geographic location in the African continent's southern region may exacerbate its climate change impacts. Africa has experienced surface temperature increases above the global average (IPCC, 2021) and is regarded as one of the most vulnerable continents to climate change due to its low adaptive capacity (IPCC, 2001; Callaway, 2004). Furthermore, southern Africa is considered the most vulnerable region in Africa to climate change impacts (IPCC, 2007) due to its climate's large spatial and temporal variability (IPCC, 2007; Gallego-Ayala and Juizo 2011). Subsequently, climate change impacts on southern Africa's water resources are expected to be even more pronounced than previously anticipated (Kusangaya *et al.*, 2014), posing a serious threat to South Africa's water resources, given its climate change outlook (Ziervogel *et al.*, 2014).

The developing trend in South Africa's climate towards lower rainfalls and higher temperatures leads to decreased terrestrial moisture (Graham *et al.*, 2011; Engelbrecht *et al.*, 2015), ultimately affecting streamflow components (Legesse *et al.*, 2010). Precipitation directly affects the quantity of water entering a hydrological system (Trenberth, 1999); therefore, decreases in precipitation have adverse effects on streamflow. Temperature directly affects the

quantity and rate of evaporation (Arnell and Liv, 2001); hence, due to higher temperatures, rainfall falling overland may be quickly evaporated back into the atmosphere, subsequently reducing water availability for run-off and infiltration (Gleick, 1989). Interception and water uptake from vegetation further exacerbates water's availability for run-off and infiltration, thereby reducing groundwater recharge (Healy, 2010). Decreases in groundwater recharge translate to lowering of the water table and, hence, reduced subsurface flow into the stream network (Matalas *et al.*, 1998). Consequently, streamflow projections for South Africa indicate substantial decreases by 2050, compromising access to water for human consumption, socio-economic development, agriculture, and the aquatic environment (Kusangaya *et al.*, 2014).

The Upper Crocodile River Basin (UCRB), shown in Figure 1.1, exemplifies the climatic and anthropogenic factors affecting the current and future sustainability of South Africa's water resources. The UCRB is characterised as having the greatest human impact in South Africa (Department of Water Affairs South Africa [DWAF], 2008), as it accommodates the urban settlements of northern Johannesburg, Midrand, and southern Pretoria (Tshwane). As a result, there is a considerable water demand from various economic sectors in the basin (Abiye *et al.*, 2015), totalling 556 million m^3/year (DWAF, 2008). However, water resources within the UCRB could not meet this demand and necessitated enhancement from the neighbouring Vaal River Basin to the south (Abiye *et al.*, 2015; Leketa and Abiye, 2019). The transfer of 550 million m^3/year of water from the Vaal Basin subsequently increased wastewater disposal from treatment plants to the rivers draining the UCRB (Leketa and Abiye, 2019), thereby exacerbating the quality of the UCRB's surface water resources (DWAF, 2008). It has been projected that the annual urban water requirements in the UCRB will increase from 292 million m^3 to 409 million m^3 by 2025 (DWAF, 2008), compromising the water quality in the basin. The Hartbeespoort Dam (Fig. 1.1) will potentially be most impacted by increased urban wastewater disposal and climate changes in the UCRB, as it is the first restrictive flow body downstream from Johannesburg and Pretoria. Moreover, Hartbeespoort Dam is renowned for its pollution crises due to high nutrient loads from wastewater treatment plants, leaking sewers,

and urban and agricultural run-offs (Dudula, 2007), labelling it as one of the most severely eutrophicated water bodies in South Africa (Cukic and Venter, 2012).

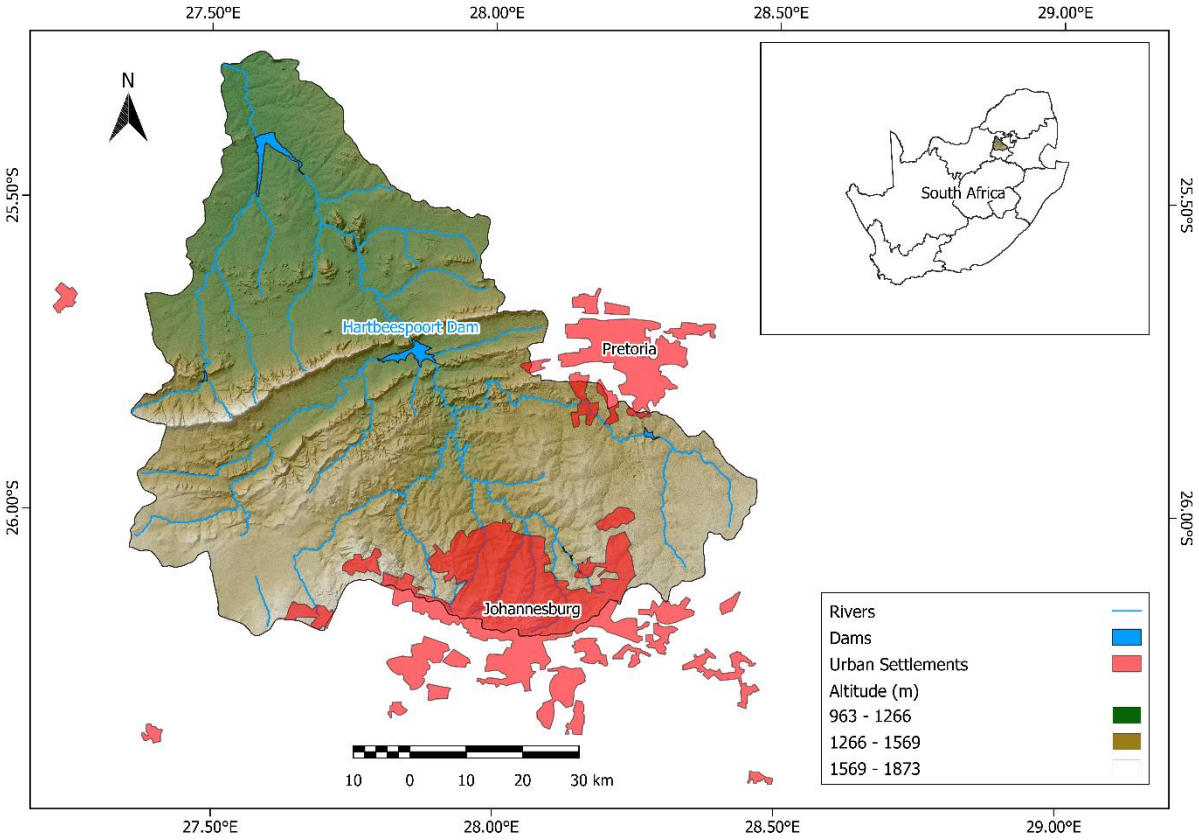


Figure 1.1: Locality map of the Upper Crocodile River Basin, its water resources, and urban developments

The UCRB is, therefore, expected to be adversely affected by climate and human activity changes. The predicted decrease in rainfall and increase in temperature, coupled with the expected exponential population growth, and associated effluent discharge, pose significant threats to groundwater and surface water availability (Kusangaya *et al.*, 2014). Moreover, the increased wastewater disposal attributed to urbanisation and industrial growth within the UCRB is envisaged to aggravate the pollution levels of its water resources as there is less natural flow to dilute the lower quality wastewater (Leketa and Abiye, 2019). Therefore, managing the UCRB's water resources in response to climate and human activity changes is critical for ensuring water quality and sustainability in the basin.

Water resources managers have frequently employed hydrological models to assess the impacts of climate and human activity changes on catchment hydrology (Dey and Mishra, 2017). Hydrological models provide a framework for conceptualising and investigating the

relationship between climate and water resources (Choi and Deal, 2008), and are commonly used for water resources planning and management in data-scarce countries like South Africa (Kusangaya *et al.*, 2014). This study, therefore, assesses the applicability and accuracy of the Soil and Water Assessment Tool (SWAT) in simulating streamflow in a South African catchment with a strong anthropogenic influence, in response to climate and human activity changes.

1.2 Aims and Objectives

1.2.1 Aim

The principal aim of this study is to simulate the hydrological response of the Upper Crocodile River Basin to climate and land-use changes using the Soil and Water Assessment Tool.

1.2.2 Research Objectives

1. Prepare a SWAT model that simulates the movement and distribution of surface and groundwater in the UCRB using climate and the physical characteristics of the basin.

2. Calibrate the streamflow of the model to delineate the factors influencing the hydrological response of the UCRB and to ensure precise model streamflow predictions.

3. Validate the model in order to certify its streamflow prediction accuracy.

4. Determine the impacts of land-use and climate changes on the UCRB's water resources, particularly the Hartbeespoort Dam.

CHAPTER 2: LITERATURE REVIEW

2.1 Assessing the influence of climate and human activity changes on basin hydrology

Numerous methods have been utilised to distinguish the independent impacts of climate variability and anthropogenic activity on streamflow (Dey and Mishra, 2017). These methods are separated based on the procedure employed to relate basin inputs (e.g., precipitation) and outputs (e.g., run-off) or characterise the hydrological processes within a catchment. Resultantly, four approaches are highlighted to assess the effects of human practices and climate change on stream discharge, namely: experimental, conceptual, analytical, and hydrological modelling (Dey and Mishra, 2017). The hydrological modelling approach is addressed separately under Section 2.2.

Experimental approaches aim to evaluate the impact of climate and anthropogenic activity changes using two analysis periods, namely, control and testing periods. The former determines the basis for basin hydrology, whereas the latter seeks to quantify the influence of climate and human activity changes in relation to the control period. Two experimental approach methods have been introduced for hydrological analysis: the paired catchment and time-trend methods. The paired catchment method is primarily used to examine the impact of vegetation changes on streamflow variation (Bosch and Hewlett, 1982) and utilises two catchments that exhibit similar physical properties with a proximal distance between them (Brown *et al.*, 2005). Following the control period, one catchment is subjected to change while the other remains as a control. This negates climate variability influences and, therefore, variations in streamflow are attributed to vegetation changes (Brown *et al.*, 2005). In contrast, the time-trend method uses one catchment and two testing periods. The first testing period considers streamflow variation in response to climate change, neglecting any human impact, while the second period assesses the combined effect of climate and human activity on streamflow. Resultantly, the overall and relative contributions of human activity and climate change can be estimated (Zhao *et al.*, 2009).

The conceptual approach emphasises the importance of actual evapotranspiration (AET) regarding streamflow determination in response to natural and artificial factors. Two methods have been developed using this approach: Budyko and Tomer-Schilling (Dey and Mishra, 2017). The Budyko method suggests that the annual water balance measurements demonstrate

the competition between available water and available energy (Ahn and Merwade, 2014). In addition, Budyko (1974) noted the difficulty in measuring actual evapotranspiration from water balance calculations, owing to its effects from climate variables, potential evapotranspiration (PET), and anthropogenic activities (Dey and Mishra, 2017). Therefore, the Budyko method uses Equation 1, in which the ratio of mean AET to mean annual precipitation (AET/P) is a function of the ratio of mean PET to the mean annual precipitation (PET/P) and catchment properties. This method is applied using long-term trends in PET, AET, and their relationship with precipitation to determine climate and human influences. Variations in climate conditions and soil properties affect PET and P only, whereas human activities such as urbanisation and land-use changes only impact AET (Dooge, 1992).

$$\frac{AET}{P} = f\left(\frac{PET}{P}, watershed\ properties\right) \tag{1}$$

Tomer and Schilling (2009) developed an approach that gauges an ecosystem's water and energy use through PET, AET, and precipitation datasets (Dey and Mishra, 2017). Shifts in the plot of water excess (P_{ex}) versus energy excess (E_{ex}), as shown in Equation 2 and Equation 3, respectively, are associated with climate, vegetation, and human activity changes in an ecosystem.

$$P_{ex} = \frac{P - AET}{P} \tag{2}$$

$$E_{ex} = \frac{PET - AET}{PET} \tag{3}$$

Two analytical methods have been developed to assess the hydrological impacts of human activities and climate change which are: climate elasticity and hydrological sensitivity. Schaake (1990) established the climate elasticity method to understand streamflow response under variable climatic conditions (Dey and Mishra, 2017). This procedure utilises the ratio of the proportional change in streamflow and the proportional changes in climate variables such as precipitation and potential evapotranspiration to delineate the relative impact of climate change on streamflow variation (Fu *et al.*, 2007). The hydrological sensitivity technique aims to quantify the changes in mean streamflow with respect to changes in precipitation and potential evapotranspiration and is expressed as a percentage (Zuo *et al.*, 2014). Thus, any further changes regarding mean streamflow are deduced as anthropogenic influences.

The experimental, analytical, and conceptual approaches to assessing streamflow variation as a result of climatic and anthropogenic influences have been applied successfully in numerous studies worldwide (Ahn and Merwade, 2014; Dey and Mishra, 2017). Due to these studies' variable basin properties and climates, some researchers have exposed limitations or failures in these methods. The analytical methods do not assess the individual impacts of anthropogenic activities on streamflow, requiring the effects of human activity to be quantified through relativity or extrapolation (Dey and Mishra, 2017). Paired catchment studies recognised that the extensive variability in the characteristics of medium and large catchments was not considered by this method (Zhao *et al.*, 2010). Moreover, Li *et al.* (2009) highlighted the difficulty in locating catchments with similar properties under identical climatic conditions. The time-trend method focuses on the climatological variables affecting streamflow but fails to consider a catchment's geomorphological properties influencing run-off generation (Dey and Mishra, 2017). The Tomer-Schilling procedure has shortcomings as it does not directly quantify streamflow variations but instead identifies whether they are attributed to climate change or human activity. Lastly, the Budyko method was acknowledged to be a practical yet straightforward theory that may be limited by diverse catchments (Dooge, 1992).

2.2 Hydrological Modelling

Hydrological models have become a vital tool for the study of hydrological processes and the influence of modern human activity on the hydrological system (Devia *et al.*, 2015). According to Tessema (2011), hydrological models treat the hydrological cycle as a system comprising various inputs and outputs, linked using a set of equations. Therefore, choosing the hydrological model implemented for a study is essential and should be selected based on context-specific factors, such as data availability, catchment complexity, and the intricacy of model structure (Dey and Mishra, 2017).

Several hydrological models have been developed to analyse the effects of natural and artificial factors on basin hydrology, such as the Geomorphology-Based Hydrological Model (GBHM), the Variable Infiltration Capacity (VIC), the Spatial Tools for River basins and Environment and Analysis of Management options (STREAM), and the Precipitation-Runoff Modelling System (PRMS) (Dey and Mishra, 2017). These models can be distinguished into two broad categories (deterministic and stochastic) based on the presence of random variables and their spatial and temporal variability (Chow *et al.*, 1988). Stochastic models produce model outputs that are at least partially random; therefore, these models use statistical predictions in their modelling approach. Conversely, deterministic models do not consider randomness in their

approach. As a result, deterministic models always produce the same output for a given input, highlighting their usefulness as forecasting tools (Devia *et al.*, 2015).

Hydrological models can be subdivided into lumped, semi-distributed, and distributed models on a spatial basis. Lumped models consider a catchment as a single component and make computations based on catchment averages for certain parameters and variables (Niel *et al.*, 2003). Semi-distributed models divide a catchment into smaller sub-basins and simulate the hydrological properties in each of these units. Lastly, distributed models use cells to describe a catchment's spatial heterogeneity (Devia *et al.*, 2015). Stochastic and deterministic models can, therefore, be further classified using this approach. Stochastic models are classed as space correlated or space independent subject to the spatial influence of random variables. However, deterministic models are classified into three groups, namely: deterministic lumped, deterministic semi-distributed, and deterministic distributed. Deterministic lumped models are applied to single points or regions within a catchment and do not account for the spatial distribution of numerous hydrological processes (Niel *et al.*, 2003). Deterministic semi-distributed models partition a catchment into hydrological response units (HRUs) based on land-use/land cover, soil, and topographic properties and separately simulate the hydrological processes in each HRU (Devia *et al.*, 2015). Deterministic distributed models separate a watershed into grids and simulate the hydrological processes in each grid using model variables with spatial accountability (Feyen *et al.*, 2000).

Each of these approaches (lumped, semi-distributed, and distributed) has numerous strengths and weaknesses concerning their simulation of the hydrological processes at a catchment scale. The lumped models' conceptual parameterisation is simple and computationally efficient; however, it fails to adequately account for the spatial variability in hydrological processes (Niel *et al.*, 2003). In contrast, semi-distributed and distributed models have improved consideration for catchment properties and spatial relationships affecting hydrological response (Devia *et al.*, 2015). But it is to note that semi-distributed models have shortcomings regarding simplifying or grouping a basin's spatial properties, resulting in reduced accuracy of hydrologic process simulation. In addition, although distributed models provide the greatest consideration for catchment spatial heterogeneity, the scale of data required, consequently, reduces its applicability in ungauged catchments (Devia *et al.*, 2015).

2.3 Soil and Water Assessment Tool (SWAT) description

SWAT is a continuous-time, deterministic semi-distributed hydrological model developed at the United States Department of Agriculture's Agricultural Research Service (Neitsch *et al.*, 2011; Arnold *et al.*, 2012). It operates on a river basin or watershed scale with the aim of predicting the impact of land management practices on sediment, water, and agricultural chemical yields for large and intricate watersheds having various management, land-use, and soils over long periods (Neitsch *et al.*, 2011; Arnold *et al.*, 2012; Krysanova and Srinivasan, 2015). To satisfy its aim, SWAT is physical based and uses regression equations to delineate the relationship between input and output variables (Neitsch *et al.*, 2011). Input variables include information regarding vegetation, land management practices, topography, soil, and weather (Mengistu *et al.*, 2019); which is used to model the processes associated with nutrient cycling, sediment, and water movement (Neitsch *et al.*, 2011; Arnold *et al.*, 2012). Subsequently, SWAT quantifies the long-term impacts of changing land management practices, vegetation, climate, water quality, and other variables using readily available data (Arnold *et al.*, 2012).

SWAT has received numerous upgrades since its inception in the early 1990s and now operates through several geographic information systems (GIS) interfaces (Krysanova and Srinivasan, 2015), enabling model parameterisation and initialisation. Initialisation occurs through data input concerning topography, land-use/land cover, soils, land management, and climate (Neitsch *et al.*, 2011). SWAT utilises topographic data to partition a watershed into numerous sub-basins depending on elevation and further divides sub-basins into HRUs using similarities between land-uses, management practices, topography, and soil characteristics (Arnold *et al.*, 2012; Krysanova and Srinivasan, 2015). SWAT simulates the hydrology in each HRU using two phases: the land phase and the routing phase, simulating water movement overland towards the main river channel and water movement through the stream network, respectively (Arnold *et al.*, 2012).

Numerous studies have implemented SWAT to meet various research objectives, such as: evaluating the effects of best management practices on basin hydrology (Sood and Ritter, 2010) and quality (Motsinger *et al*., 2016; Himanshu *et al.*, 2019); examining the impacts of pollution sources on water resources (Pohlert *et al*., 2005; Yang *et al.*, 2011); simulating nutrient (Bosch, 2008) and sediment (Zettam *et al*., 2017) transport and their associated influences; assessing the individual impacts of land-use (Baker and Miller, 2013) and climate (Narsimlu *et al.*, 2013) changes on hydrology; as well as their combined effects (Vaghefi *et al*., 2015). Moreover,

SWAT's successful applicability is noted in different regions and across various climates, including Australasia (Watson *et al*., 2003; Cao *et al*., 2006; Saha *et al*., 2014; Me *et al*., 2015), Europe (Romanowicz *et al*., 2005; Glavan *et al*., 2011; Abbaspour *et al*., 2015; Serpa *et al*., 2015), Asia (Li *et al*., 2009; Ghaffari *et al*., 2010; Narsimlu *et al*., 2013; Wagner *et al*., 2013), South America (Stehr *et al*., 2008; Fukunaga *et al*., 2015; Romagnoli *et al*., 2017;), and North America (Jayakrishnan *et al*., 2005; Tong *et al*., 2009; Srinivasan *et al*., 2010). In the African context, SWAT has been employed extensively across North Africa (Bouraoui *et al*., 2005; Fadil *et al*., 2011), West Africa (Schuol and Abbaspour, 2006; Schuol *et al*., 2008) and East Africa (Mango *et al*., 2011; Baker and Miller, 2013).

In South Africa, SWAT was first applied by Govender and Everson (2005), who assessed SWAT's ability to model streamflow occurring in two small Kwa-Zulu Natal catchments with differing land-use practices. Govender and Everson (2005) noted SWAT's ability to successfully simulate streamflow based on soils, climate, and land-use changes. However, their study identified that SWAT had shortcomings regarding simulating crop growth and the associated increased water demand in afforested catchments. Querner and Zanen (2013) examined SWAT's suitability in analysing innovations in agriculture within the Letaba basin of the Limpopo Province. Their research highlighted SWAT's potential weaknesses as the model could not be calibrated due to its size and the magnitude of input parameters required. Welderufael *et al.* (2013) utilised SWAT in a quaternary catchment of the Modder River Basin (Free-State Province) to assess the effects of rainwater harvesting on water resources. The authors concluded that SWAT was able to determine the influence of different land-use types on water resources; however, noted potential inaccuracies attributed to a lack of available soil data. Gyamfi *et al.* (2016) applied SWAT to the Olifants Basin in the Limpopo Province to assess the impacts of land-use changes on basin hydrology. Their study emphasised SWAT's usefulness as a water resources decision-making tool in South Africa through successful simulation of basin response to land-use changes. Ngubane (2017) aimed to model the hydrology of the Ingula pumped storage scheme catchments in the Kwa-Zulu Natal and Free-State provinces using SWAT. Ngubane (2017) highlighted SWAT's suitability for simulating the hydrology of mountainous and data-scarce catchments in southern Africa in response to climate and land-use changes through successful calibration and validation. Thavhana *et al.* (2018) aimed to use SWAT to simulate run-off in the Luvuvhu River catchment of the Limpopo Province. Thavhana *et al.* (2018) observed that SWAT struggled to simulate the hydrological extremes in the basin; however, concluded that SWAT could still be helpful for general water

resources assessments. Mengistu *et al.* (2019) provided a method for the calibration and validation of SWAT in South Africa using two catchments: a donor and a target catchment located in Gauteng and the Northern Cape, respectively. Their study aimed at the regionalisation approach, whereby a gauged donor catchment is used to provide model parameters for an ungauged target catchment with similar properties. Mengistu *et al.* (2019) emphasised that the transfer of calibrated parameters from one catchment to another using SWAT may result in potential uncertainties regarding model outputs.

Hydrological research within the UCRB have focused on surface water and groundwater interactions (Abiye, 2011; Abiye *et al.*, 2011; Abiye, 2013; Abiye, 2014; Abiye *et al*., 2015) or groundwater recharge processes (Zondi, 2017; Leketa *et al*., 2018; Leketa *et al.*, 2019); however, few studies have assessed the potential impacts of land-use and climate changes on the hydrology of the UCRB. Leketa and Abiye (2019) used the Precipitation-Runoff Modelling System to determine the impact of climate variables on the hydrology of the southern portion of UCRB. Through successful simulation their study noted the potential pollution of the UCRB's surface water resources due to reduced streamflow attributed to climate change. Although Leketa and Abiye (2019) have simulated UCRB hydrology using PRMS, no studies were performed assessing the accuracy of the hydrological models in simulating the UCRB's response to both climate and land-use changes. In addition, no previous studies have attempted to characterise the UCRB's hydrology in its entirety or attempted to apply SWAT to a South African basin of such large-scale couple with extensive and diverse land-use practices.

2.4 Description of Study Area

The UCRB, also known as 'Catchment A21', is a tertiary catchment encompassing eleven quaternary catchments (A21A – A21L) (Fig. 2.1.), which constitutes part of the Crocodile West and Marico Water Management Area as per the Department of Water and Sanitation (DWS) classification. The basin covers an area of approximately 6336 km^2 (DWAF, 2008) within the Gauteng and North-West provinces of South Africa, extending between latitudes 25.27° to 26.199° S, and longitudes 27.357° to 28.467° E (DWAF, 2004). Due to the presence of higher elevations in the south of the basin (Fig. 2.1.), the UCRB is drained in a general northerly direction. The confluence of the Jukskei and Hennops rivers in the east of the basin produce the Crocodile River, which contributes to 90% of Hartbeespoort Dam's inflow (Leketa *et al.*, 2018). The Magalies River contributes minor inflow to Hartbeespoort Dam from the west. The Crocodile River flows northward from Hartbeespoort Dam into the Roodekoppies Dam before eventually discharging into the Limpopo River via the Lower Crocodile River Basin (Leketa

et al., 2018). Apart from the Hartbeespoort and Roodekoppies dams, the UCRB contains two other significant water bodies: Rietvlei Dam and Buffelspoort Dam.

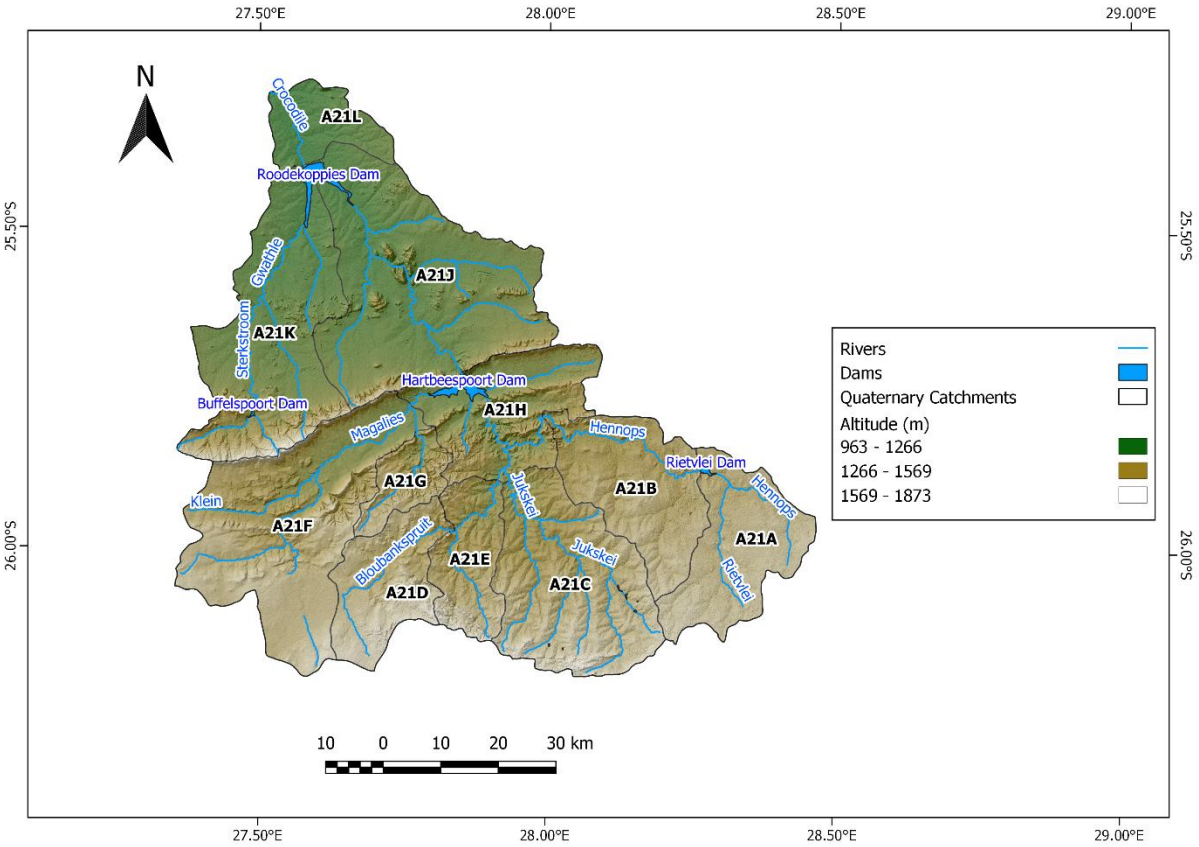


Figure 2.1: Quaternary catchments, stream networks, and reservoirs within the UCRB

2.5 Climate Setting

The UCRB forms part of South Africa's interior and is, therefore, characterised by a subtropical highland climate (Leketa *et al.*, 2018) with a low yet highly variable mean annual rainfall of 700 mm (Abiye, 2011) and mean annual evapotranspiration of approximately 1700 mm (DWAF, 2008). Plots concerning average monthly precipitation and maximum and minimum surface temperatures from two weather stations near the UCRB, namely Buffelspoort II AGR and Pretoria University Proefplaas, shown in Figure 2.2, indicate a directly proportional relationship between precipitation and temperature in the basin. Resultantly, the UCRB is noted to experience cold, dry winters between May and July (Leketa, 2019), with winter temperatures ranging from a minimum of 1 °C to a maximum of 20 °C between April and September (DWAF, 2004). In contrast, the UCRB generally receives rainfall between the summer months of October and March, which occurs as convective rainfall in the form of afternoon thundershowers and occasional hailstorms (Barnard, 2000; DWAF, 2004; Leketa, 2019). This

rainfall is instigated by the hot temperatures experienced during summer, commonly ranging from a minimum of 10 °C to a maximum of 30 °C (DWAF, 2004).

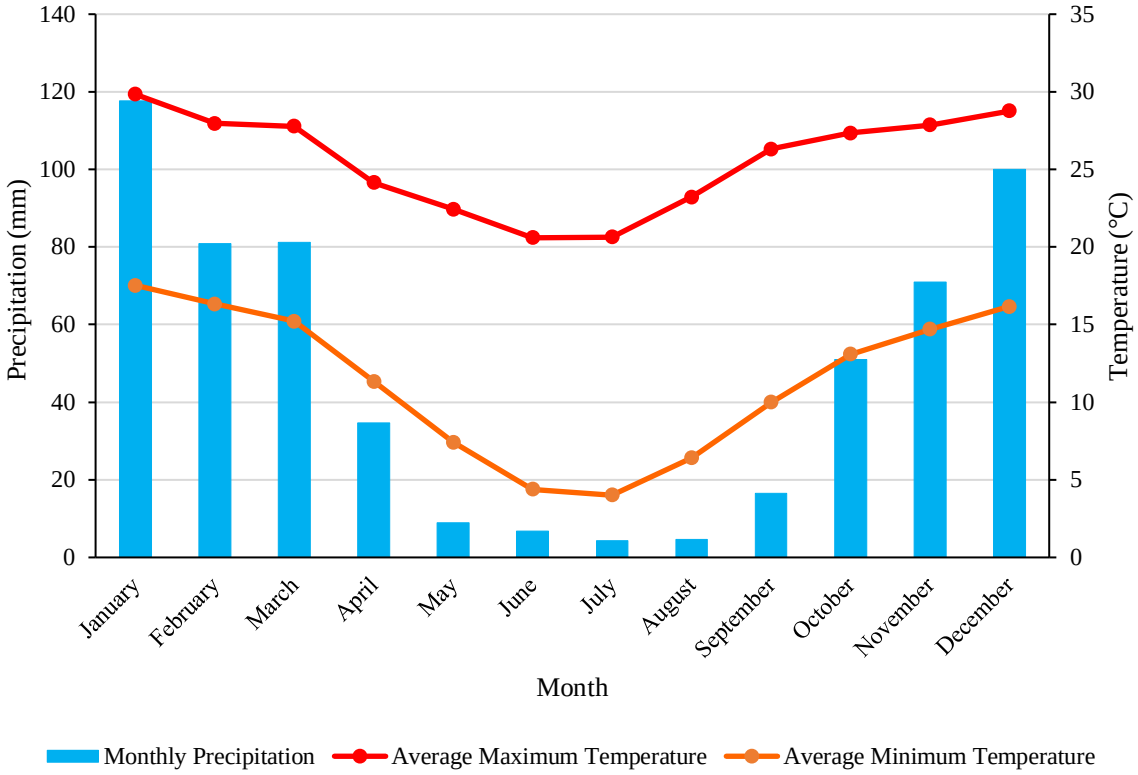


Figure 2.2: The monthly average rainfall, and maximum and minimum temperatures for the Buffelspoort II AGR and Pretoria University Proefplaas weather stations from 1980 to 2020

2.6 Geological Setting

The basis for the geology of the UCRB and South Africa is constituted by a portion of thick continental crust, developed in southern Africa between 3.7 and 2.7 Ga, known as the Kaapvaal Craton (Robb and Meyer, 1995). The Kaapvaal Craton is characterised by an Archean basement consisting of granodiorites, gabbros, granitic gneiss, and serpentinites (McCarthy and Rubidge, 2005), which have been weathered, eroded, and altered by tectonic processes since their emplacement. Overlying the Archean basement are rocks of the Witwatersrand, Ventersdorp, and Transvaal supergroups, the Bushveld Igneous Complex, and the Karoo Supergroup, which have a general northerly younging direction relative to Johannesburg (Barnard, 2000; Johnson *et al.*, 2006; Leketa, 2019).

The Witwatersrand Supergroup unconformably overlies the Kaapvaal Craton and comprises a succession of metamorphosed sedimentary rocks consisting of alterations of conglomerates, quartzites, grits, and shales (Brock and Pretorius, 1964) with tillites, ironstones, and a band of

intercalated lava found in the lower segment of the Supergroup (Anhaeusser, 1971). The Witwatersrand Supergroup is sequentially divided into the West Rand Group (2970-2914 Ma), comprising the Orange Grove quartzites and ferruginous magnetic shales, and the Central Rand Group (2894-2714 Ma), composed of quartzites, shales, and conglomerates (Pretorius, 1976).

The Ventersdorp Supergroup was emplaced after 2714 Ma (Robb and Meyer, 1995) and, therefore, overlies the Witwatersrand Supergroup. It is characterised by intermediate to mafic volcanic, sedimentary, and volcano-sedimentary rock units (Van der Westhuizen *et al.*, 1991); however, in the UCRB, the Ventersdorp Supergroup predominantly outcrops as tuffs and andesites from the Klipriviersberg Group (Barnard, 2000).

Rocks of the Transvaal Supergroup unconformably overlie the granite basement in the north and conformably overlie the Ventersdorp Supergroup in the east of the UCRB (Anhaeusser, 1971). The Transvaal Supergroup consists of two groups: the Chuniespoort Group and the Pretoria Group, formed between 2500 and 2100 Ma (Leketa, 2019). Within the UCRB, the Chuniespoort Group comprises quartzites of the Black Reef Formation and dolomites of the Malmani Subgroup (Eriksson *et al*., 2006; Leketa, 2019). The Pretoria Group overlies the Chuniespoort group and is characterised by several formations, namely: the Timeball Hill shale and quartzite, Hekpoort andesite, Strubenkop shale, Daspoort sandstone, Silverton lava and shale, Magaliesberg quartzite, and Rayton shale, sandstone, and volcanic rocks (Eriksson *et al*., 2006).

The Bushveld Igneous Complex comprises a succession of magmatic intrusions separated into the Rustenburg Layered Suite, Rashoop Granophyre Suite, and the Lebowa Granite Suite (Barnard, 2000). The Bushveld Igneous Complex outcrops in the northern part of the UCRB and consists of gabbros, norites, and anorthosites of the Rustenburg Layered Suite; Nebo-granites of the Lebowa Granite Suite; and granodiorites of the Rashoop Granophyre Suite (Cawthorn, 2006).

The Karoo Supergroup comprises the youngest rocks of the UCRB, which have small outcrops in the eastern part of the catchment. The Karoo Supergroup is composed of mudstones, sandstones, and tillites of the Dwyka Group and sandstones, shales, and coal of the Ecca Group (Leketa, 2019).

2.7 Hydrogeological Setting

From a structural perspective, the UCRB has undergone deformation resulting in numerous shear zones and strike-slip faults which penetrate different rock units (Abiye, 2011). Consequently, the UCRB consists of aquifers with variable hydraulic properties whose yields depend on weathering and the development of secondary structures (Abiye *et al.*, 2015). These aquifers can be classified into four different types: fractured aquifers, karstic aquifers, intergranular aquifers, and intergranular and fractured aquifers (Barnard, 2000; Abiye, 2011; Abiye *et al.*,2011, Abiye *et al.*, 2015).

Fractured aquifers consist of rocks containing fractures, joints, and/or fissures that retain and transmitting large quantities of water. These aquifers are commonly found in the granitic gneisses of the Archean basement and in the Witwatersrand Supergroup quartzites of the UCRB (Leketa, 2019).

Karstic aquifers comprise carbonate rocks, such as limestone and dolomite, which have undergone karstification to produce cavities for the storage and transmission of water. Depending on the degree of karstification, these aquifers can produce large conduits for groundwater transmission or retard groundwater flow. Karstic aquifers are found within the Malmani Subgroup of the UCRB, which Abiye (2011) noted to occur at greater depths and have higher productivity in comparison to fractured aquifer systems within the UCRB.

Intergranular aquifers are composed of unconsolidated, porous material occurring as river channel deposits, sand, and gravel in alluvial zones or as rocks that have undergone significant weathering to a porous state. Therefore, intergranular aquifers are found along riverbanks and in the weathered zones of granites across the UCRB (Leketa, 2019).

Intergranular and fractured aquifers comprise rocks containing both unconsolidated material and fractures (Barnard, 2000). These types of fractures commonly comprise a two-layer system consisting of regolith of high permeability due to intense weathering, which overlies a fractured hard rock aquifer. This aquifer type occurs in the basement granites and Bushveld Igneous Complex of the UCRB (Barnard, 2000).

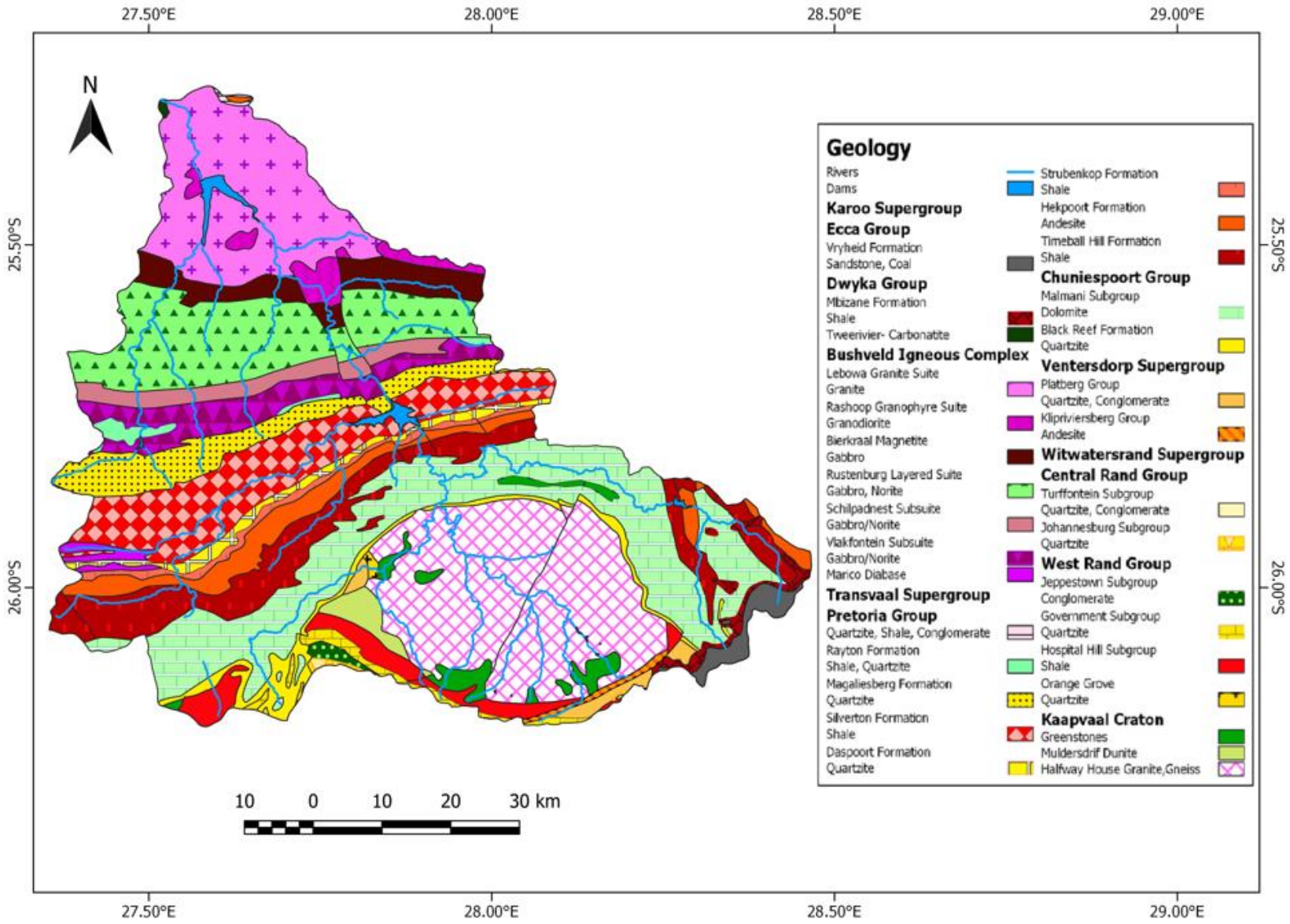


Figure 2.3: Geological Map and Stratigraphic Legend of the UCRB

CHAPTER 3: METHODOLOGY

The development of a SWAT model which accurately described the basin hydrology of a large and complex catchment such as the UCRB required the collection and refinement of data regarding climate and the physical characteristics of the basin. SWAT necessitated the spatial representation of these basin characteristics for the enhanced simulation of catchment hydrology. As a result, the SWAT2012 model was coupled with the Quantum Geographic Information System (QGIS) (Version 3.10- A Coruña) via an extension to QGIS known as QSWAT 3 (Version 1.1). QSWAT enabled the spatial delineation of the catchment extent and the factors influencing the basin's hydrological properties through a systematic attribute, vector, and raster dataset input in the following stages: watershed delineation, hydrological response unit creation, SWAT edit, and SWAT run (Arnold *et al.*, 2012). These stages were used to synthesize the SWAT model prior to calibration and validation of the model for the visualization of streamflow results under climate and land-use changes, as shown in Figure 3.1.

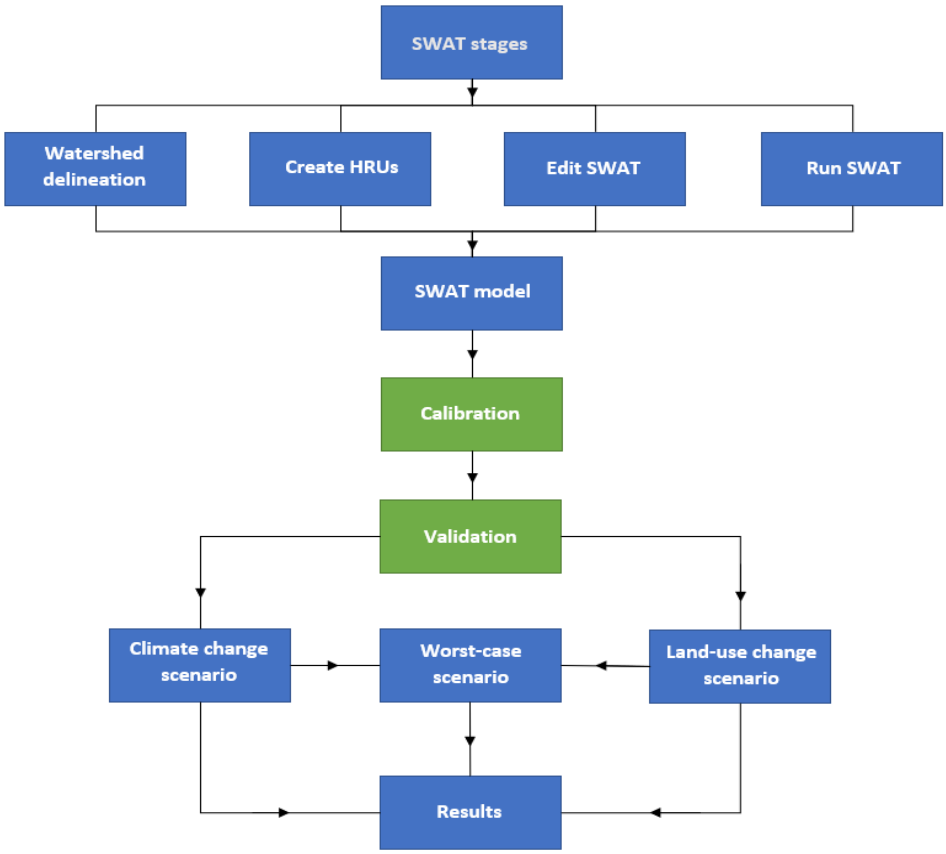


Figure 3.1: Flow diagram showing the methodology used to generate results for the UCRB SWAT model

3.1 Watershed Delineation

The first step in SWAT model synthesis is concerned with the watershed and stream network configuration by partitioning a catchment into numerous sub-basins for improved model simulation (Dile *et al.,* 2015). SWAT permitted watershed delineation using one of the two methods: the predefined watershed or the grid cell method. The predefined watershed method utilised existing data regarding the stream network, sub-basins, and topography of a watershed to partition a catchment into its sub-basins. In contrast, the grid cell method used the elevation properties of a catchment, represented by grids, to delineate its sub-basins. Resultantly, the grid cell method was inferior to the predefined watershed method, as it did not preserve the routing reaches or topographic flow paths (Arnold *et al.,* 2012) in the UCRB. However, due to the complex nature of the UCRB demanding a more detailed characterisation of its basin properties, the grid cell method was, thus, used for this study.

The grid cell method enabled the description of the sub-basins of the UCRB through a two-step process. The first step involved defining the catchment and stream network's position, extent, and elevation using a digital elevation map (DEM), river map, and a user-defined threshold value. According to Cotter *et al.* (2003), a DEM is one of the critical input files for hydrological models used in approximating numerous variables in a watershed. Moreover, the DEM resolution can significantly influence watershed characteristics such as shape, slope, length, and surface area (Nazari-Sharabian *et al.*, 2020). Therefore, a 30 m resolution DEM, shown in Figure 3.2, was used to characterise the extent of the UCRB and defined most of the elevation-related properties of the basin, such as altitude and topography. The river map outlined the position and shape of the stream network. Hence, the combination of the DEM and river map input succeeded in delineating the elevation of the stream network and the direction of flow within the UCRB. The threshold value is defined as the minimum number of DEM cells draining into a single cell for it to be included in the stream network (Neitsch *et al.*, 2011). Resultantly, lower threshold values caused more cells to be incorporated and, thus, reflected a higher drainage density. Therefore, a threshold value of 26 000 cells (or 23.4 km^2) was deemed appropriate to delineate the stream network adequately and accurately within the UCRB (Fig 3.2.).

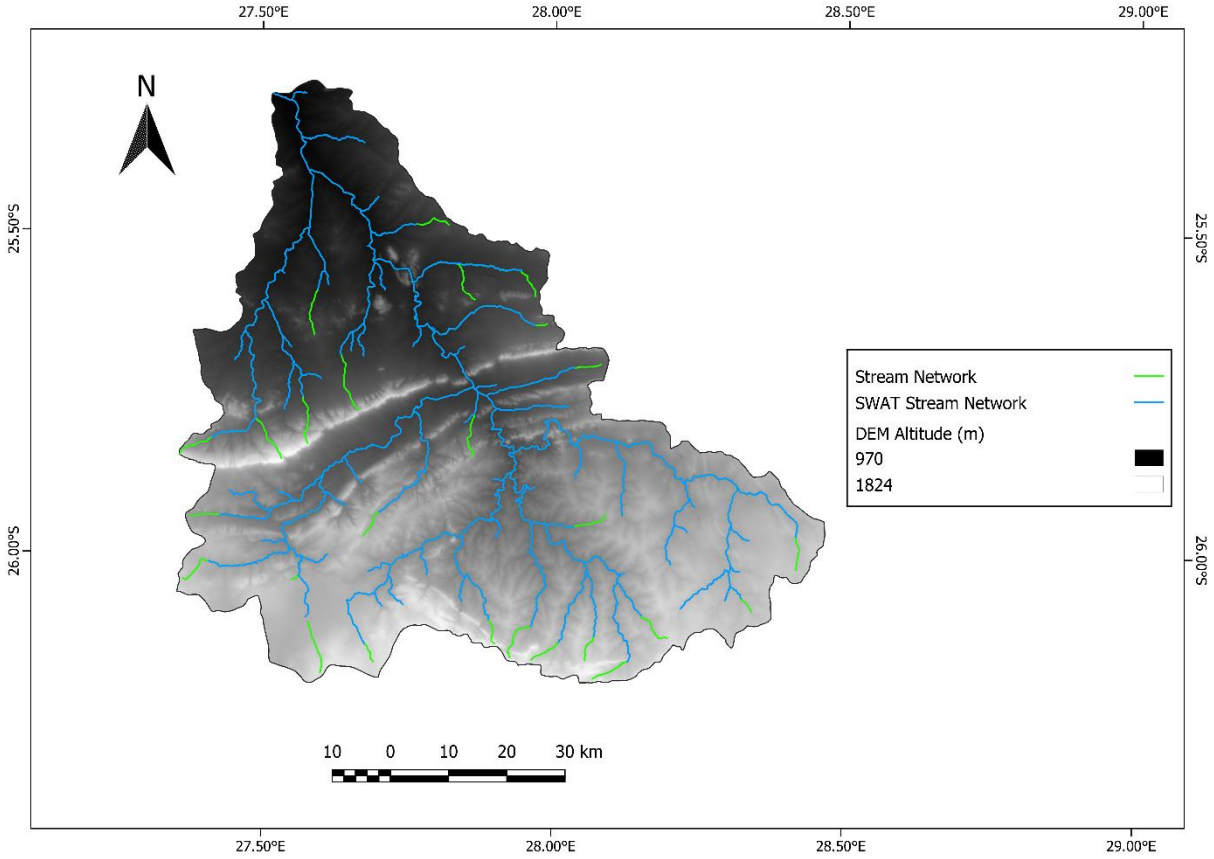


Figure 3.2: The DEM and River map involved in producing the stream network for the UCRB

The second step in grid cell watershed delineation involved separating the UCRB into several sub-basins. SWAT divided sub-basins to ensure that each sub-basin contained at least one tributary or main channel reach. In addition, two types of impoundments (reservoirs, ponds, or wetlands) were permissible as inclusions to each sub-basin (Arnold *et al.*, 2012). As a result, SWAT required the delineation of the positions of inlets, outlets, and reservoirs within the UCRB prior to sub-basin separation.

The DEM, river map, and threshold value, whose attributes are described in Table 3.1, simulated a stream network (blue- Fig. 3.2.) which was nearly identical to that of the UCRB's stream network (green- Fig. 3.2.). Moreover, the input of the locations of three inlets, one outlet, and four reservoirs segmented the stream network and divided the UCRB's watershed into 139 sub-basins. Collectively, these sub-basins produced an overall basin with a close approximation to the UCRB, as shown in Figure 3.3.

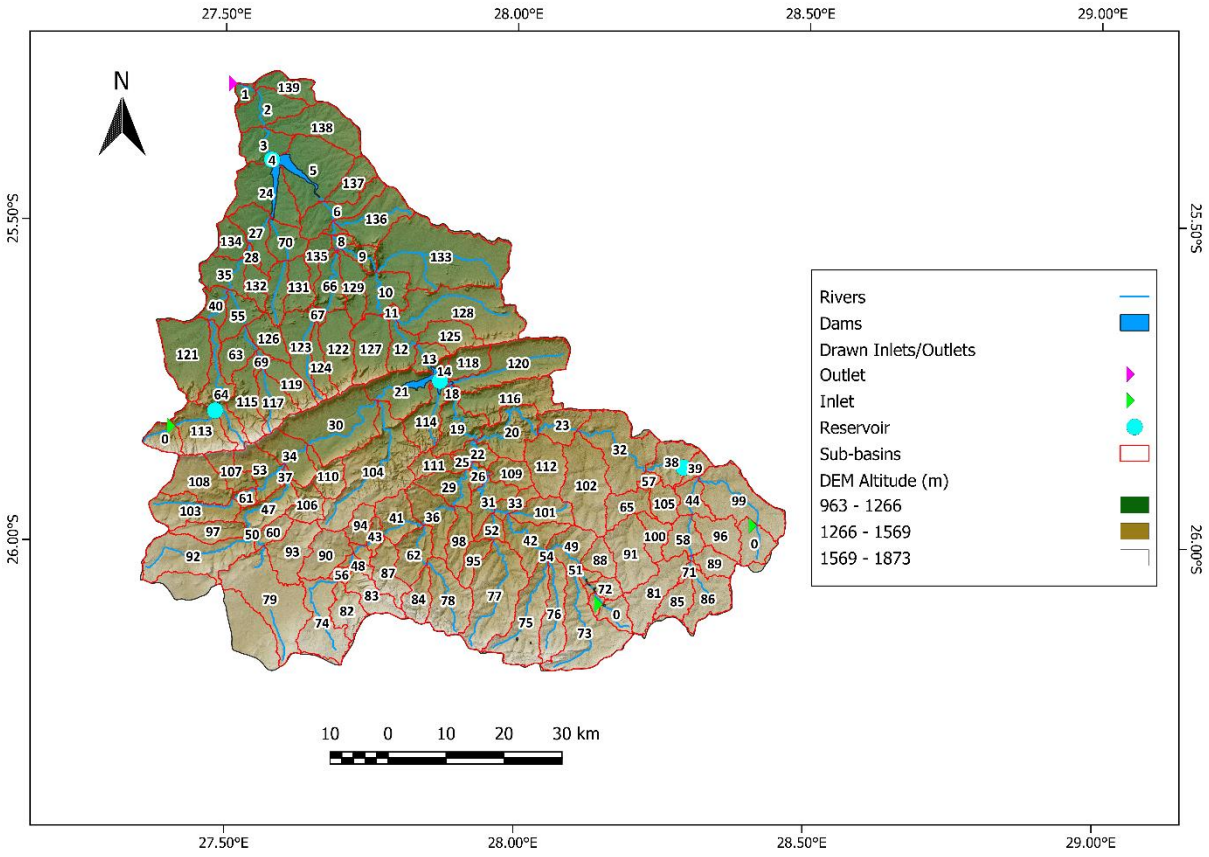


Figure 3.3: The delineated watershed of the UCRB including its inlets, outlets, reservoirs, and sub-basins

Table 3.1: Description and sources of data used in delineating the watershed of the UCRB

Name	Source	GIS data type	Resolution
Digital Elevation Map	https://earthexplorer.usgs.gov/	GeoTIFF	30 metres
River Map	https://egis.environment.gov.za/	ESRI Shapefile	N/A
Threshold Value	Manual input	N/A	N/A
Dam Map	https://egis.environment.gov.za/	ESRI Shapefile	N/A
Inlets, Outlets and Reservoirs	Manual input	ESRI Shapefile	N/A
Point Sources	SWAT automatic input	ESRI Shapefile	N/A

SWAT enabled the addition of point sources to each sub-basin. These include water, sediment, and nutrient loadings to the stream network from sources not associated with the land area (Arnold *et al.*, 2012). Thus, point sources consider artificial inflations to the stream network from sources like wastewater treatment plants. These sources were employed in the UCRB to characterise the wastewater discharge, which added 139 point sources to the watershed, one for each sub-basin, shown in Figure 3.4.

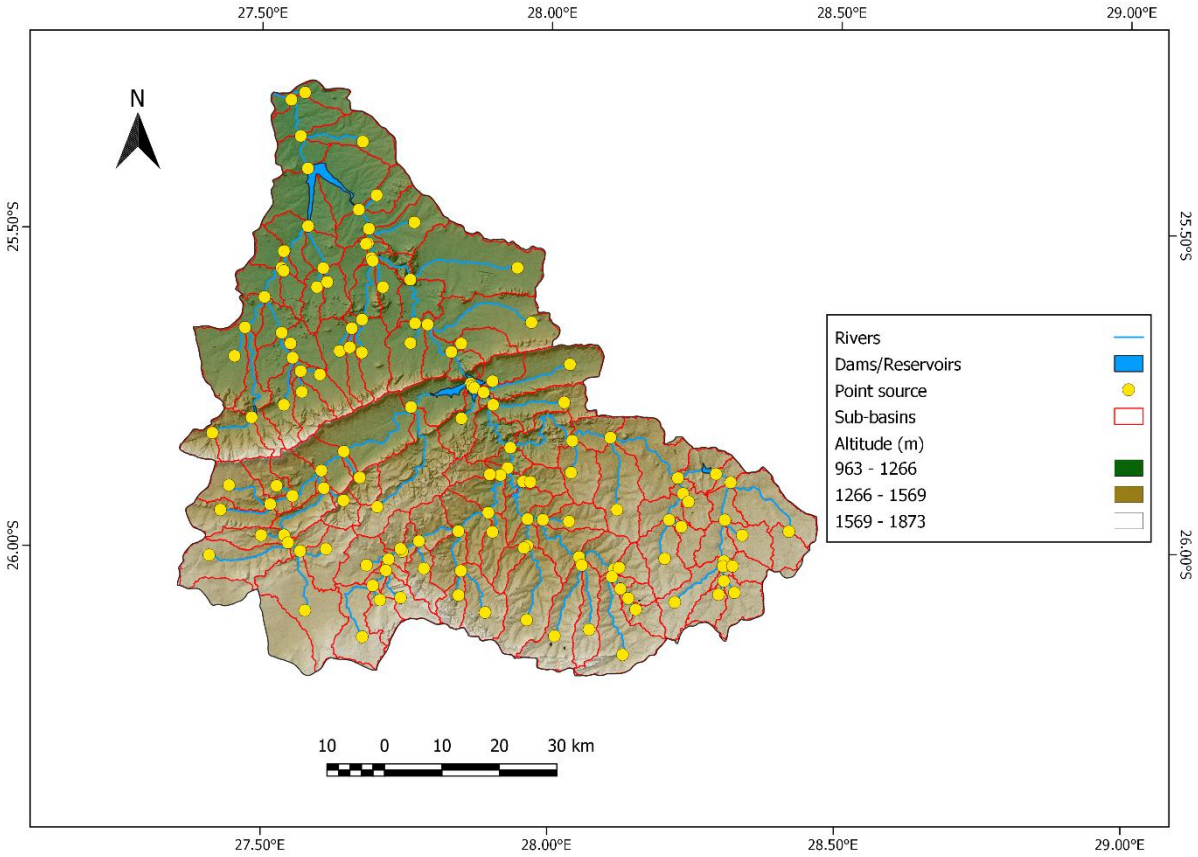


Figure 3.4: Location of point sources in relation to the stream network of the UCRB

3.2 Create Hydrological Response Units

The next step in generating the model concerned subdividing the sub-basins, defined during watershed delineation, into several hydrological response units (HRUs) to improve the description of the UCRB's properties influencing streamflow. SWAT defines HRUs as combinations of soils and land-use/land cover practices that differ significantly regarding their hydrologic characteristics to cause unique changes in streamflow (Neitsch *et al.*, 2011; Dile *et al.*, 2015).

The land-use/land cover practices occurring over the UCRB were obtained from South Africa's Department of Environment, Forestry, and Fisheries, who developed a map defining the land-use practices operating throughout the country for 2018, known as South Africa's Land Cover dataset 2018 (SANLC 2018). The SANLC 2018 (available at: https://www.environment.gov.za/projectsprogrammes/egis_landcover_datasets) defined the spatial relations between 73 different land-use/land cover classes and was clipped to the extent of the UCRB. Figure 3.5 shows that 58 of these classes occurred over the UCRB in 2018, highlighting the diverse nature of the basin. However, the land-use/land cover classes

implemented for the SANLC 2018 dataset could not be integrated into the SWAT model, which utilised 22 different land-use/land cover classes in its modelling procedure (Neitsch *et al.*, 2011), shown in Table 3.2. Thus, a land-use lookup table, depicted in Appendix A- Table A.1, was used to associate the SANLC 2018 classes to SWAT using appropriate SWAT codes.

Table 3.2: SWAT codes and their description used in the land-use look up table

	SWAT code	**Description**
1	**WATR**	Water
2	**SWRN**	South Western Range
3	**SWRN**	South Western Range and Bare Rock
4	**SWRN**	South Western Range and Quarries/Mines
5	**FRSE**	Evergreen Forest
6	**FRSD**	Deciduous Forest
7	**FRST**	Mixed Forest
8	**WETF**	Woody Wetlands
9	**WETN**	Emergent/Herbaceous Wetlands
10	**RNGB**	Range Shrubland
11	**RNGE**	Grasslands/Herbaceous
12	**ORCD**	Orchards/Vineyards
13	**PAST**	Pasture/Hay
14	**AGRR**	Row Crops
15	**AGRC**	Small Grains
16	**AGRL**	Generic
17	**URML**	Urban Medium density
18	**URHD**	Urban High Density
19	**UCOM**	Urban Commercial
20	**UINS**	Urban Institutional
21	**UIDU**	Urban Industrial
22	**UTRN**	Urban Transportation

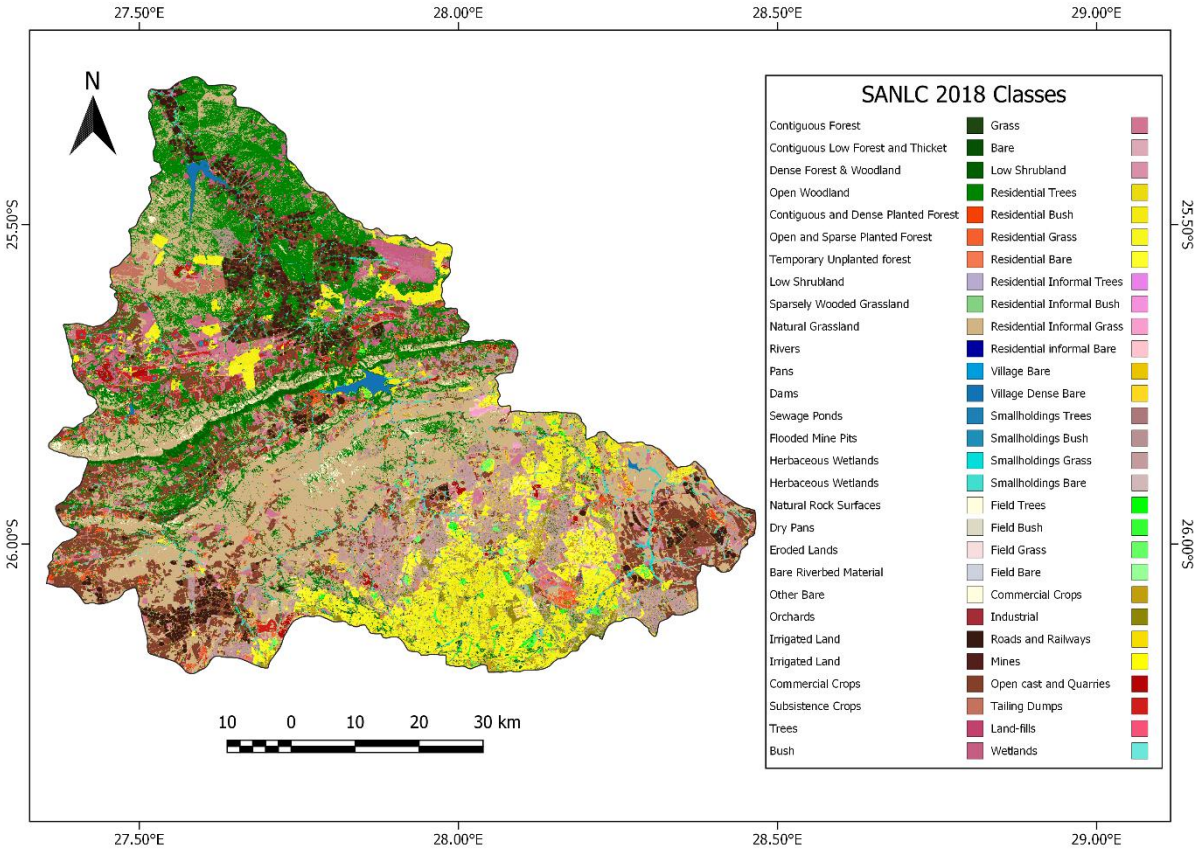


Figure 3.5: The SANLC 2018 land-use/land cover classes operating over the UCRB in 2018

The UCRB's soil data was sourced from the United Nations Food and Agricultural Organization's (FAO) Harmonized World Soil Database (HWSD- Version 1.2) (available at: http://www.fao.org/soils-portal/data-hub/soil-maps-and-databases/harmonized-world-soil-database-v12/en/). The HSWD, developed in 2009, combined existing regional and national soil updates worldwide and, therefore, contained over 15 000 soil mapping units, spatially represented by a raster image, as well as a database file detailing the properties of these soil layers. The HWSD raster image was clipped to the UCRB's extent, which identified 65 soil mapping units within the basin (Figure 3.6). The attributes of these soils were recognised by SWAT through data input into a usersoil table, contained within QSWAT's reference database, which was linked to SWAT using a soil-lookup table, shown in Appendix A- Table A.2.

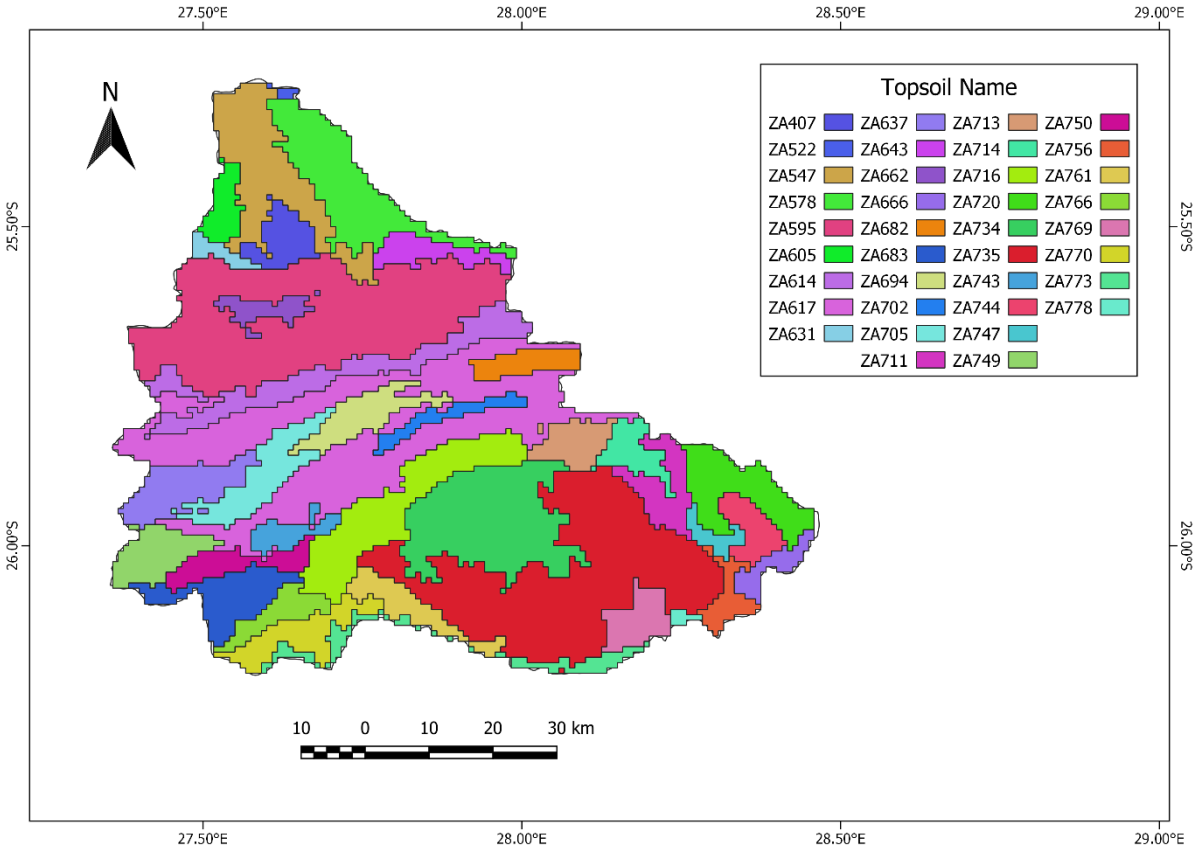


Figure 3.6: The HSWD topsoil names and locations in the UCRB

The HSWD database file comprised soil attribute data required for input into SWAT's usersoil table, such as the identification of soil layers (MUID), the depth of soil layers (SOL_Z), the maximum rooting depth of soil layers (SOL_ZMX), their moist soil albedo (SOL_ALB), as well as the bulk density of soil layers (SOL_BD), their clay content (SOL_CLAY), silt content (SOL_SILT), sand content (SOL_SAND), rock fragment content (SOL_ROCK), and carbon content (SOL_CBN),which were input directly into the usersoil table. However, the HSWD did not contain some soil properties necessary for SWAT, such as the soil's hydrological group (HYDRO_GRP), available water capacity (SOL_AWC), hydraulic conductivity (SOL_K), and erodibility (USLE_K). Therefore, information pertaining to these soil properties required calculation through relevant hydrological programs or equations before incorporation into SWAT's usersoil table.

The soils' available water capacity and hydraulic conductivity were calculated using the Soil-Plant-Air-Water (SPAW) Hydrology program (available at-https://www.ars.usda.gov/research/software/). SPAW hydrology is a daily hydrologic budget model developed by the United States Department of Agriculture (USDA) for agricultural fields and ponds. As such, SPAW Hydrology was considered appropriate regarding calculating

soil hydrological properties using basic soil information. Subsequently, the program enabled the input of soil clay content, silt content, sand content, carbon content, and rock fragment content (obtained from the HSWD database file), from which the soil's available water capacity and hydraulic conductivity were estimated.

The soil hydrological group is defined as a group of soils having similar run-off potential under similar land-cover and storm conditions (Neitsch *et al.*, 2011). SWAT, therefore, required soils to be classified into four different hydrological groups, indicated in Table 3.3, based on their infiltration characteristics.

Table 3.3: Description of the different soil hydrological groups and their infiltration rate (adapted from Neitsch et al. 2011)

Soil hydrological group	Hydrological properties	Infiltration rate (mm/hr)
A	Soils composed primarily of gravel and sands that are deep and well drained. These soils have a high infiltration rate even when entirely wetted and, therefore, have a low runoff potential.	7.6-11.4
B	Soils having moderate infiltration rates and moderate rates of water transmission. These soils often contain moderately fine to moderately coarse textures.	3.8-7.6
C	Soils with low infiltration and water transmission rates which predominately consist of a layer of moderately fine to fine texture which impeded the downward movement of water.	1.3-3.8
D	Soils composed primarily of clay having slow rates of water transmission and very slow infiltration rates.	0-1.3

Calculation of the soils' infiltration rate and the identification of the soil hydrological group was based on a study conducted by Che (1995), who used the correlation between soil permeability and average particle diameter to estimate the soil permeability coefficient. Che (1995) developed two empirical formulae (Equation 4 and Equation 5) to determine the soil infiltration rate.

$$X = (20Y)^{1.8} \quad (2)$$

$$Y = \frac{Scp}{10} * 0.03 + 0.002 \quad (3)$$

Where X is the permeability coefficient (infiltration rate), Y is the average particle diameter of the soil, and Scp represents the percentage of the soil's sand content.

The universal soil erodibility factor ($USLE_K$) is defined as the soil loss rate per erosion index unit of the sample soil measured on a unit plot and indicates the susceptibility of soils to erosion (Neitsch *et al.*, 2011). However, Williams (1995) noted that experimental measurement of a soil's erodibility factor were often costly and time-consuming and hence, proposed a simplified equation, shown by equation 6, to calculate soil erodibility based on soil composition.

$$USLE_K = f_{csand} * f_{cl-si} * f_{orgc} * f_{hisand} \tag{4}$$

$USLE_K$ is the soil erodibility factor, f_{csand} is the coarse sand erosion factor, f_{cl-si} is the clay loam soil erosion factor, f_{orgc} is the soils organic matter factor, and f_{hisand} is the high sand soil erosion factor. The terms of this equation were calculated as follows:

$$f_{csand} = 0.2 + 0.3 * EXP^{\left[-0.0256 * m_s * \left(1 - \frac{m_{silt}}{100}\right)\right]} \tag{5}$$

$$f_{cl-si} = \left(\frac{m_{silt}}{m_c + m_{silt}}\right)^{0.3} \tag{6}$$

$$f_{orgc} = 1 - \left(\frac{0.0256 * OrgC}{OrgC + EXP^{(3.72 - 2.95 * OrgC)}}\right) \tag{7}$$

$$f_{hisand} = 1 - \left(\frac{0.7 * \left(1 - \frac{m_s}{100}\right)}{\left(1 - \frac{m_s}{100}\right) + EXP^{\left[-5.51 + 22.9\left(1 - \frac{m_s}{100}\right)\right]}}\right) \tag{8}$$

where m_s is the percentage sand content of the soil, m_{silt} is the soil's percentage silt content, m_c is the percentage clay content of the soil and $OrgC$ is the organic carbon content of the soil.

The calculated hydrological group, available water capacity, hydraulic conductivity, and erodibility of each soil were input into SWAT's usersoil table and appended to the QSWAT reference database. Thereafter, SWAT was able to produce HRUs for the UCRB using the spatial maps for soils and land-uses and their associated reference tables. Furthermore, SWAT

enabled the input of user-defined slope and elevation bands to improve run-off simulation. Slope bands were used to further separate the UCRB based on slope steepness, whereas elevation bands identified sub-basins with large elevation changes to account for the uneven distribution of rainfall due to orographic effects. As a result, five slope bands (0-5°, 5-10°, 10-15°, 15-25°, >25°) and a 200 m elevation band threshold were used for the UCRB.

The combination of slope and elevation bands in conjunction with the soils and land-uses identified 8863 HRUs for the UCRB, shown in Appendix A- Figure A.1. However, the 8863 HRUs were not used in model development. Instead, SWAT allowed for HRUs to be filtered by land-use, soil, and slope using appropriate threshold values. Accordingly, SWAT ignored any HRUs in which the percentage of land-uses, soils, or slopes were below the specified threshold to improve computational efficiency (Dile *et al.*, 2015). Using a threshold value of 20% for land-use and 10% for slopes and soils produced 413 HRUs for the UCRB, which was implemented for the model.

3.3 Edit SWAT

The third stage of producing a SWAT model concerned defining and describing all the additional factors affecting the UCRB's hydrology such as climate, reservoirs, and wastewater treatment plants.

Characterising the climate over the UCRB involved the initial preparation of a weather generator table (WGEN_user), located in QSWAT's reference database. This table functioned to identify climate trends to assist SWAT in simulating the UCRB's hydrology over the observed period (Neitsch *et al.*, 2011; Arnold *et al.*, 2012). As such, constructing the WGEN_user table required the statistical analysis of monthly or daily weather data. The South African Weather Service (SAWS) provided daily records regarding maximum and minimum surface temperatures, precipitation, wind speed, wind direction, relative humidity, and solar radiation for two weather stations found within or proximal to the UCRB, namely: Buffelspoort II AGR (25.7530° S; 27.4820° E) and Pretoria University Proefplaas (25.7520° S; 28.2580° E), shown in Figure 3.7, from 1 January 1980 to 31 July 2020. However, the dewpoint temperature necessitated by SWAT was absent from these records. Therefore, the dew.exe program (available at: https://swat.tamu.edu/software/) was used to calculate the average daily dewpoint temperature using average humidity and temperature data from SAWS. In addition, the WGN Excel macro extension, known as WGNmaker4.xls, was used to create the

WGEN_user table as it was designed to calculate weather station statistics and to create user weather station files for SWAT.

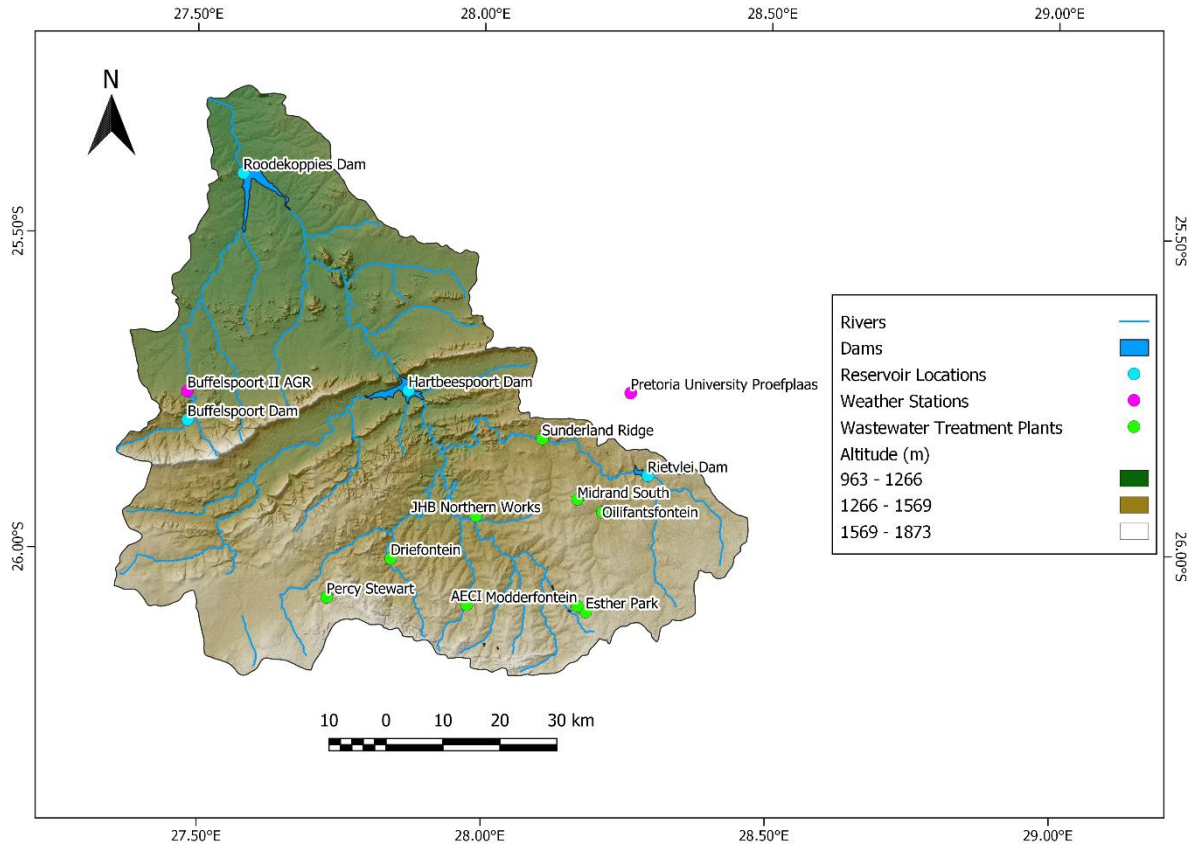


Figure 3.7: The locations of the weather stations, reservoirs, and wastewater treatment plants within the UCRB

The WGNmaker4.xls used text files, prepared using SAWS measured data, to calculate the monthly averages, standard deviations, skew coefficients, and probabilities for each climatic variable in each weather station. Results from the WGNmaker4.xls were input into the WGEN_user table, which allowed SWAT's weather generator to fill in missing data or simulate weather data (Neitsch *et al.*, 2011). The WGEN_user table was used in conjunction with text files; containing daily data including maximum and minimum temperature, precipitation, solar radiation, relative humidity, and wind speed to describe the climate occurring over the UCRB.

The reservoir tab under Edit SWAT Inputs described the properties of the dams influencing changes in water level and reservoir storage and, therefore, the resultant downstream release of water. SWAT quantified these changes using two reservoir characteristics, the emergency spillway and principal spillway, which referred to the maximum and normal reservoir capacity, respectively. The emergency spillway volume (RES_EVOL) and surface area (RES_ESA), as

well as the principal spillway volume (RES_PVOL) and surface area (RES_PSA), were used along with the initial reservoir volume (RES_VOL) to define the physical characteristics of the dams impacting their water level fluctuations and flood control attributes and hence, the hydrology of the UCRB. The emergency and principal spillways attributes and the initial dam volumes were estimated from available historical information from the DWS (Table 3.4). Moreover, the releases from the reservoirs were characterised using SWAT's outflow simulation codes (IRESCO), which determined reservoir discharges using one of four methods, namely: the measured daily outflow, the measured monthly outflow, the simulated annual release rate for an uncontrolled reservoir, and the simulated controlled outflow target release rate.

Table 3.4: The physical attributes of the UCRB's reservoirs used in SWAT model development

Dam/Reservoir	Sub-basin	RES-ESA (ha)	RES_EVOL (10^4 m^3)	RES_PSA (ha)	RES_PVOL (10^4 m^3)	RES_VOL (10^4 m^3)
Roodekoppies	**4**	1728.1	11850	1571	10300	9500
Hartbeespoort	**16**	2271.7	21400	2065.2	18640	16000
Rietvlei	**39**	207.9	1400	189	1230	950
Buffelspoort	**113**	149.3	1200	135.7	1025.1	900

Due to the paucity of data from the DWS concerning the average reservoir rates of the UCRB's dams, the monthly or daily measured outflow methods could not be employed for the model. In addition, the annual release rate was considered insufficient regarding its characterisation of reservoir discharge variability as it provided a constant daily outflow from each reservoir for the entire simulation period. Therefore, the target release rate method was used in model synthesis. According to Neitsch *et al.* (2011), the target release approach attempts to imitate the regulations used by dam operators when deciding on the water quantities emitted from a reservoir. Although it is a simplistic method, it can rationally simulate low flow and high flow periods (Neitsch *et al.*, 2011). The target release method required data entry regarding the beginning (IFLOD1R) and ending month (IFLOD2R) of the non-flood season, the number of days required to attain the target storage from the present reservoir storage (NDTARGR), and the monthly target storage (STARG).

The target release approach functioned by setting the principal spillway volume to the maximum flood control reservation and the emergency spillway volume to the no flood control

reservation. As such, the downstream reservoir release was calculated using these flood control reservations for the flooding and the non-flood seasons. During the non-flood season, no flood control reservation was required, and the monthly target storage was designated to the emergency spillway volume. Conversely, the flood control reservation was a function of reservoir soil water content during the flood season and required the monthly target storage to be specified. In order to describe the outflow from the four major reservoirs of the UCRB (Figure 3.7), the non-flood season was not implemented for the model. Instead, the reservoirs were treated as if the flooding season was continuous throughout the year, and the monthly target storage for the flooding season was set to the reservoir principal spillway volume. This ensured that the dam outflow reflected the desire to achieve full reservoir operating capacity irrespective of water abundant or strenuous conditions occurring in the UCRB. Lastly, the number of days needed to reach the target storage during the flood season were estimated using available daily reservoir releases related to dam storage, obtained from the DWS, shown in Table 3.5.

Table 3.5: The attributes of the target release approach used to describe the outflow from the UCRB's reservoirs

Dam/Reservoir	**Sub-basin**	**NDTARGR (days)**	**STARG (10^4 m^3)**
Roodekoppies	**4**	18	10300
Hartbeespoort	**16**	16	18640
Rietvlei	**39**	6	1230
Buffelspoort	**113**	6	1025.1

Similarly, the attributes of the wastewater treatment plants could be described using the point source tab under Edit SWAT Inputs. This involved selecting the sub-basins containing wastewater treatment plants and inputting daily wastewater loadings for each appropriate sub-basin. Nine wastewater treatment plants were found within the UCRB (Table 3.6; Figure 3.7) and their daily discharges to the main channel were acquired from the Department of Water Affairs (DWAF, 2004).

Table 3.6: The locations and effluent loadings from wastewater treatment plants within the UCRB

Sewage Treatment Plant	Sub-basin	Latitude	Longitude	Discharge (m^3/day)
Oilifantsfontein	**64**	25.942 S	28.213 E	38 000
Sunderland Ridge	**20**	25.827 S	28.106 E	35 000
Esther Park	**57**	26.101 S	28.185 E	400
JHB Northern Works	**25**	25.949 S	27.990 E	220 000
AECI	**53**	26.091 S	27.976 E	7 000
Modderfontein	**57**	26.092 S	28.169 E	16 000
Midrand South	**24**	25.922 S	28.168 E	5000
Percy Stewart	**61**	26.081 S	27.728 E	25 000
Driefontein	**56**	26.017 S	27.842 E	15 000

3.4 Run SWAT

The final step in SWAT model synthesis concerned simulating streamflow in UCRB for the desired period. SWAT permitted daily, monthly, or yearly simulations for the entire period supported by weather data (Neitsch et al., 2011). Furthermore, SWAT allowed for a warm-up or equilibration period (NYSKIP) to be input for the model. The equilibration period defined the number of years for which SWAT simulated the hydrological cycle before quantifying streamflow in the basin (Neitsch *et al.*, 2011). The accuracy of SWAT's streamflow simulations was assessed in relation to six discharge stations distributed across the UCRB (Figure 3.8). The selection of these stations was based on the comprehensive coverage of stream inflow into Hartbeespoort Dam (A2H012, A2H034, A2H044, A2H045), stream outflow from the dam (A2H083), and the outflow from the entire UCRB (A2H019). Additionally, these recording stations had the most complete records regarding monthly streamflow measurements for accuracy analysis (Table 3.7). As this study aimed to simulate the UCRB's hydrology in response to climate and land-use changes, further calibration and validation of the model were necessary to certify that the model made accurate streamflow predictions from its basin response.

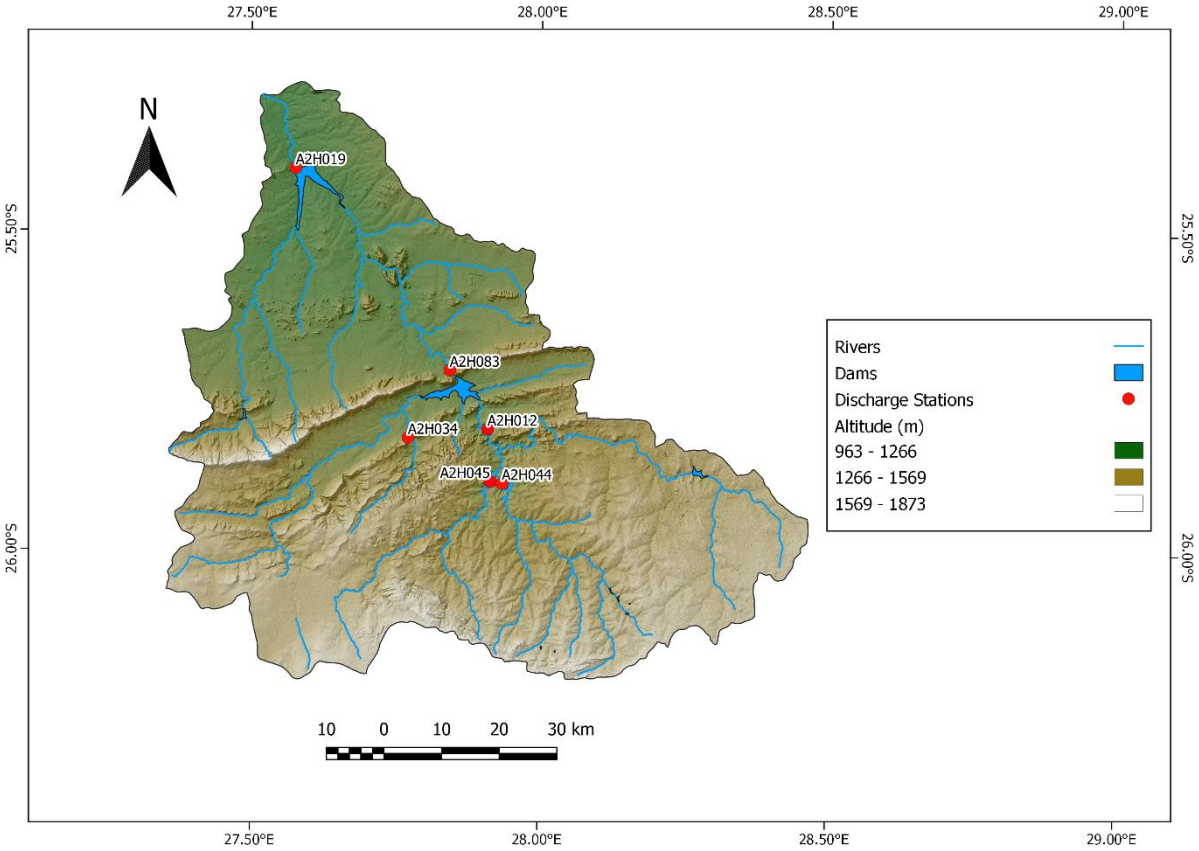


Figure 3.8: The positions of the discharge stations used for accuracy analysis in context of the UCRB's river network

Table 3.7: The attributes of the stream discharge stations used to assess the precision of streamflow simulations in the UCRB

Stream gauge	Name	Sub-basin	Latitude	Longitude	Catchment area (km^2)	Data availability
A2H012	Krokodil River @ Kalkheuwel	**19**	25.811° S	27.910° E	2551	1922/10/01 to 2020/09/03
A2H019	Krokodil River @ Beestkraal	**3**	25.404° S	27.575° E	6131	1951/03/01 to 2016/03/31
A2H034	Skeerpoort River @ Scheerport	**104**	25.825° S	27.772° E	150	1964/03/03 to 2020/09/03
A2H044	Jukskei River @ Vlakfontein	**26**	25.896° S	27.935° E	798	1971/07/18 to 2020/09/03
A2H045	Krokodil River @ Vlakfontein	**29**	25.893° S	27.915° E	653	1972/05/25 to 2020/09/03
A2H083	Krokodil River @ Hartbeesfontein	**13**	25.719° S	27.844° E	4116	1980/03/01 to 2016/02/29

3.5 Calibration

Calibration is the process of altering input parameter values and initial conditions within sensible ranges until the simulated results correlate with observed data (Zeckoski *et al.*, 2015). Therefore, calibration requires the accuracy analysis of model outputs and process simulation to ensure satisfactory watershed and scenario depiction (Sorooshian and Gupta, 1983) and reduce model prediction uncertainty (Engel *et al.*, 2007). The SWAT Calibration and Uncertainty Program (SWATCUP) was employed to calibrate the UCRB model. SWATCUP is a software program developed to calibrate and validate SWAT models (Abbaspour, 2015), which links several precision evaluation procedures to SWAT, such as particle swarm optimization (PSO), generalized likelihood uncertainty estimation (GLUE), parameter solution (ParaSol), Markov chain Monte Carlo (MCMC), and sequential uncertainty fitting (SUFI2). Thus, SWATCUP enables the sensitivity and uncertainty analysis of SWAT parameters and hence, the calibration and validation of the UCRB model.

According to Abbaspour (2015), a significant issue surrounding the calibration of watershed models is the uncertainty regarding their predictions. Watershed models suffer from substantial model uncertainties associated with conceptual models and their parameters and inputs. Conceptual model uncertainties arise from simplifications in the conceptual model; the inclusion of model processes that are absent from the physical environment; the exclusion of model processes that occur in a catchment; and the incorporation of model processes without spatial delineation. Input uncertainties are ascribed to errors regarding input variables (e.g., rainfall and temperature), whereas parameter uncertainties occur due to parameter non-uniqueness in inverse modelling. Parameters reflect hydrologic processes; therefore, parameters affect one another during calibration, similar to how hydrologic processes affect the hydrological cycle. Resultantly, many combinations of parameters may produce the same output. For this reason, calibrating a model using a deterministic approach, whereby a set of parameters produce a singular output, is erroneous (Abbaspour, 2015).

This study, therefore, implemented SWATCUP's SUFI2 evaluation procedure for the calibration of the UCRB model. SUFI2 used a stochastic approach to calibration, where the errors and uncertainties in modelling work are acknowledged, owing to ignorance of the processes occurring in the natural environment (Abbaspour, 2015). As such, parameters used in SUFI2 were expressed as ranges, accounting for all model uncertainties. Propagation of these uncertainties resulted in uncertainties concerning output variables, which SUFI2 expressed as

95% probability distributions and, thus, produced an envelope of model outputs referred to as 95% prediction uncertainty (95 PPU).

The parameters used for SUFI2's calibration procedure were delineated through SWATCUP's global sensitivity analysis. Sensitivity analysis is the process of determining the rate of change of model outputs with respect to parameter changes and is, therefore, crucial to identifying parameters and their precisions required for calibration (Moriasi *et al.*, 2007). SWATCUP's parameter sensitivities were determined by calculating the multiple regression system, shown in Equation 11, which regressed the parameters against a function of model accuracy to provide two statistics of parameter sensitivity, namely the t-stat value and the p-value (Abbaspour, 2015).

$$g = \alpha + \sum_{i=1}^{m} \beta_i b_i \tag{11}$$

The t-stat is defined as the coefficient of a parameter (β) divided by its standard error and measures the precision with which the regression coefficient is determined. The p-value is obtained by comparing a parameter's t-stat value with those in the Student's t-distribution table and assesses the null hypothesis that the coefficient is equal to zero. Resultantly, low p-values (< 0.05) indicated high parameter sensitivity as changes in parameter values were related to changes in model outputs, whereas, larger absolute values for t-stat indicated increased parameter sensitivity.

Calibration using SUFI2 necessitated the input of sensitive parameters and their ranges. SWATCUP enabled three parameter identifiers (absolute, relative, and replace) to be linked to each parameter during calibration. These parameter identifiers aimed to improve model calibration and better characterise the spatial heterogeneity of the basin by replacing the SWAT parameter value with another (replace), adding the selected value to the existing SWAT parameter (absolute), or multiplying the SWAT parameter by (1 + the selected value) (relative). SUFI2 then simulated different combinations of parameter values through iterations, decreasing the parameter ranges around the best result in each case. The best result in each iteration was determined using statistics developed by SWATCUP and general model performance measures, which assessed the accuracy of simulated streamflow compared to recorded data.

SWATCUP implemented two statistics, the p-factor and r-factor, to quantify the fit between the simulation results, expressed as 95 PPU, and the recorded data expressed as a single signal

(Abbaspour, 2015). The p-factor defined the percentage of observed data enveloped by modeling result, whereas the r-factor referred to the thickness of the 95 PPU envelope. As a result, larger p-factor and smaller r-factor values reflected a limited parameter range which was accurate compared to recorded data. Thus, sufficiently large p-factors (> 0.7) and small r-factors (~ 1) were used as the baseline of good model performance for the UCRB. In addition, SWATCUP used ten different model performance measures (objective functions) to assess the accuracy of simulations. However, only three of these measures were used to describe the accuracy of the UCRB model simulations, namely: the Nash-Sutcliffe efficiency (NSE), percent bias (PBIAS), and the coefficient of determination (R^2).

The coefficient of determination is used in conjunction with Pearson's correlation coefficient (*r*) (Equation 12) to describe the degree of collinearity between simulated and measured data (Moriasi *et al.*, 2007; Moriasi *et al.*, 2015). The correlation coefficient indicates the extent of the linear relationship between recorded and simulated data and ranges from -1 to 1. Therefore, $r = 0$ is indicative of no linear relationship, whereas $r = 1$ and $r = -1$ indicate the ideal positive and negative linear relationship, respectively (Moriasi *et al.*, 2007).

$$r = \frac{\sum_{i=1}^{n}(O_i - \bar{O})(P_i - \bar{P})}{\sqrt{\sum_{i=1}^{n}(O_i - \bar{O})^2}\sqrt{\sum_{i=1}^{n}(P_i - \bar{P})^2}} \tag{12}$$

Where O_i and P_i are the observed and simulated discharges, whereas $\bar{O}$ and $\bar{P}$ are the observed and simulated average discharge (denotation used for all subsequent model performance measure equations).

R^2 delineates the proportion of the variance in observed data explained by the model and ranges from 0 to 1 (Equation 13) (Moriasi *et al.*, 2007; Moriasi *et al.*, 2015). Higher values are indicative of less error variance and, therefore, are characteristic of superior model performance. R^2 values greater than 0.5 are considered of acceptable model performance (Santhi *et al.*, 2001; Van Liew *et al.*, 2003; Moriasi *et al.*, 2007).

$$R^2 = \left[\frac{\sum_{i=1}^{n}(O_i - \bar{O})(P_i - \bar{P})}{\sqrt{\sum_{i=1}^{n}(O_i - \bar{O})^2}\sqrt{\sum_{i=1}^{n}(P_i - \bar{P})^2}}\right]^2 \tag{13}$$

Krause *et al.* (2005) noted that regression graphs should always be used when reporting R^2 as only regression line gradients close to one and intercepts near zero are indicative of good model performance regarding R^2. The *r* and R^2 performance indicators are implemented extensively in hydrological modeling (Moriasi *et al.*, 2015) and thus serve as a standard for model performance evaluation. Nevertheless, Legates and McCabe (1999) and Krause *et al.* (2005) noted that *r* and R^2 are overly sensitive to extremely high values (outliers) and are insensitive to additive and proportional differences between simulated and recorded data.

The percent bias measures the average tendency of simulated data to be larger or smaller than the observed data (Gupta *et al.*, 1999; Moriasi *et al.*, 2007; Moriasi *et al.*, 2015). PBIAS is expressed as a percentage with an optimal value of 0.0 and a range between -∞ and ∞ (Equation 14). Therefore, low magnitude values are representative of accurate model simulation, whereas, negative values indicate model overestimation bias, and positive values characterise model underestimation bias (Gupta *et al.*, 1999). Resultantly, PBIAS values with a magnitude of ≤15% from the optimal value are indicative of satisfactory model performance (Moriasi *et al.*, 2015). In addition, PBIAS provides a benchmark for model evaluation as it is robust and frequently used due to its usefulness for continuous long-term simulations and its indication of poor model performance (Gupta *et al.*, 1999). However, Moriasi *et al.* (2015) suggested that PBIAS can provide a deceiving rating of model performance if a model overestimates as much as it underestimates, leading to a satisfactory PBIAS result (proximal to 0.0) from an unsatisfactory simulation.

$$PBIAS = \frac{\sum_{i=1}^{n}(O_i - P_i)}{\sum_{i=1}^{n} O_i} * 100 \quad (14)$$

NSE is a normalised statistic developed by Nash and Sutcliffe (1970) that determines the relative magnitude of residual variance compared to observed data variance (Equation 15). As such, NSE indicates how well the plot of recorded versus simulated data fits the 1:1 line and ranges between -∞ and 1, with 1 being the optimal value (Moriasi *et al.*, 2007). NSE values between 0 and 1 are regarded as acceptable model performance levels, whereas negative values are considered as unacceptable model performance as the observed data mean is a preferable predictor compared to the simulated value (Moriasi *et al.*, 2007). Notably, NSE is recognised to have numerous disadvantages and limitations, such as its inability to identify model bias, its deficiency regarding single-event simulations (Moriasi *et al.*, 2015), as well as its over-sensitivity to outliers (Krause *et al.*, 2005). Despite this, NSE is used extensively due to its

usefulness in continuous long-term simulations and its ability to evaluate model accuracy using different output variables (e.g., streamflow, sediment, and nutrients) (Moriasi *et al.*, 2015).

$$NSE = 1 - \frac{\sum_{i=1}^{n}(O_i - P_i)^2}{\sum_{i=1}^{n}(O_i - \bar{O})^2} \quad (15)$$

The model performance measures used to characterise the accuracy of SWAT's UCRB simulations were identified to each have multiple shortcomings. However, these performance measures collectively produce a well-rounded characterisation of model accuracy as it compensated for the failings of individual performance measures. Subsequently, Moriasi *et al.* (2015) developed evaluation criteria for the three objective functions to better describe model simulation accuracy (Table 3.8).

Table 3.8: The performance criteria for the objective functions used to analyse the accuracy of UCRB simulation (adapted from Moriasi et al., 2015)

	Performance Evaluation Criteria			
Performance Measure	**Very Good**	**Good**	**Satisfactory**	**Not Satisfactory**
R^2	$R^2 > 0.85$	$0.75 < R^2 \leq 0.85$	$0.60 < R^2 \leq 0.75$	$R^2 \leq 0.60$
PBIAS (%)	PBIAS < ±5	±5 ≤ PBIAS < ±10	±10 ≤ PBIAS < ±15	PBIAS ≥ ±15
NSE	NSE > 0.80	0.70 < NSE ≤ 0.80	0.50 < NSE ≤ 0.70	NSE ≤ 0.50

The objective functions used provided statistical performance measures for calibration accuracy; however, according to Moriasi *et al.* (2015), both graphical and statistical performance measures are crucial for strong model performance evaluation as graphical performance measures provide evidence as to where a model is performing inadequately. Therefore, this study implemented hydrographs as the graphical performance measure to assess model simulation accuracy. Hydrographs are time series plots of simulated and measured flow, which aid in the identification of model bias and the differences in timing and magnitude of peak flows (Moriasi *et al.*, 2007). Additionally, the integration of hydrographs with the selected objective functions were beneficial, as NSE is the best objective function for representing the overall fit of a hydrograph (Servat and Dezetter, 1991).

3.6 Validation

Validation is the process by which a calibrated model exhibits its capability of reproducing a set of observations or predicting future conditions without further adjustment of calibrated parameters (Zheng *et al.*, 2012). In other words, model validation is the process of depicting that a given model is able to generate sufficiently accurate simulations based on project goals (Refsgaard, 1997). Thus, validation involves running the model using parameters that were measured or determined during calibration (Moriasi *et al.*, 2007). Accordingly, the SUFI2 procedure was also used to validate the UCRB model. But it is to note that the validation period did not concur with the period of calibration to ensure that the parameters developed during calibration reflected a realistic basin response and did not only justify the basin response for the calibrated period. The accuracy of model streamflow simulations during the validation period were evaluated using the same graphical and statistical performance measures outlined during calibration.

CHAPTER 4: RESULTS

4.1 Initial Model

The initial model was run on a monthly basis to provide a discernible view of the influence of climate and human activity alterations on basin hydrology. The period selected for simulation aimed at describing the modern climate and land-uses affecting UCRB streamflow. Therefore, five equilibration years were used to enhance streamflow quantification, and the initial model simulated monthly average streamflow in the UCRB for 18 years, from 1 January 1998 to 31 December 2015. The accuracy of SWAT's initial streamflow predictions was evaluated compared to the six discharge stations using the objective functions highlighted during calibration.

A summary of the initial model's streamflow simulations in the UCRB sub-basins is shown in Table 4.1. These results revealed that the initial model had acceptable linear correlations with observed data in sub-basins 3, 13, 19, 26, and 29 (R^2 of 0.73, 0.68, 0.61, 0.54, and 0.63, respectively). However, further analysis of the regression graphs presented in Figure 4.1 indicated that the adequate R^2 obtained in sub-basins 3, 13, and 19 did not reflect an accurate linear correlation with measured streamflow due to the large intercepts of their trendlines. In addition, the regression graph of sub-basin 104 (Fig. 4.1f.) illustrated its unsatisfactory correlation with recorded data ($R^2 = 0.21$).

Table 4.1: The initial SWAT model simulation results evaluated in comparison to stream discharges recorded in the UCRB from 1998 to 2016

Sub-basin	Stream Gauge	NSE	PBIAS	R^2	Observed mean (m^3/s)	Simulated mean (m^3/s)	Observed σ (m^3/s)	Simulated σ (m^3/s)
3	A2H019	0.53	-37.20	0.73	9.87	15.72	15.84	17.73
13	A2H083	0.37	-32.28	0.68	9.19	13.57	11.08	13.44
19	A2H012	0.16	-24.24	0.61	12.63	16.67	8.39	10.46
26	A2H044	0.41	6.58	0.54	6.66	6.24	4.69	5.12
29	A2H045	0.16	-27.64	0.63	1.82	2.52	1.36	1.71
104	A2H034	-3.47	-37.41	0.21	0.47	0.75	0.24	0.48
Average		**-0.31**	**-25.37**	**0.57**	**6.77**	**9.25**	**6.94**	**8.16**

σ = Standard Deviation

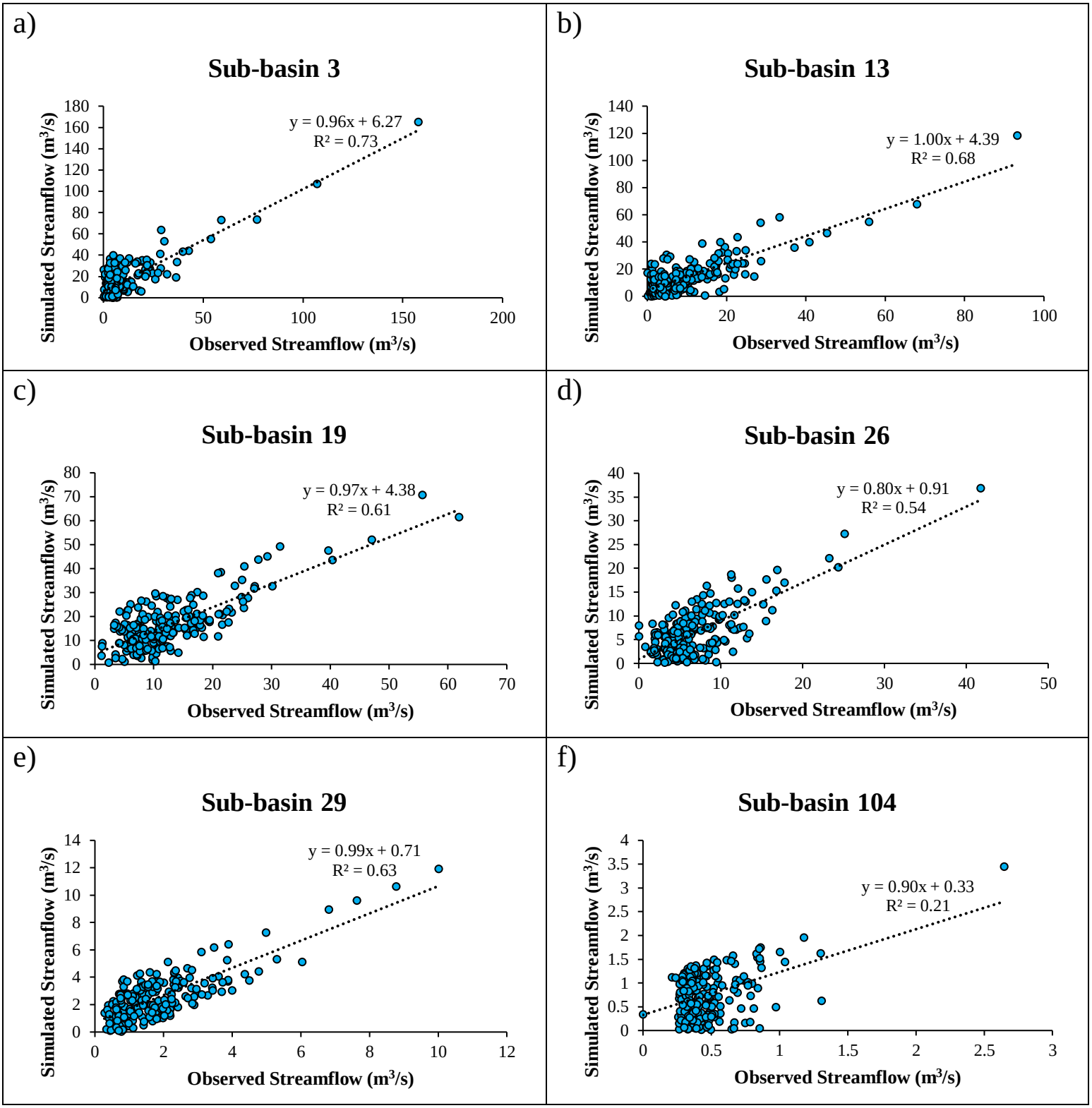


Figure 4.1a-f: Regression graphs showing the linear relationships between the measured and simulated streamflow in each of the sub-basins used for analysis (1998-2016)

PBIAS results highlighted that the initial model had the inherent tendency of overestimating streamflow in sub-basins 3, 13, 19, 29, and 104, generating PBIAS values of -37.20, -32.28, -24.24, -27.64, and -37.41, respectively. Conversely, the 6.58 PBIAS value in sub-basin 26 indicated model streamflow underestimation. NSE analysis expressed that the initial model's streamflow predictions were more accurate than the recorded data mean in sub-basins 3, 13, 19, 26, and 29, owing to positive NSE values of 0.53, 0.37, 0.16, 0.41, and 0.16, respectively. However, the -3.47 NSE value obtained in sub-basin 104 suggests that its simulation precision was inferior to the measured data average.

As emphasised by the objective functions, the discrepancies between the simulated and observed streamflow in each sub-basin were substantiated by their streamflow hydrographs, shown in Figures 4.2-4.7. These hydrographs depict that streamflow simulation fluctuated considerably compared to the recorded streamflow in each sub-basin. Moreover, the initial model was observed to overestimate peak flows in all sub-basins.

The hydrographs and model performance measures indicated that streamflow predictions from the initial model were not precise with measured data. Therefore, further calibration and validation of the model were necessary to improve simulation accuracy. It is to note that the acceptable NSE and R^2 results, obtained for most sub-basins, deemed the initial model a suitable basis for the calibration process.

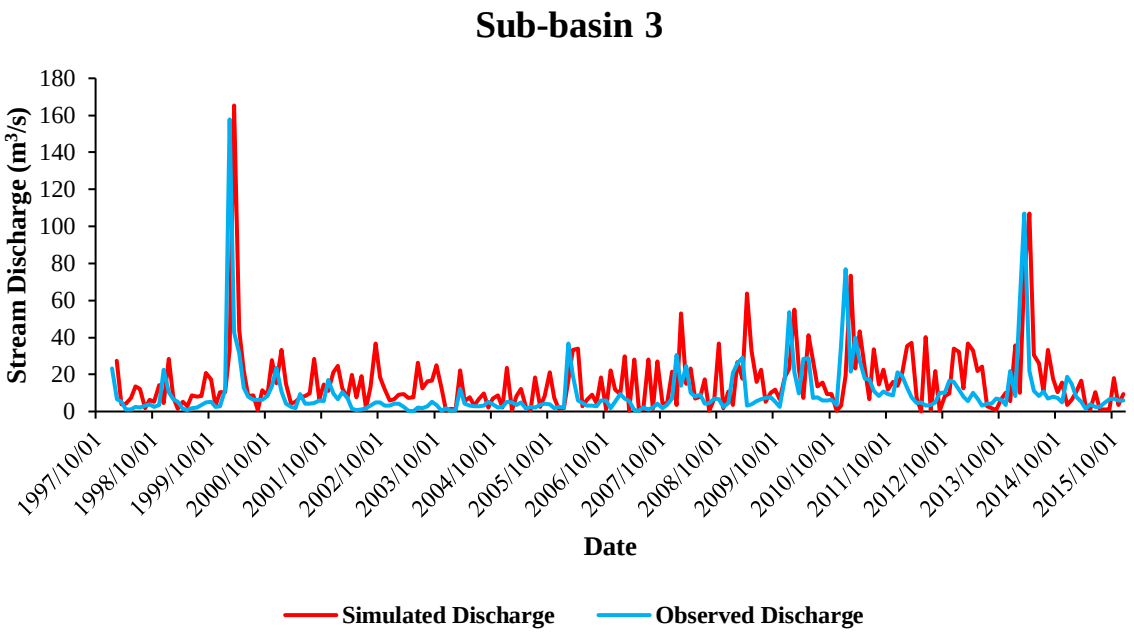


Figure 4.2: The initial model results in sub-basin 3 compared to the observed data at discharge station A2H019 (1998-2016)

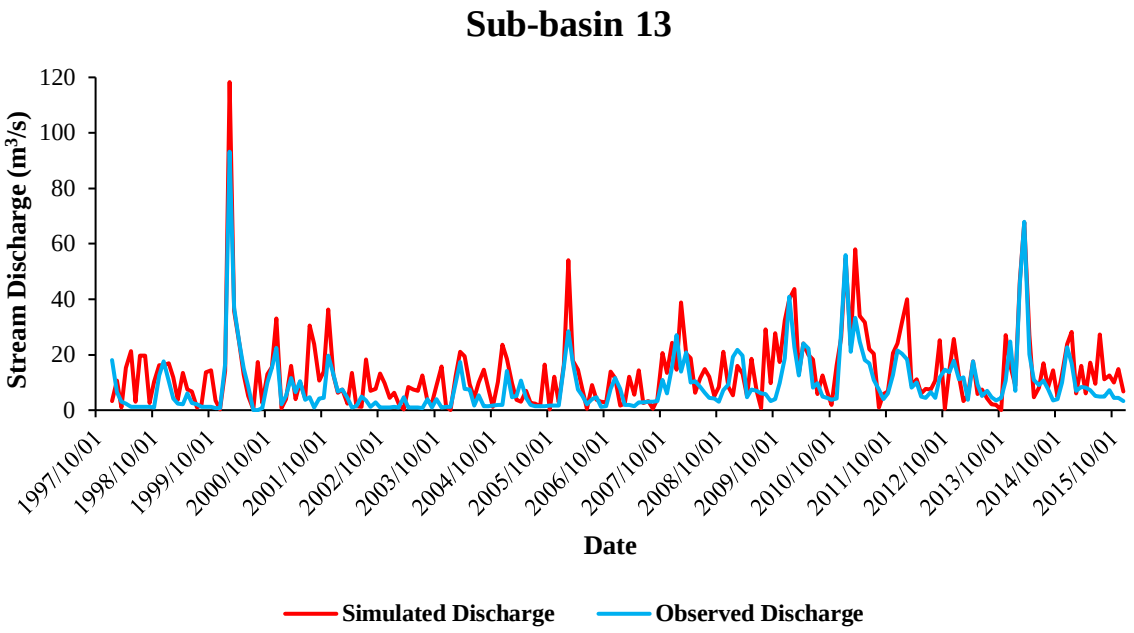


Figure 4.3: The hydrograph showing the differences in streamflow from the simulations in sub-basin 13 compared to the measured streamflow at recording station A2H083 (1998-2016)

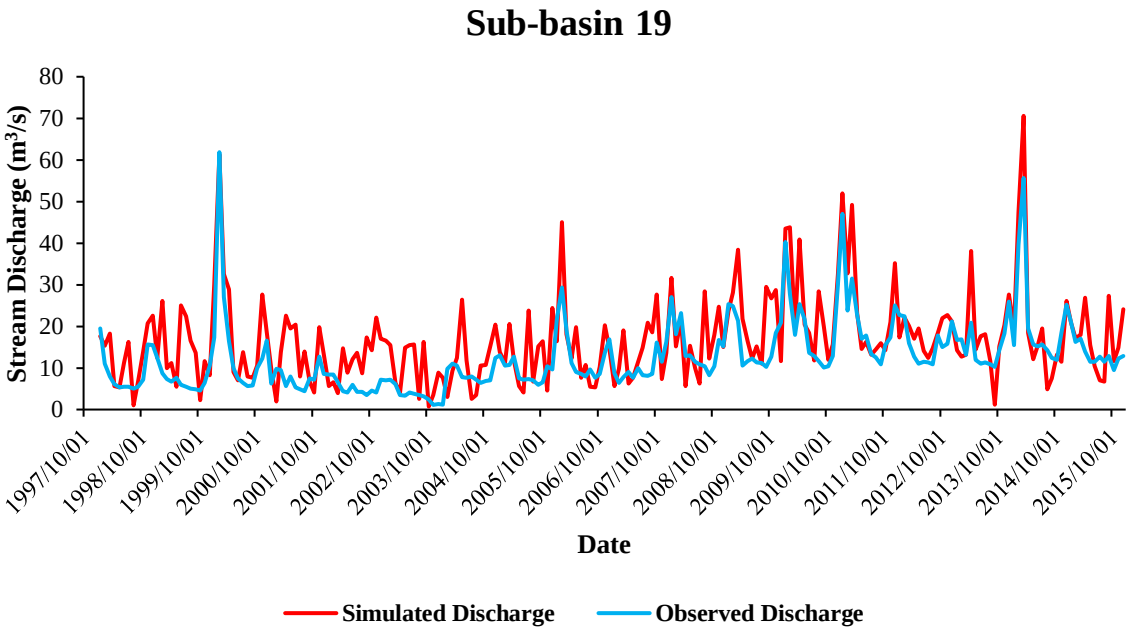


Figure 4.4: The initial model streamflow simulations in sub-basin 19 compared to the observed streamflow at the A2H012 discharge station from 1998 to 2016

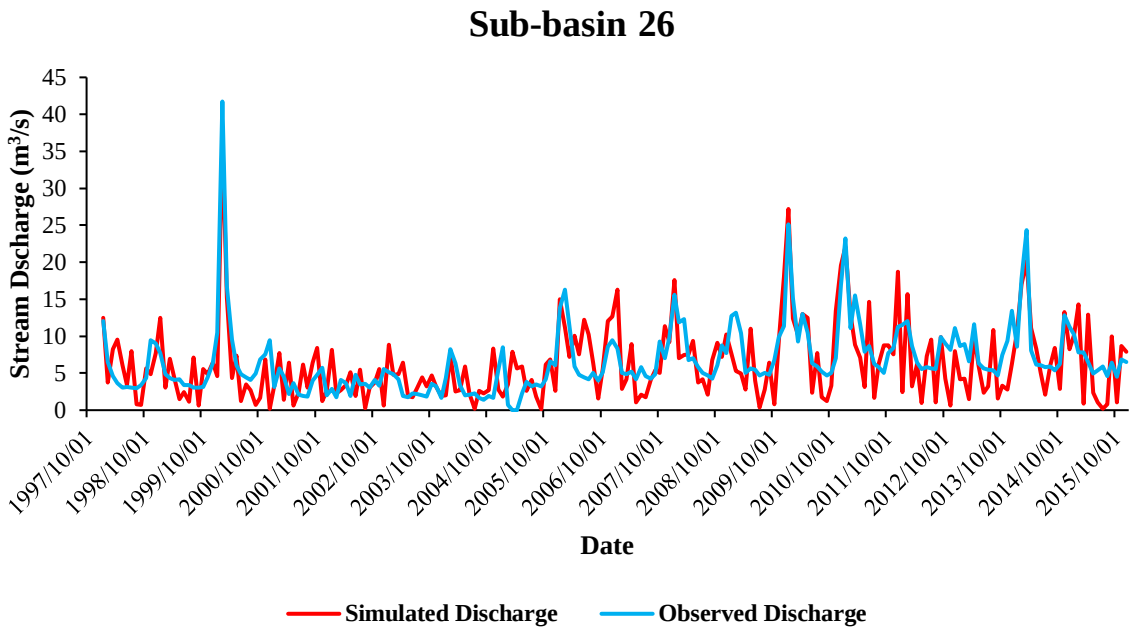


Figure 4.5: The variations in monthly streamflow between the initial simulations in sub-basin 26 and the recorded discharge at the A2H044 station (1998-2016)

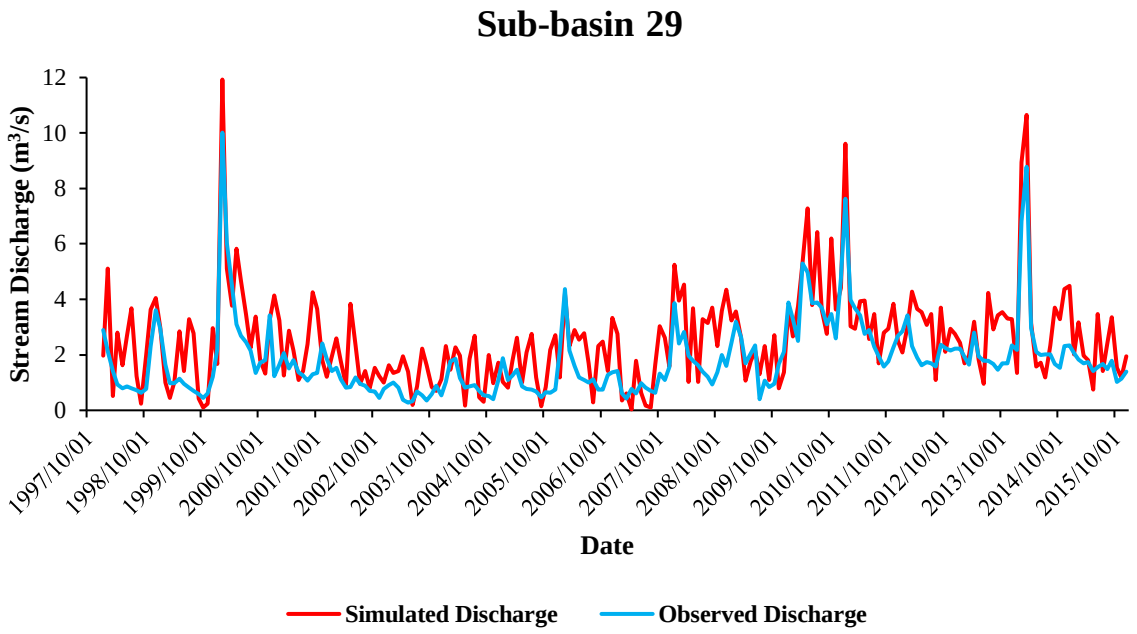


Figure 4.6: The streamflow hydrograph showing the discrepancies between the measured data at the A2H045 discharge station and SWAT's initial simulations in sub-basin 29 (1998-2016)

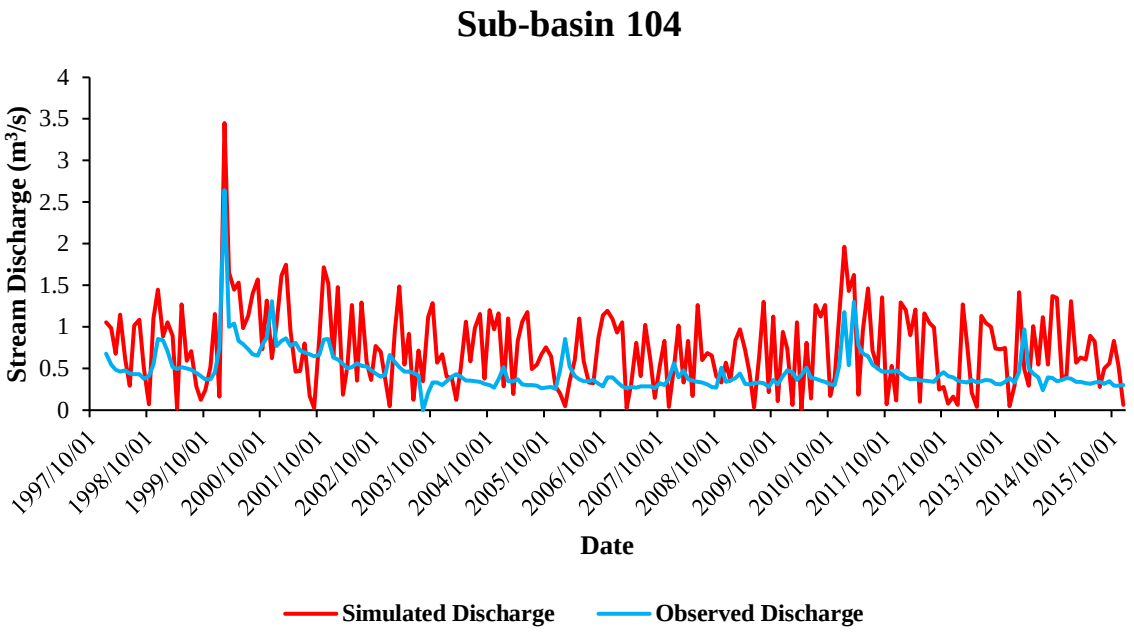


Figure 4.7: Streamflow hydrograph showing the differences between streamflow simulations in sub-basin 104 compared to those measured at the A2H034 recording station (1998-2016)

4.2 Calibration

4.2.1 Parameter Sensitivity

A total of 18 parameters were identified for sensitivity analysis based on the findings of previous SWAT studies performed in South Africa (Gyamfi *et al.*, 2016; Ngubane, 2017; Thavhana *et al.*, 2018; Mengistu *et al.*, 2019) and successful calibrations across Europe (Abbaspour *et al.*, 2015) (Table 4.2). The parameters selected covered several aspects governing basin hydrology, such as basin properties (FFCB, SURLAG), HRU properties (SLSUBBSN, OV_N, ESCO, EPCO), soil properties (SOL_K, SOL_AWC), groundwater flow (ALPHA_BF, GW_DELAY, GW_REVAP, GWQMN, REVAPMN, SHALLST), main channel flow (CH_K2, CH_N2, ALPHA_BNK), and management practices (CN2). Global sensitivity analysis results, shown in Table 4.3 and Appendix B- Figure B.1, indicated that thirteen parameters were sensitive to streamflow within the UCRB ($P < 0.05$). Moreover, five parameters (ALPHA_BF, SURLAG, GWQMN, GW_REVAP, ESCO) were regarded as less sensitive ($P > 0.05$) and were removed from consideration for calibration.

Table 4.2: Parameters considered for sensitivity analysis in SWATCUP

Parameter	Description
ALPHA_BF	Baseflow alpha factor (1/days)
GW_DELAY	Groundwater delay time (days)
GW_REVAP	Groundwater percolation coefficient
GWQMN	Depth of water in the shallow aquifer threshold required for return flow to occur (mm H_2O)
REVAPM	Threshold depth of water in the shallow aquifer for percolation into the deep aquifer to occur (mm H_2O)
SHALLST	Initial depth of water in the shallow aquifer (mm H_2O)
SLSUBBSN	Average slope length (m)
OV_N	Manning's "n" value for overland flow
ESCO	Soil evaporation compensation factor
EPCO	Plant uptake compensation factor
SOL_K	Saturated hydraulic conductivity of the soil (mm/hr)
SOL_AWC	Available water capacity of the soil layer (mm H_2O/mm soil)
CH_K2	Effective hydraulic conductivity in main the main channel (mm/hr)
CH_N2	Manning's "n" value for the main channel
ALPHA_BNK	Baseflow alpha factor for bank storage (days)
FFCB	Initial soil water storage as a fraction of field capacity water content
SURLAG	Surface runoff lag coefficient
CN2	Initial SCS runoff curve number

Table 4.3: The sensitivity ranking, p-value- and t-stat value of the different parameters considered for calibration

Parameter Name	Sensitivity Ranking	P-value	T-stat
ALPHA_BNK	**1**	0.00000	-23.00929
CN2	**2**	0.00000	-15.51008
OV_N	**3**	0.00000	11.69576
SOL_K	**4**	0.00001	-5.81077
CH_K2	**5**	0.00003	5.64016
FFCB	**6**	0.00008	-5.44854
SLSUBBSN	**7**	0.00014	3.84061
CH_N2	**8**	0.00470	2.84006
REVAPMN	**9**	0.01834	2.36681
SHALLST	**10**	0.02731	-2.21378
EPCO	**11**	0.05061	-1.95970
GW_DELAY	**12**	0.05374	-1.93368
SOL_AWC	**13**	0.08024	1.75301
ESCO	**14**	0.12933	-1.51937
GW_REVAP	**15**	0.24461	-1.16496
GWQMN	**16**	0.25085	1.14968
SURLAG	**17**	0.34024	-0.95463
ALPHA_BF	**18**	0.38986	-0.86066

The calibration period began on the first month of SWAT streamflow simulation. However, the 3 to 5 year calibration period recommended by Moriasi *et al.* (2007) was not implemented for the UCRB model as Moriasi *et al.* (2015) emphasised that the objective functions used for precision analysis tend to vary considerably depending on the prevalence of wet and dry years. As a result, the calibration period was extended to include both wet and dry years for further characterisation of the UCRB's response to water availability increases and decreases, respectively. Therefore, the model was calibrated against 13 years of monthly recorded data, beginning 1 January 1998 to 31 December 2009, using the multi-site approach to calibration.

4.2.2 Calibrated Parameters

The most sensitive parameters to streamflow in the UCRB (Table 4.3) were initially input to SUFI2 with a broad range for calibration. Performing nine calibration iterations, each containing 500 simulations, subsequently reduced parameter limits and provided a set of parameter ranges (Table 4.4) that achieved the best efficiency between observed and simulated streamflow within the UCRB. These parameter sensitivities were supported by a sensitivity analysis graph (Appendix B- Figure B.2) and scatter plots generated by SWATCUP indicating the change in NSE value with changing parameter values (Appendix B- Figure B.3).

Table 4.4: Sensitivity ranking of the parameters used in calibration, including their identifiers, maximum, minimum, and fitted values that achieved the best calibration result

	Parameter	T-stat	P-value	Parameter identifier	Minimum	Maximum	Fitted Value
1	**SOL_K**	17.9368	0.0000	Relative	0.887951	1.43648	**0.923947**
2	**CN2**	9.5273	0.0000	Relative	-0.177476	-0.013154	**0.113360**
3	**SOL_AWC**	3.1703	0.0016	Relative	0.627981	1.069515	**0.927783**
4	**OV_N**	2.7404	0.0064	Replace	0.088593	0.264253	**0.236674**
5	**ALPHA_BNK**	1.8559	0.0641	Replace	0.766267	1.000000	**0.986095**
6	**CH_N2**	1.6357	0.1026	Replace	0.400019	0.500233	**0.429582**
7	**FFCB**	-1.4084	0.1596	Replace	0.520373	0.879171	**0.633394**
8	**GW_DELAY**	-1.2740	0.2033	Replace	5464.796387	7703.459473	**5511.808105**
9	**CH_K2**	0.7488	0.4543	Replace	0.000000	17.888680	**3.738734**
10	**SLSUBBSN**	-0.6298	0.5291	Replace	31.843937	43.454220	**37.474922**
11	**SHALLST**	-0.3402	0.7339	Replace	5168.109375	26675.406250	**11125.630859**
12	**REVAPMN**	0.1544	0.8774	Replace	12174.837891	16815.298828	**16560.074219**
13	**EPCO**	0.1263	0.8996	Replace	0.809426	0.920590	**0.851779**

Parameter sensitivity statistics revealed that the soil saturated hydraulic conductivity (SOL_K) and initial SCS runoff curve number (CN2) were most sensitive to streamflow in the UCRB

during the calibration period. In comparison, the soil available water capacity (SOL_AWC) and Manning's 'n' value for overland flow (OV_N) were marginally less sensitive. The remaining parameters had inferior streamflow sensitivities in the UCRB during calibration; however, these parameters were still necessary to affect other parameters and achieve the best calibration result.

4.2.3 Model Performance

The calibrated parameter ranges produced an average r-factor of 1.08 (Table 4.5) for the calibration period, characteristic of a small parameter range. P-factor values of 0.78, 0.72, 0.71, 0.73, 0.68, and 0.62 in sub-basins 3, 13, 19, 26, 29 and 104, respectively, indicated good model performance in sub-basins 3, 13, 19, and 26. However, sub-basins 29 and 104 generated p-factor values below the threshold of good model performance. Overall, the model produced an average p-factor of 0.71 for the calibration period, which indicated that SUFI2's uncertainty enveloped 71% of recorded data on average, descriptive of good model simulation.

Table 4.5: The calibration results showing the accuracy of simulation compared to recorded data using appropriate model performance indicators

Sub-basin	Stream Gauge	p-factor	r-factor	NSE	PBIAS	R^2	Observed mean (m^3/s)	Simulated mean (m^3/s)	Observed σ (m^3/s)	Simulated σ (m^3/s)
3	A2H019	0.78	1.02	0.86	-12.49	0.89	7.63	8.85	14.59	15.33
13	A2H083	0.72	1.13	0.77	-16.06	0.80	7.07	8.42	9.90	8.22
19	A2H012	0.71	1.07	0.69	-11.21	0.78	10.05	11.32	6.98	7.69
26	A2H044	0.73	0.94	0.71	4.91	0.77	5.57	5.31	4.44	4.95
29	A2H045	0.68	0.98	0.48	-25.97	0.71	1.44	1.94	1.16	1.20
104	A2H034	0.62	1.32	-1.13	-22.60	0.39	0.49	0.63	0.27	0.47
Average		**0.71**	**1.08**	**0.40**	**-13.90**	**0.72**	**5.37**	**6.08**	**6.22**	**6.31**

σ = Standard Deviation

Analysis of the precision of calibration using the objective functions showed that the model simulated an R^2 of 0.89, 0.80, 0.78, 0.77, 0.71, and 0.39 in sub-basins 3, 13, 19, 26, 29, and 104, respectively. It is thus deduced that sub-basin 3 was characteristic of very good model performance; sub-basins 13, 19, and 26 delineated good model performance; sub-basin 29 described satisfactory model performance; and sub-basin 104 showed unsatisfactory performance. Resultantly, the regression graphs for each sub-basin, shown in Figure 4.8, highlight that model calibration improved the linear relationship between simulated and observed streamflow in comparison to the initial model. Moreover, the average R^2 indicated

that the simulated streamflow variance explained 72% of the observed streamflow variance during calibration, descriptive of satisfactory accordance with measured data.

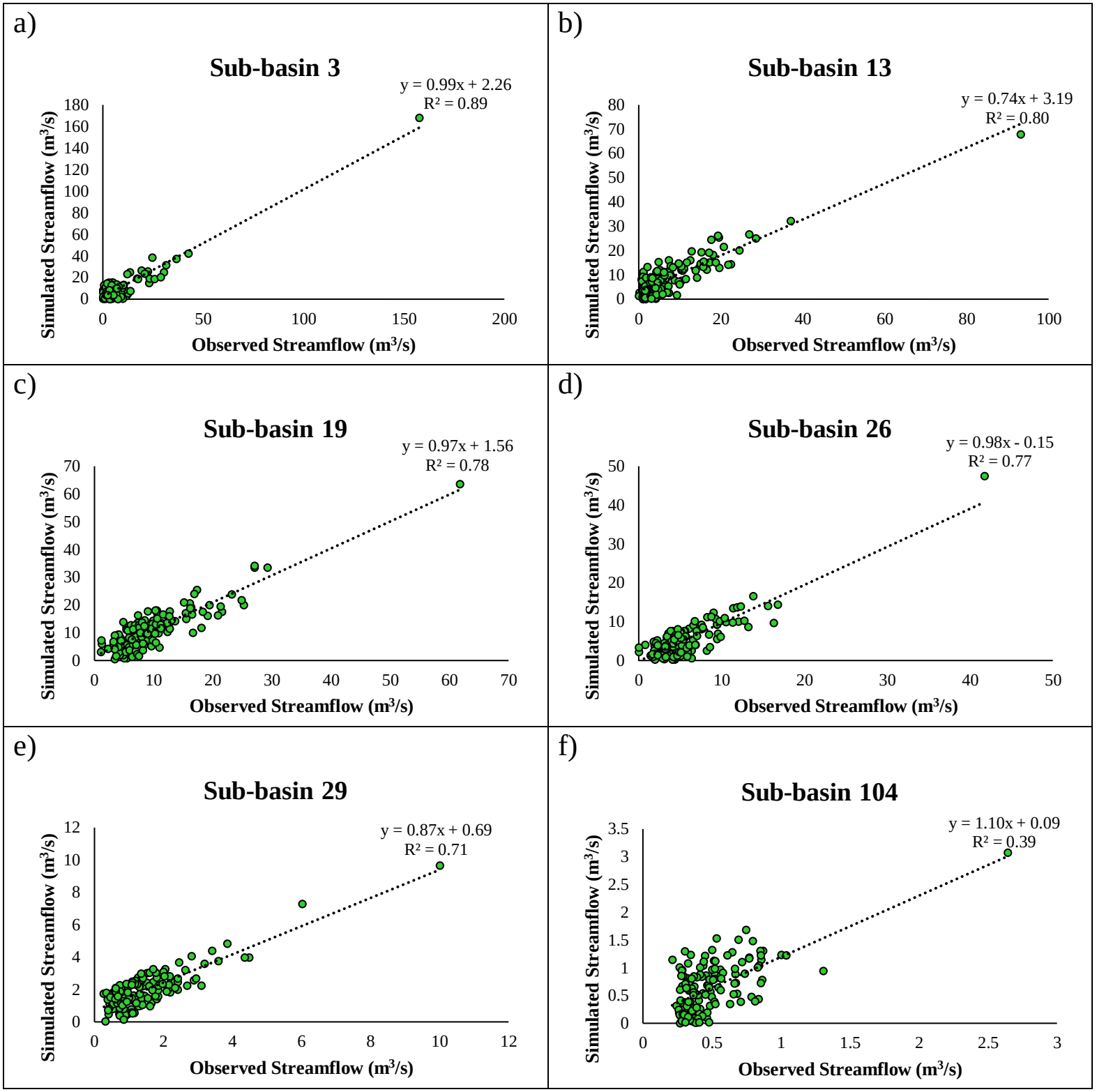


Figure 4.8a-f: The recession graphs showing the linear relationship between simulated and recorded streamflow for the period of calibration (1998-2010)

The average PBIAS result of -13.90 indicated satisfactory model overestimation during calibration. This resulted from PBIAS values of -12.49, -16.06, -11.21, 4.91, -25.97, and -22.60 in sub-basins 3, 13, 19, 26, 29, and 104, respectively. As such, sub-basins 3, 19, and 26 produced satisfactory simulations for the calibration period, whereas sub-basin 13, 29, and 104 overestimated streamflow unsatisfactorily.

NSE results expressed satisfactory model simulation in sub-basins 3, 13, 19, and 26, attributed to NSE values of 0.86, 0.77, 0.69, and 0.71, respectively. In contrast, sub-basins 29 and 104 simulated streamflow to an unsatisfactory standard, owing to NSE values of 0.48 and -1.13 (Table 4.5).

The calibration hydrographs are shown in Figures 4.9-4.14 and illustrate the improved objective function performance during calibration compared to the initial simulations. All hydrographs portray that model calibration decreased the simulated streamflow fluctuations from the initial model and reduced the discrepancies between simulated and measured streamflow. Furthermore, all hydrographs exhibited decreases concerning the overestimation of peak flows and depicted consistency regarding peak flow simulations with recorded data.

Given the satisfactory simulations across all objective functions in sub-basins 3, 13, 19, and 26, and the uniformity of peak flow simulation with observed data in all sub-basins, the calibration process was determined to improve streamflow precision with sufficient accuracy for validation.

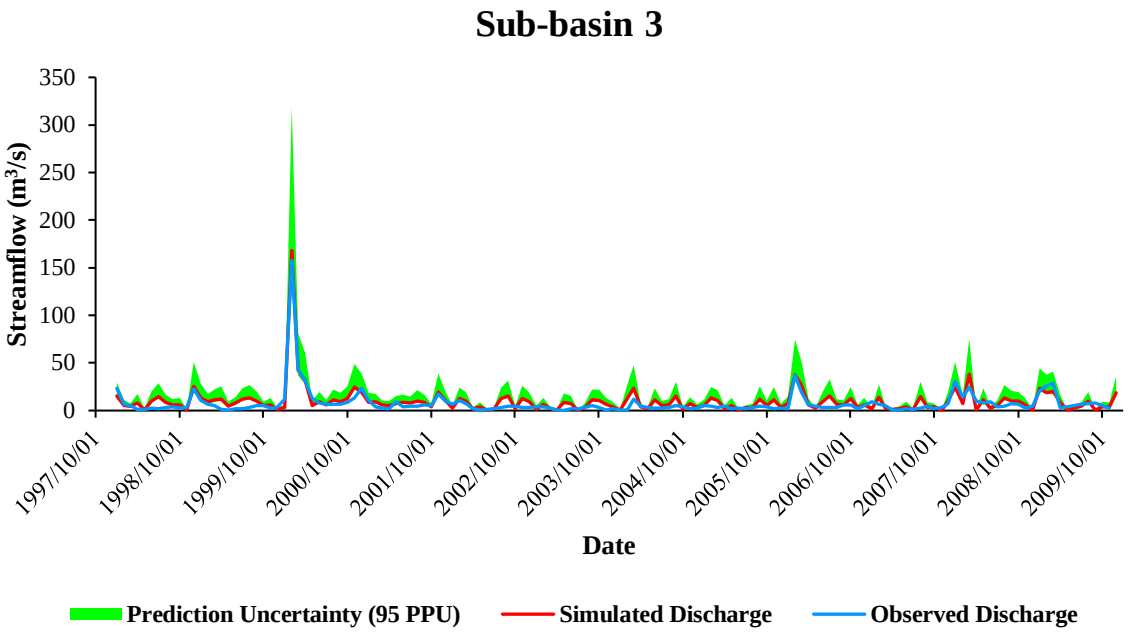


Figure 4.9: The calibration hydrograph at discharge station A2H019 from 1998 to 2010

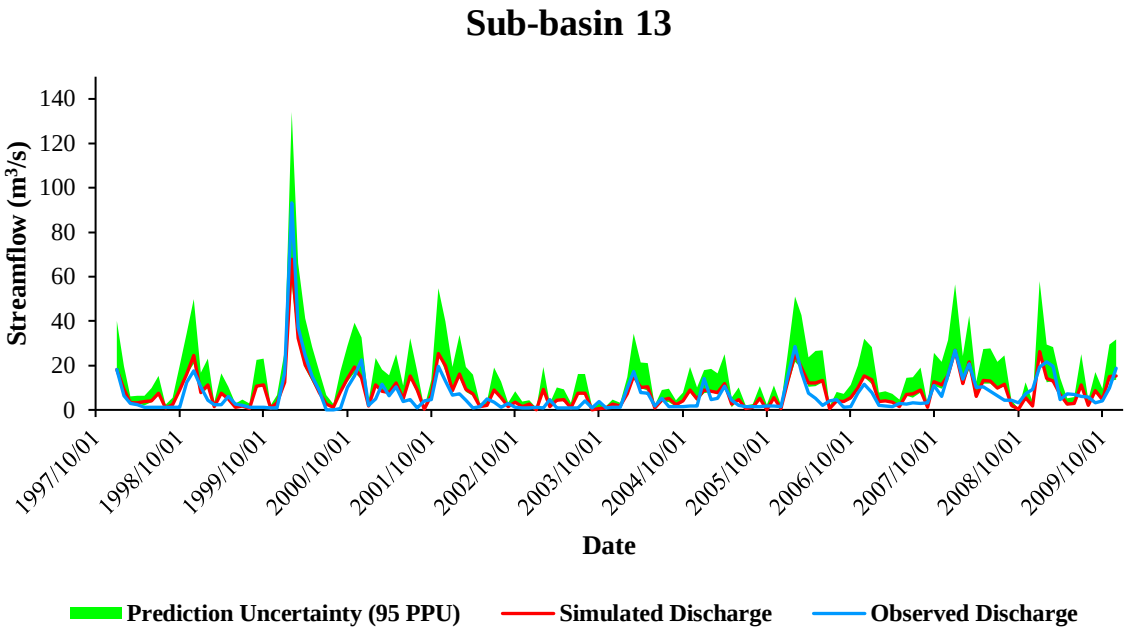


Figure 4.10: The simulated and observed streamflow hydrograph for discharge station A2H083 during the calibration period (1998-2010)

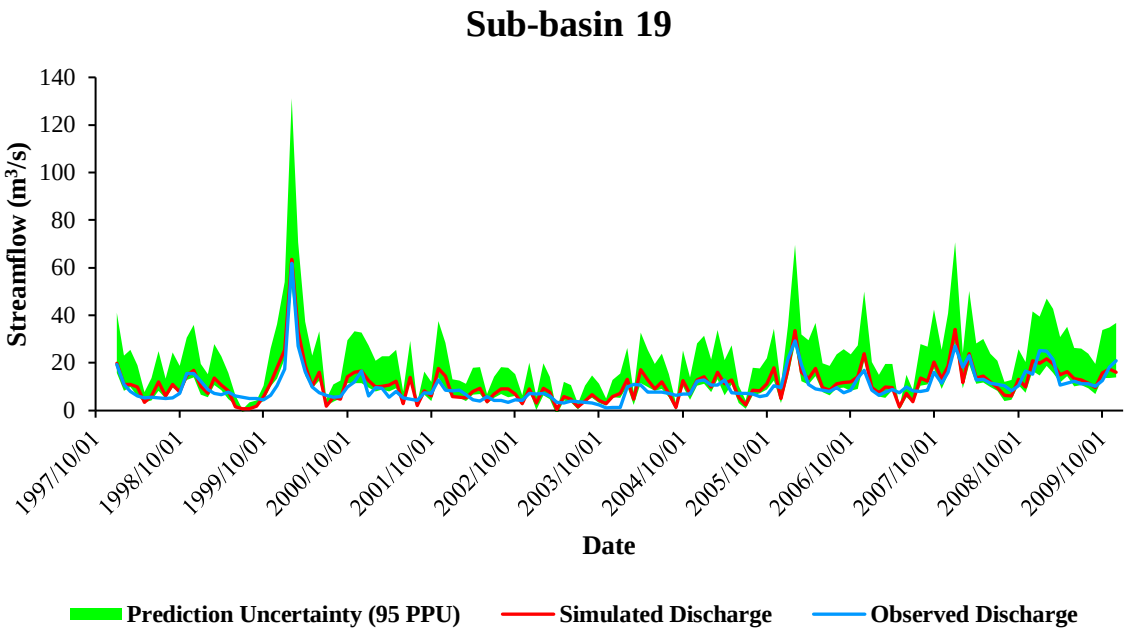


Figure 4.11: The simulated and measured streamflow at the A2H012 discharge station for the calibration period (1998-2010)

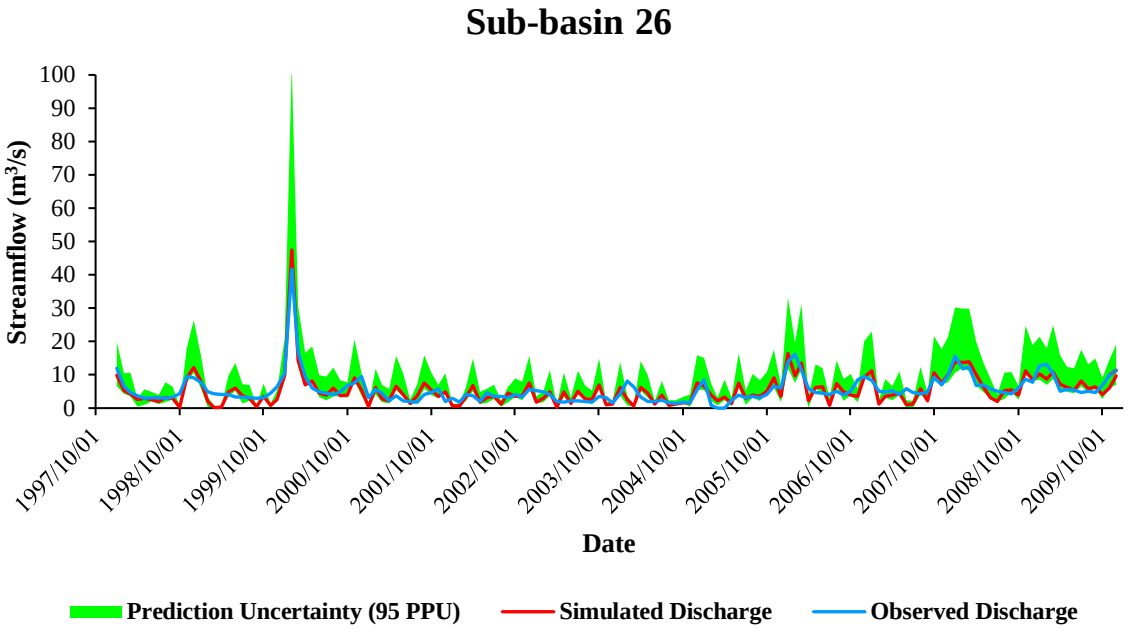


Figure 4.12: The SWAT simulated and recorded streamflow at the A2H044 discharge station for the calibration period (1998-2010)

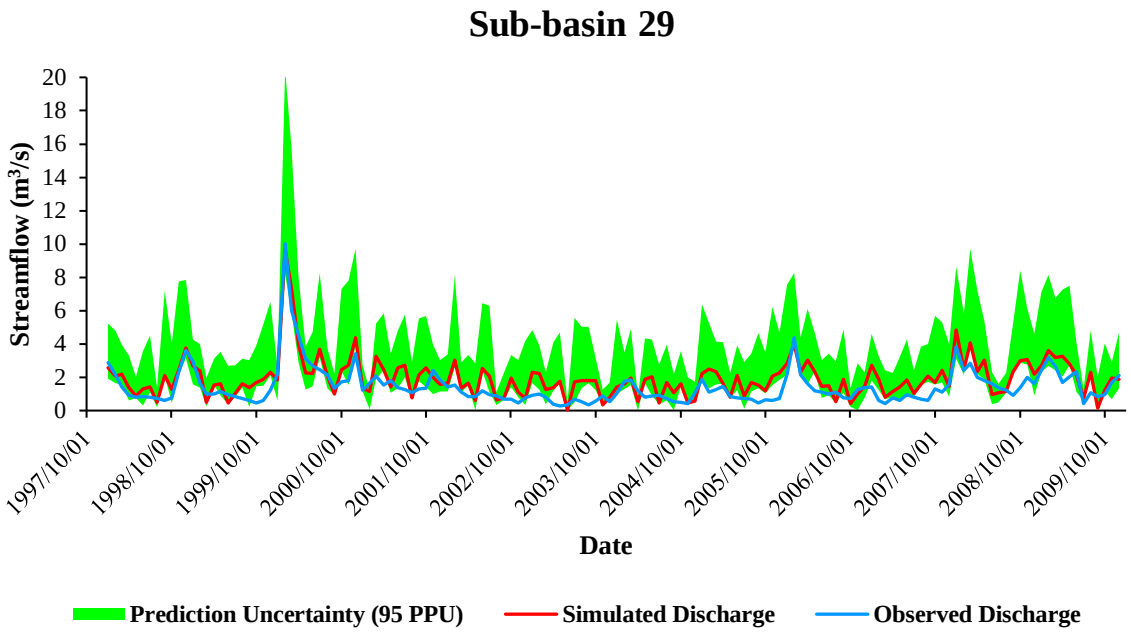


Figure 4.13: The observed vs simulated streamflow at the UCRB's A2H045 gauging station for the 13-year calibration period

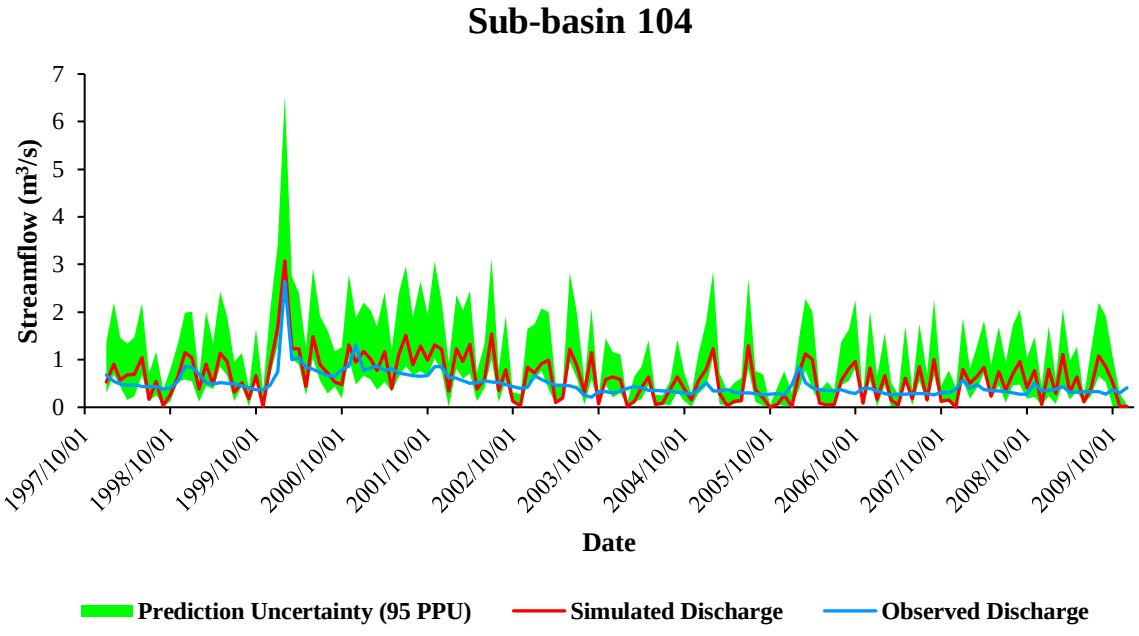


Figure 4.14: The hydrograph comparing the SWAT simulated vs recorded streamflow at the A2H034 discharge station (1998-2010)

4.3 Validation

Validation was used to verify that the calibrated model accurately simulated the UCRB's response to streamflow and, therefore, the parameter ranges, and number of simulations used for validation corresponded with calibration. In contrast, the validation period selected was dissimilar to calibration and was specified to confirm basin response to modern climate and land-use practices occurring in the UCRB. The results from the model validation that was run for six years from 1 January 2010 to 31 December 2015 are shown in Table 4.6.

Table 4.6: The validation results in each sub-basin showing the accuracy of simulation against recorded streamflow using objective functions

Sub-basin	Stream Gauge	p-factor	r-factor	NSE	PBIAS	R^2	Observed mean (m^3/s)	Simulated mean (m^3/s)	Observed σ (m^3/s)	Simulated σ (m^3/s)
3	A2H019	0.74	1.06	0.85	-14.56	0.78	15.14	16.79	18.49	20.05
13	A2H083	0.68	1.19	0.73	-15.26	0.76	13.43	15.85	12.13	12.19
19	A2H012	0.69	1.13	0.70	-12.09	0.63	17.18	19.26	8.31	15.63
26	A2H044	0.67	0.92	0.63	6.49	0.70	8.83	8.29	4.46	5.11
29	A2H045	0.65	1.01	0.39	-22.90	0.74	2.59	3.37	1.42	1.59
104	A2H034	0.57	1.28	-4.56	-23.81	0.16	0.43	0.56	0.18	0.44
Average		**0.67**	**1.10**	**-0.21**	**-13.69**	**0.63**	**9.60**	**10.69**	**7.50**	**9.17**

σ = Standard Deviation

These results indicated that model validation produced similar p-factors and r-factors to calibration. The average validation r-factor of 1.10 reflected the reduced parameter range developed during calibration. However, the p-factors of 0.74, 0.68, 0.69, 0.67, 0.65, and 0.57, simulated for sub-basins 3, 13, 19, 26, 29, and 104 respectively, showed a decrease in comparison to the calibration period. Consequently, the average p-factor for the sub-basins indicated that the parameter uncertainty encompassed 67% of observed data, which bordered the satisfactory performance threshold.

R^2 results indicated reductions in the linear correlation with measured data compared to the calibration period in sub-basins 3, 13, 19, 26, and 104, generating R^2 values of 0.78, 0.76, 0.63, 0.70, and 0.16, respectively. Notably, sub-basin 29 improved its linear correlation with observed data during validation (R^2 = 0.74). Sub-basins 3, 13, 19, 26, and 29 simulated streamflow to a satisfactory standard, whereas sub-basin 104 was unsatisfactory during validation. Resultantly, the average R^2 specified that the variance in validation streamflow explained 63% of recorded data variance, characteristic of satisfactory simulation.

PBIAS analysis showed that validation increased the magnitude of model bias in sub-basins 3, 19, 26, and 104, with values of -14.56, -12.09, 6.49, and -23.81. However, model validation reduced the bias of sub-basins 13 and 29 in relation to model calibration due to values of -15.26 and -22.90. Therefore, sub-basins 3, 19, and 26 were considered satisfactory concerning their simulation bias, sub-basin 19 bordered the PBIAS satisfactory threshold, and sub-basins 29 and 104 overestimated streamflow to an unsatisfactory standard during validation.

The NSE values exhibited decreases in all sub-basins during the validation period compared to calibration, except for sub-basin 19, which expressed a marginal increase from 0.69 to 0.70. NSE results of 0.85, 0.73, 0.63, 0.39, and -4.56, in sub-basins 3, 13, 26, 29, and 104, respectively, indicated that model validation simulated NSE to a satisfactory standard in sub-basins 3, 13, 19, and 26, whereas the remaining sub-basins 29 and 104 were unsatisfactory.

The validation hydrographs, shown in Figures 4.15-4.20, indicated similarities to the calibration hydrographs concerning their accordance with observed peak flows. The statistical and graphical performance measures showed that the calibrated model was verified to simulate monthly streamflow in the UCRB with adequate precision for assessment under climate and land-use changes. However, sub-basins 29 and 104 were omitted from evaluation as their PBIAS and NSE results during the calibration and validation periods indicated that their streamflow predictions were unreliable.

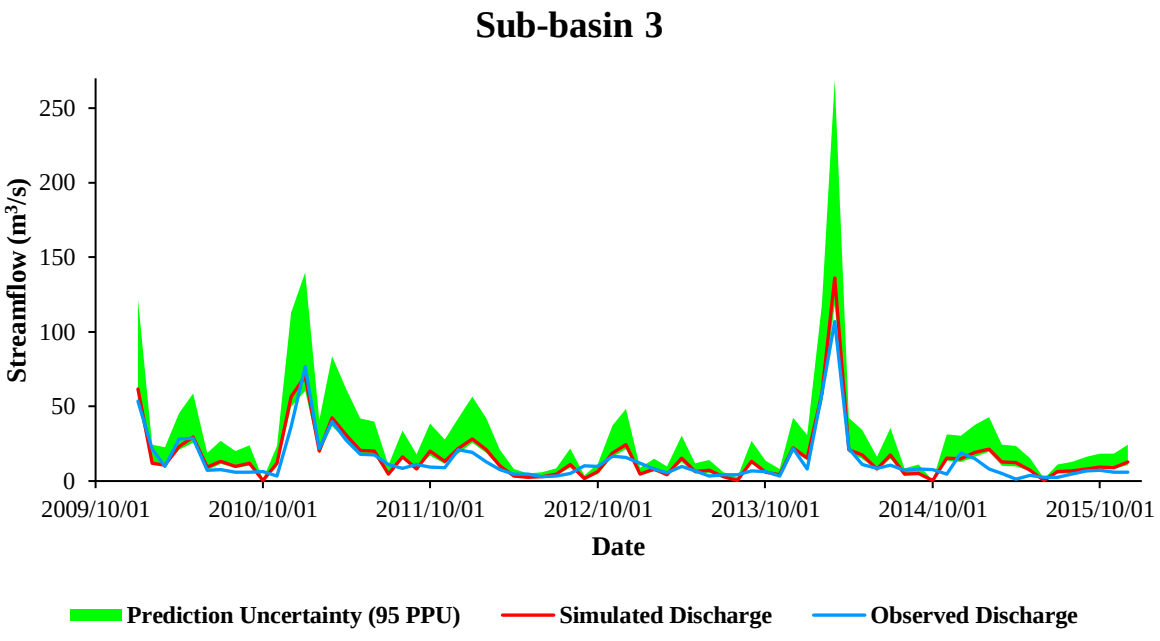


Figure 4.15: The SWAT simulated and recorded streamflow at the A2H019 discharge station for the validation period (2010-2016)

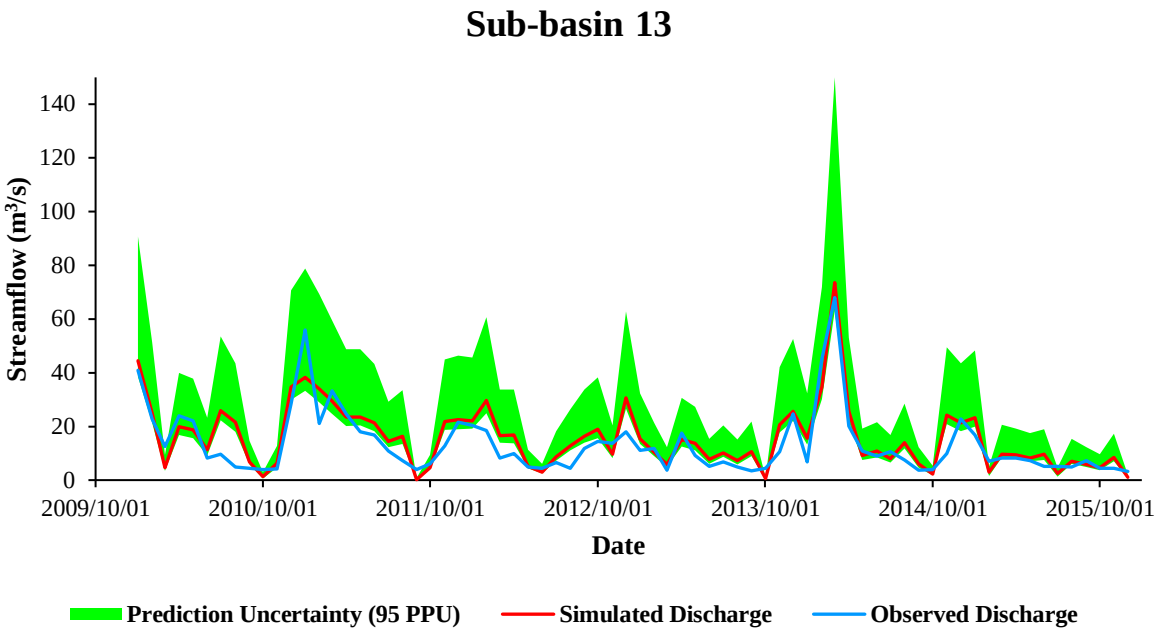


Figure 4.16: The hydrograph comparing the SWAT simulated vs recorded streamflow at the A2H083 discharge station (2010-2016)

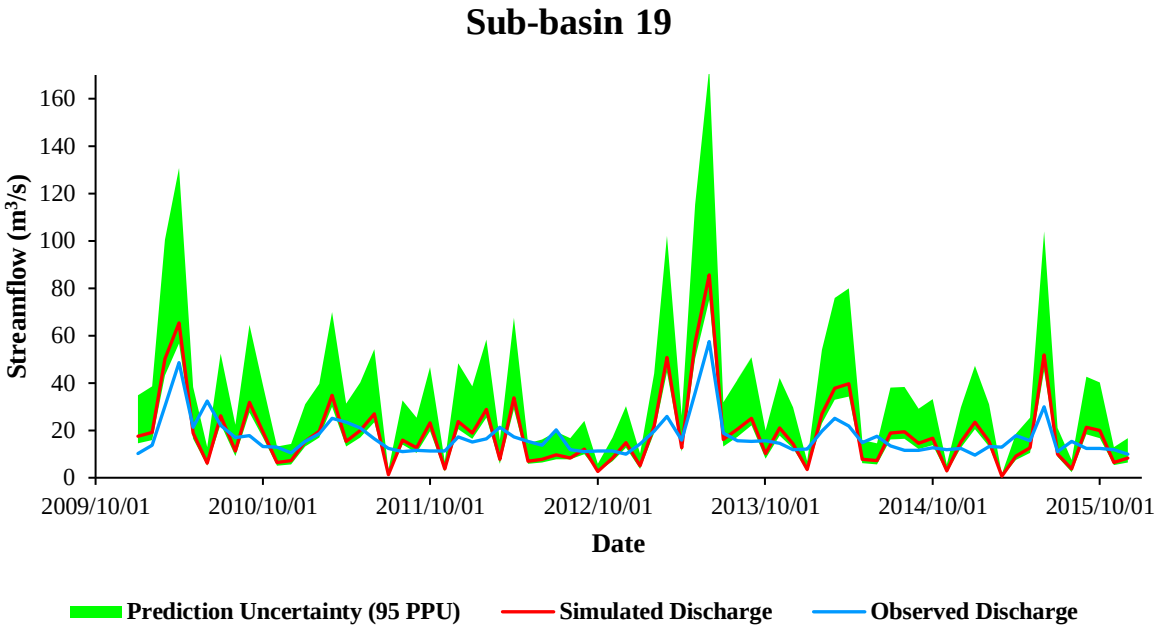


Figure 4.17: The validation hydrograph showing the SWAT simulated vs recorded streamflow at the A2H012 discharge station (2010-2016)

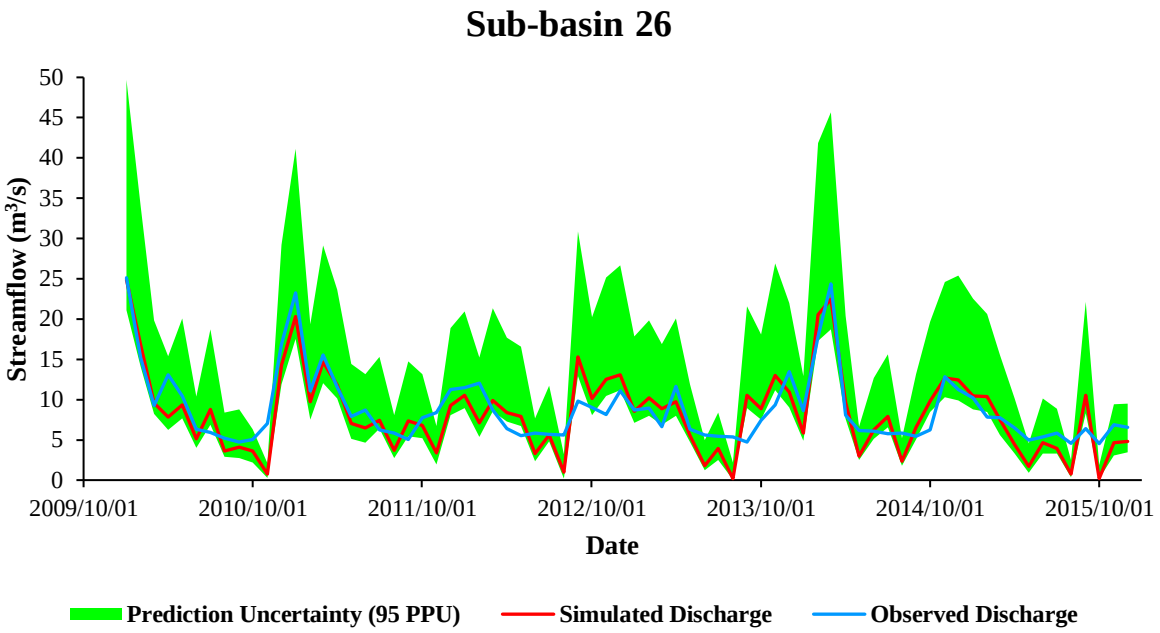


Figure 4.18: The validation hydrograph for discharge station A2H044 from 2010 to 2016

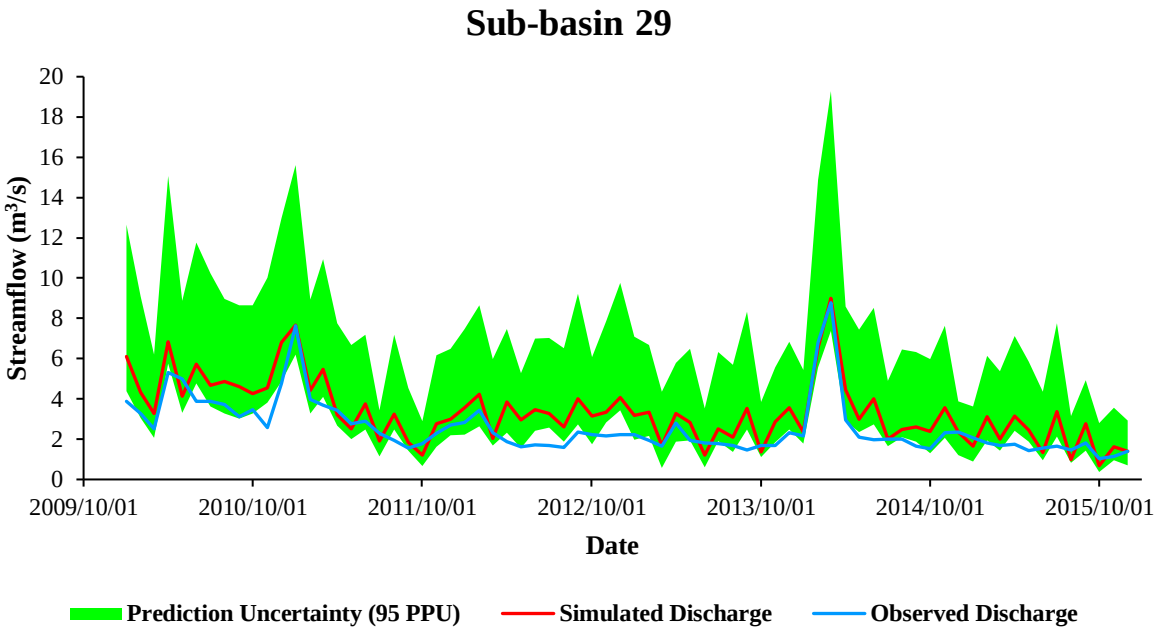


Figure 4.19: The simulated and observed streamflow hydrograph for discharge station A2H045 during the validation period (2010-2016)

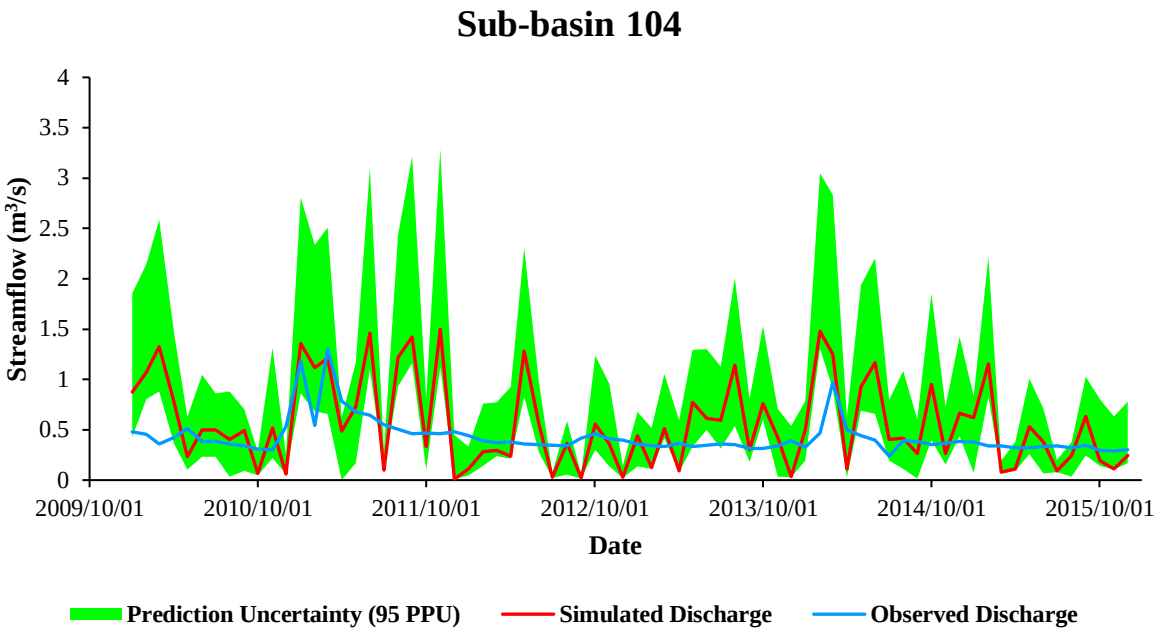


Figure 4.20: The observed vs simulated streamflow at the UCRB's A2H034 gauging station for the 6-year validation period

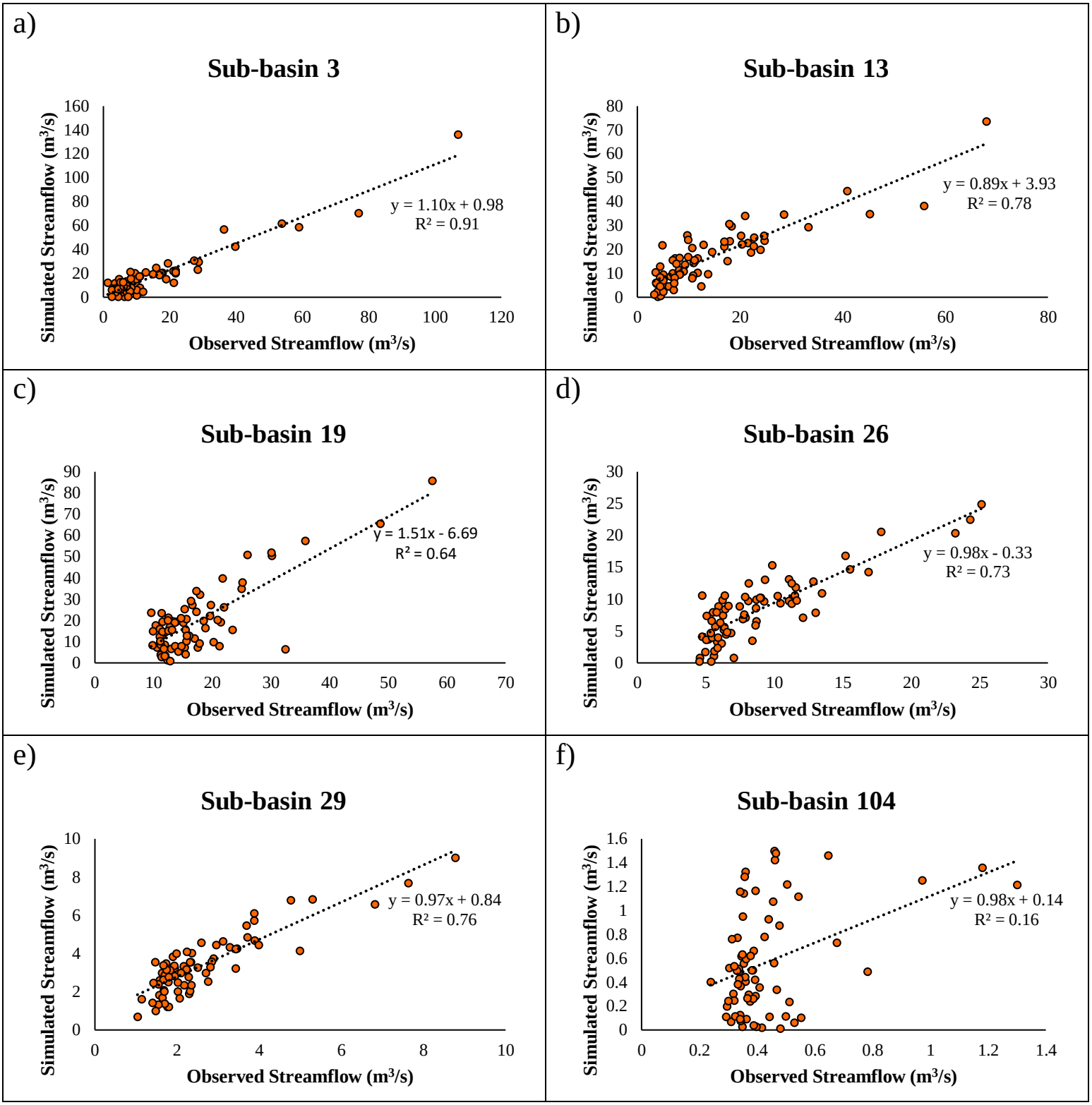


Figure 4.21a-f: The recession graphs showing the linear relationship between simulated and recorded streamflow for the validation period (2010-2016)

4.4 Climate Change Scenarios

Graphs of the annual trend in mean temperature and precipitation (Figure 4.22) were synthesised and averaged from the Buffelspoort II AGR and Pretoria University Proefplaas weather stations as a means to rationalise climate change scenarios for the UCRB. The gradients of these plots indicate that between 1980 and 2020, average surface temperatures have been rising by 0.04 °C/year with declining annual precipitations of 1.8 mm/year over the UCRB. These climatic trends agreed with southern African climate change studies by Graham *et al.* (2011), Kusangaya *et al.* (2014), and Engelbrecht *et al.* (2015), who suggested that its climate will become hotter and drier in the future. As these climate changes are associated with decreased terrestrial moisture (Graham *et al.*, 2011; Engelbrecht *et al.*, 2015), it was necessary to assess their impacts on streamflow in the UCRB.

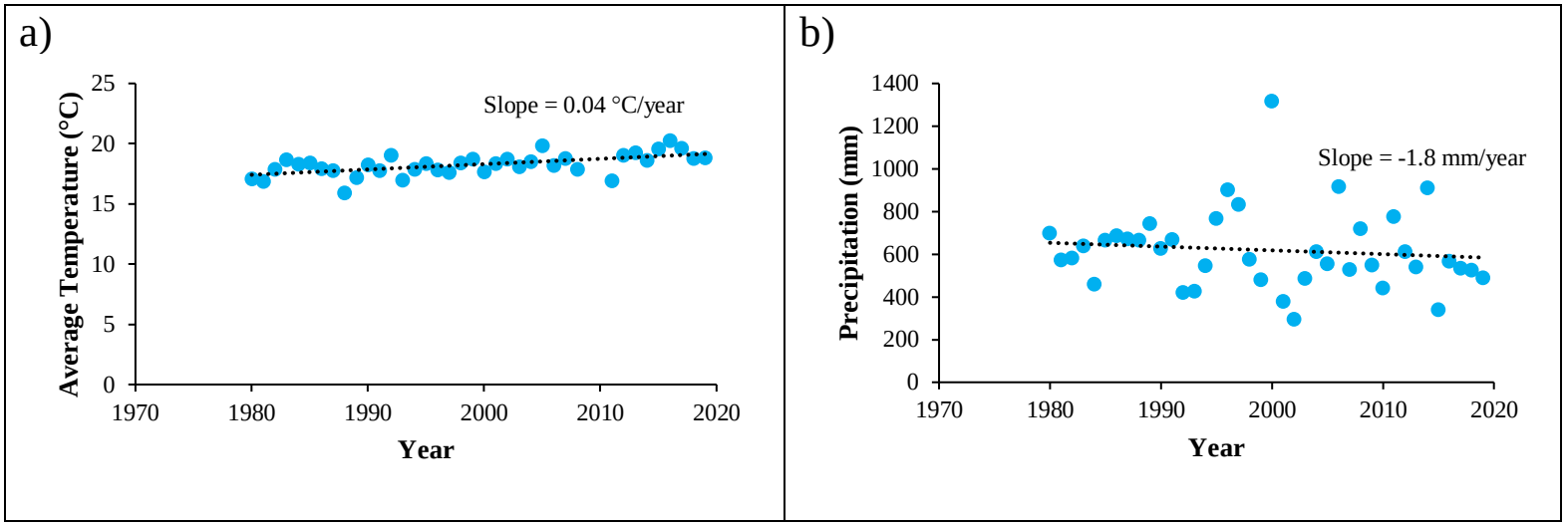


Figure 4.22: The annual average temperatures (a) and precipitations (b) experienced over the UCRB from 1980 to 2020

For this study, an increase and decrease of 1.5 °C in temperature and 20% in rainfall were used as the climate change scenarios, in line with the study by Leketa and Abiye (2019). The rainfall scenarios were deemed suitable for analysis as they concurred with the ±20% variability in precipitation projected by the IPCC for the end of the 21st century (IPCC, 2001). Moreover, the IPCC provided a special report (IPCC, 2018) delineating the potential impacts of a 1.5 °C temperature increase relative to pre-industrial levels. This report was a consequence of 196 nations signing the Paris Agreement in 2015, which aimed to limit global warming to 2 °C in the current century, with further efforts to minimize average temperature rises to 1.5 °C. Therefore, the temperature and rainfall scenarios provide a sensible extent to global climate

change by the end of the 21st century, and hence, the potential climates influencing the UCRB's streamflow.

Climate changes for the UCRB were input into the SWAT model by adjusting daily rainfall by 20% and maximum and minimum temperatures by 1.5 °C, developing new WGEN_user tables and text files associated with these changes, and running monthly model simulations under these new climates using the calibrated parameters.

4.4.1 Precipitation Change Scenarios

The hydrographs describing the monthly streamflow response of sub-basins 3, 13, 19, and 26 to increases and decreases in rainfall by 20% are shown in Figures 4.23-4.26. These hydrographs showed that changes in precipitation had substantial effects on SWAT's predicted streamflow in each sub-basin. Increasing and decreasing rainfall by 20% highlighted the enhancement of monthly streamflow simulation above the current simulation and the reduction of the predicted streamflow below the current simulation, respectively, in each sub-basin. However, Figures 4.23-4.26 portrayed that both increases and decreases in rainfall did not affect peak flow simulations compared to the current simulation in all sub-basins.

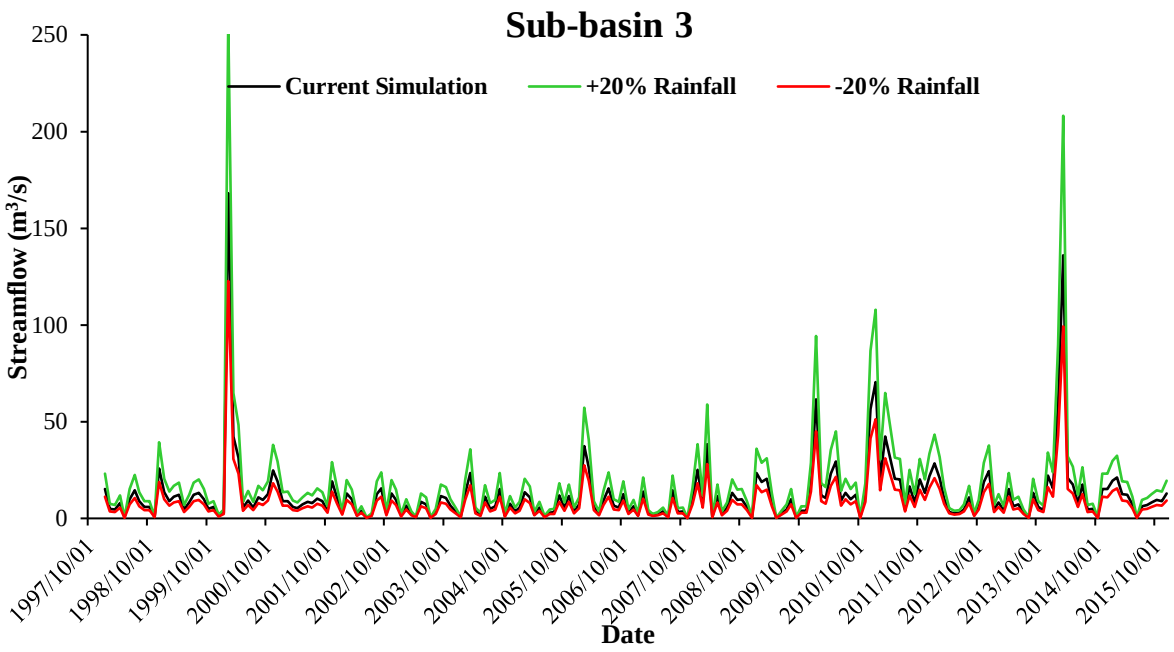


Figure 4.23: Hydrograph showing the change in streamflow in sub-basin 3 from an increase and decrease of 20% in precipitation over the UCRB from 1998 to 2016

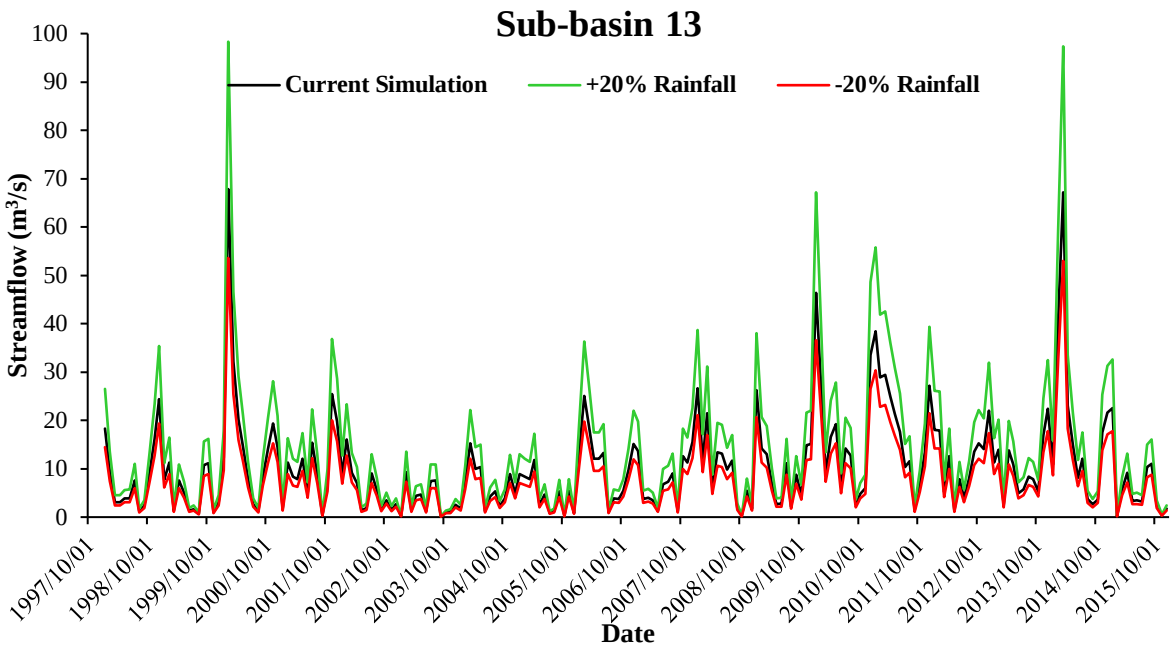


Figure 4.24: Streamflow hydrograph showing the response of sub-basin 13 to increases and decreases in precipitation by 20% (1998-2016)

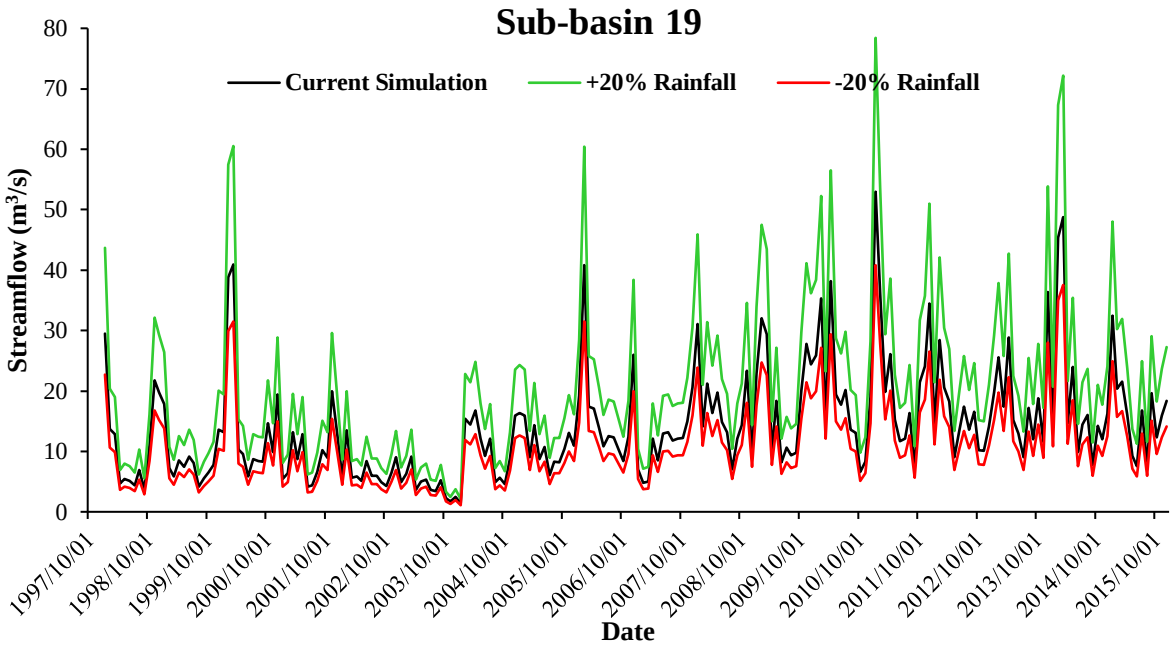


Figure 4.25: The changes in streamflow from the current simulation in sub-basin 19 due to increases and decreases in rainfall by 20% (1998-2016)

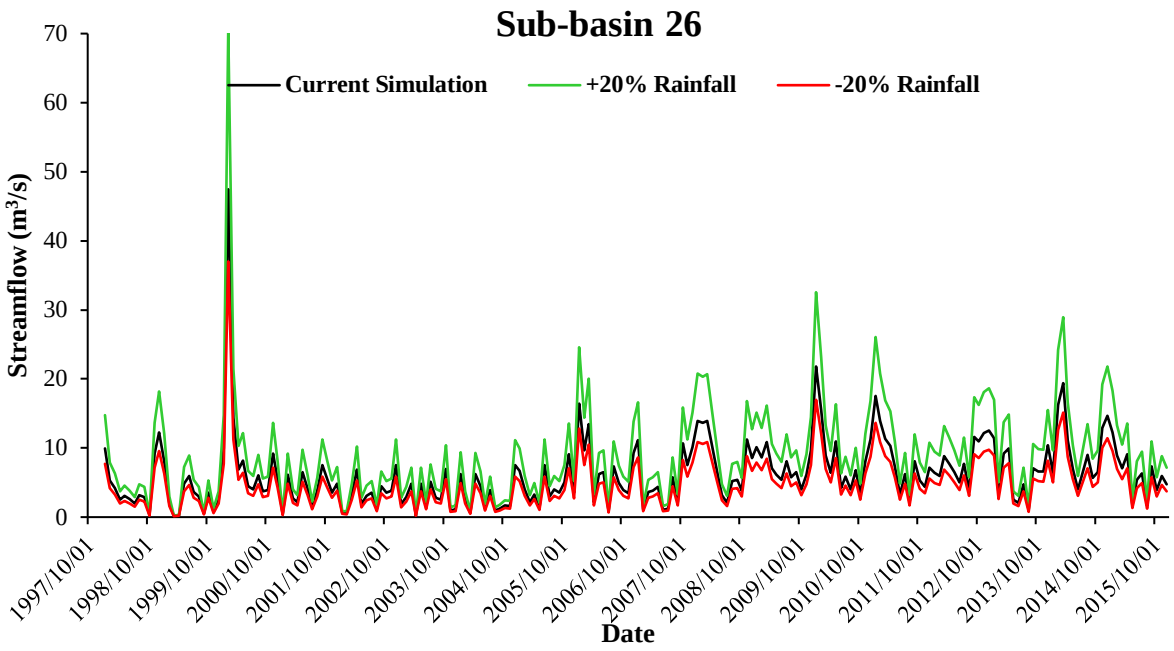


Figure 4.26: Hydrograph of sub-basin 26 indicating the change in streamflow due to a 20% change in precipitation from 1998 to 2016

4.4.2 Temperature Change Scenarios

The temperature change hydrographs, shown in Figures 4.27-4.30, demonstrated the inverse influence of temperature changes on streamflow in each sub-basin compared to the precipitation change effects. Notably, a 1.5 °C decrease in average temperature increased streamflow predictions compared to the current simulation, whereas a 1.5 °C increase in average temperature decreased streamflow predictions in each sub-basin below the current simulation. However, the temperature change hydrographs expressed similarities to the rainfall change hydrographs regarding peak flow simulations. Therefore, temperature changes did not influence the timing of peak flow occurrence.

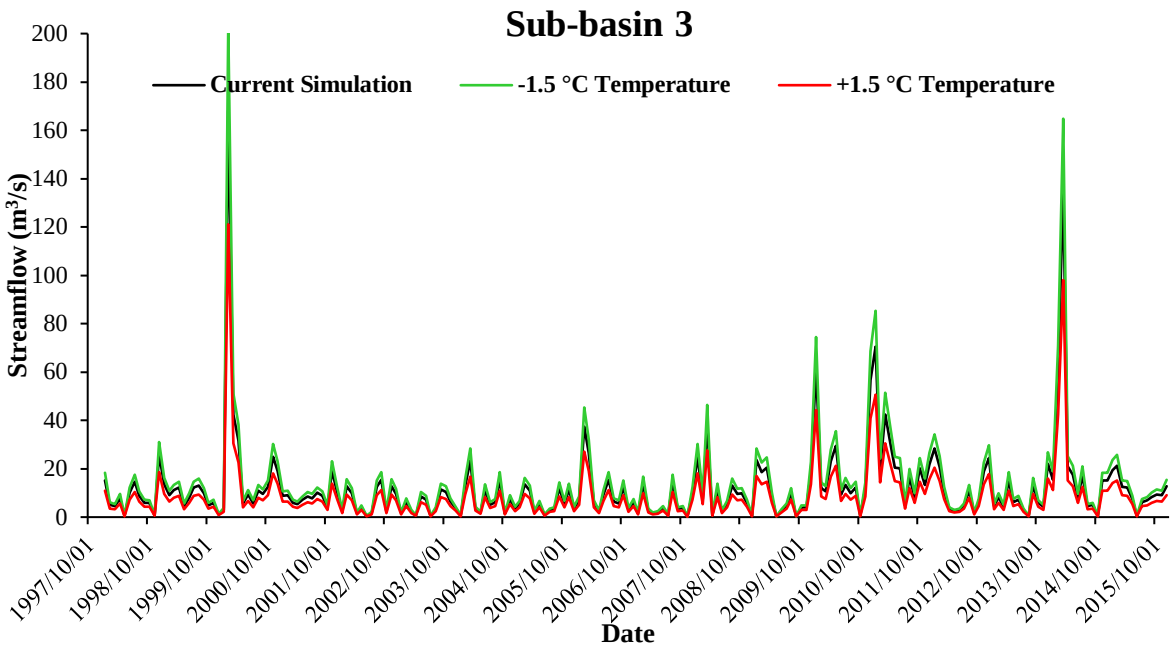


Figure 4.27: The changes in streamflow from the current simulation in sub-basin 3 due to increases and decreases in temperature by 1.5 °C (1998-2016)

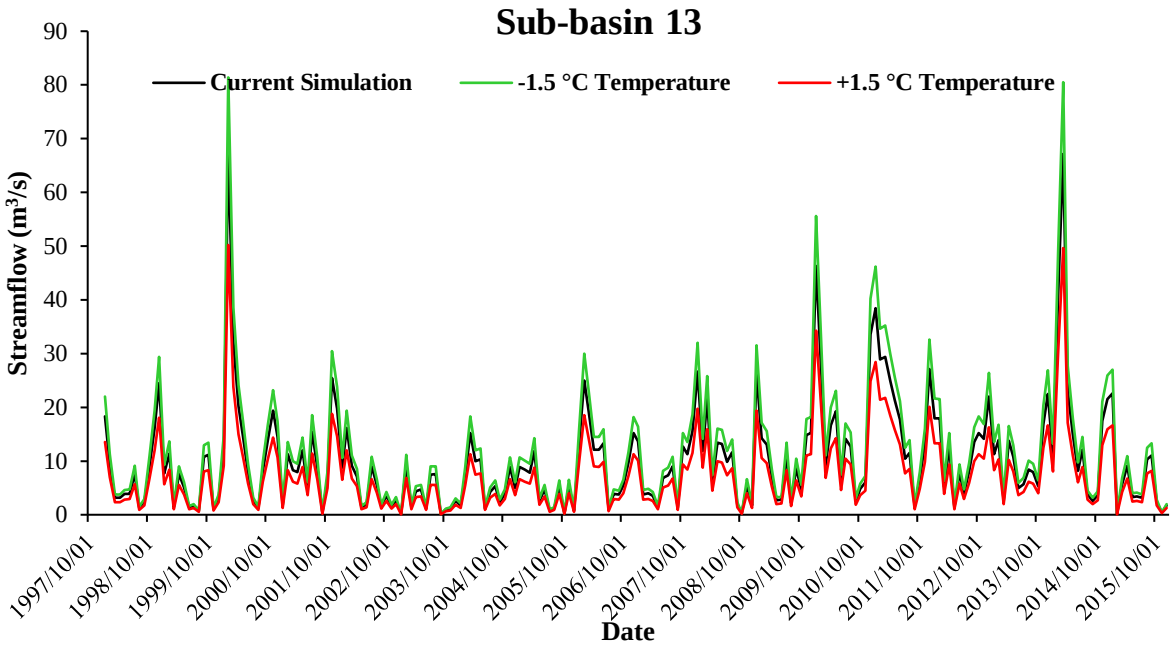


Figure 4.28: Hydrograph of sub-basin 13 indicating the change in streamflow due to a 1.5 °C change in temperature from 1998 to 2016

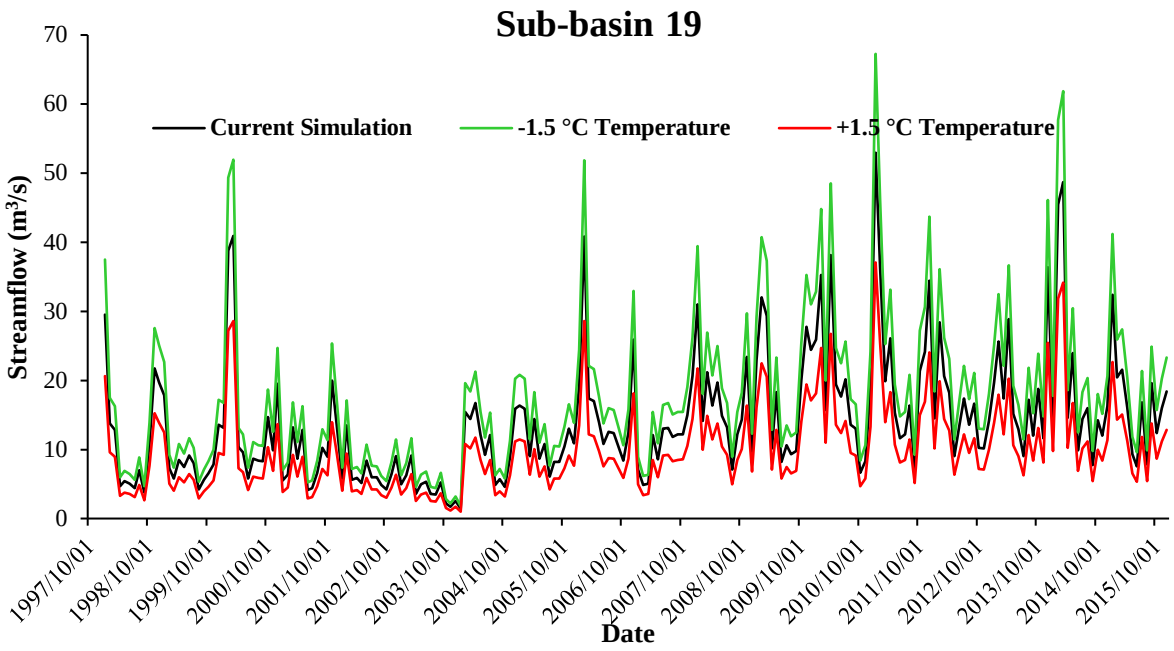


Figure 4.29: Hydrograph showing the change in streamflow in sub-basin 19 from an increase and decrease of 1.5 °C in temperature over the UCRB from 1998 to 2016

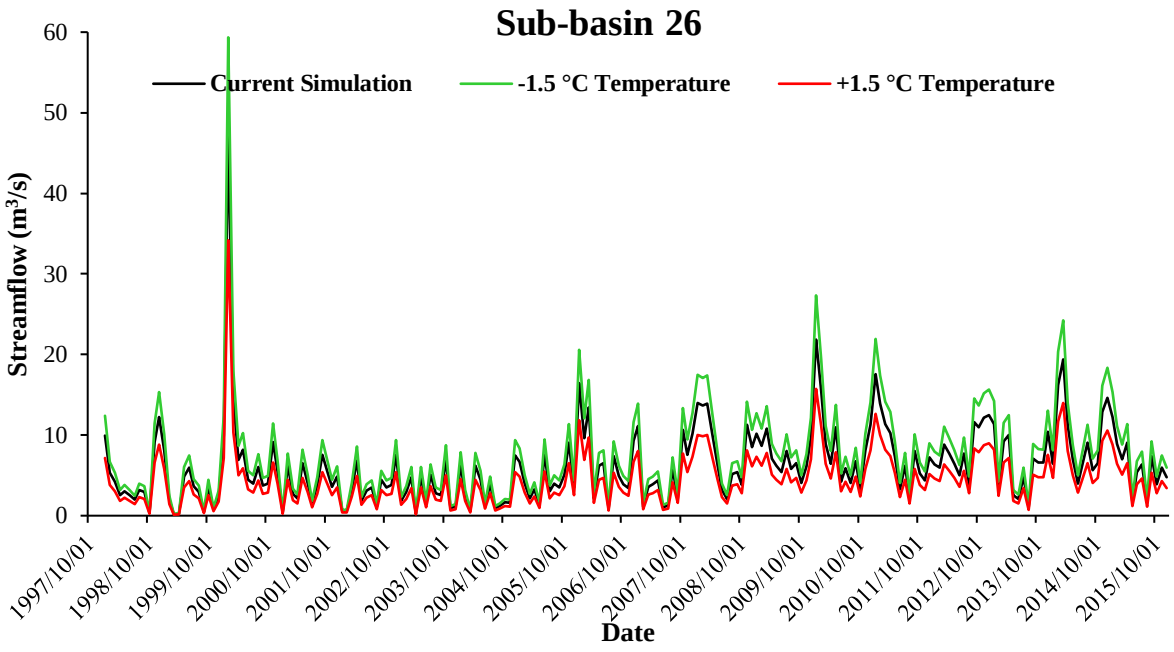


Figure 4.30: Streamflow hydrograph showing the response of sub-basin 26 to increases and decreases in temperature by 1.5 °C (1998-2016)

4.5 Land-use Change Scenarios

The land-use change used for analysis aimed to consider the social and economic factors driving human activity changes in the UCRB. According to DWAF (2008), population growth within the UCRB will continue to exceed the national average despite the UCRB's birth rate being below the national average due to economic-stimulated migration into the basin. As a result, the UCRB's 5.5 million population in 2005 is expected to increase to between 6.4 and 8.3 million by 2030. In addition, most of this growth is predicted to be in the urban growth centres of Johannesburg, Midrand, and Pretoria (DWAF, 2008). Therefore, given the association of the UCRB with large-scale urbanisation (Abiye *et al.*, 2015), a 5% increase in urbanisation was used as the land-use change assessment. The land-uses operating over the UCRB were altered using SWAT's land-use update table, located in the Edit SWAT input stage of model development (Appendix B- Figure B.4). The sub-basins containing mixed forests (FRST) and grasslands (RNGE) surrounding Johannesburg, Midrand and Pretoria were altered to medium density urban settlements (URML) until the overall basin was increased by 5% in urban developments (Appendix B- Figure B.5). The results of the increased urbanisation on streamflow in each sub-basin are shown in Figures 4.31-4.34.

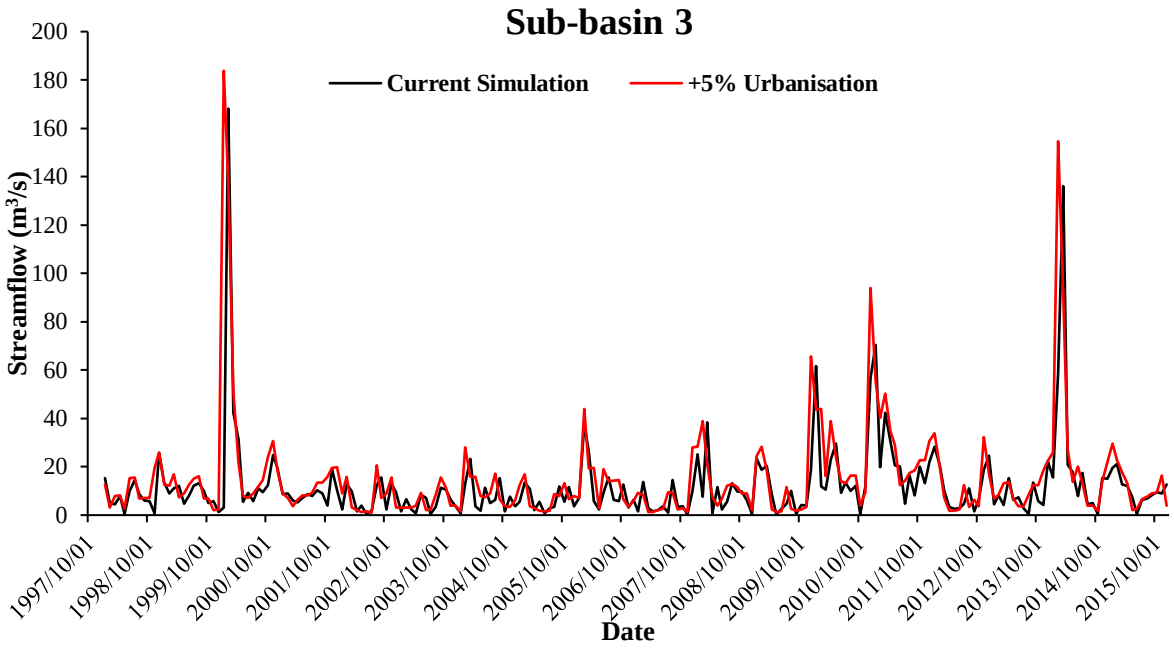


Figure 4.31: The streamflow influence of a 5% increase in urbanisation compared to the current simulation in sub-basin 3(1998-2016)

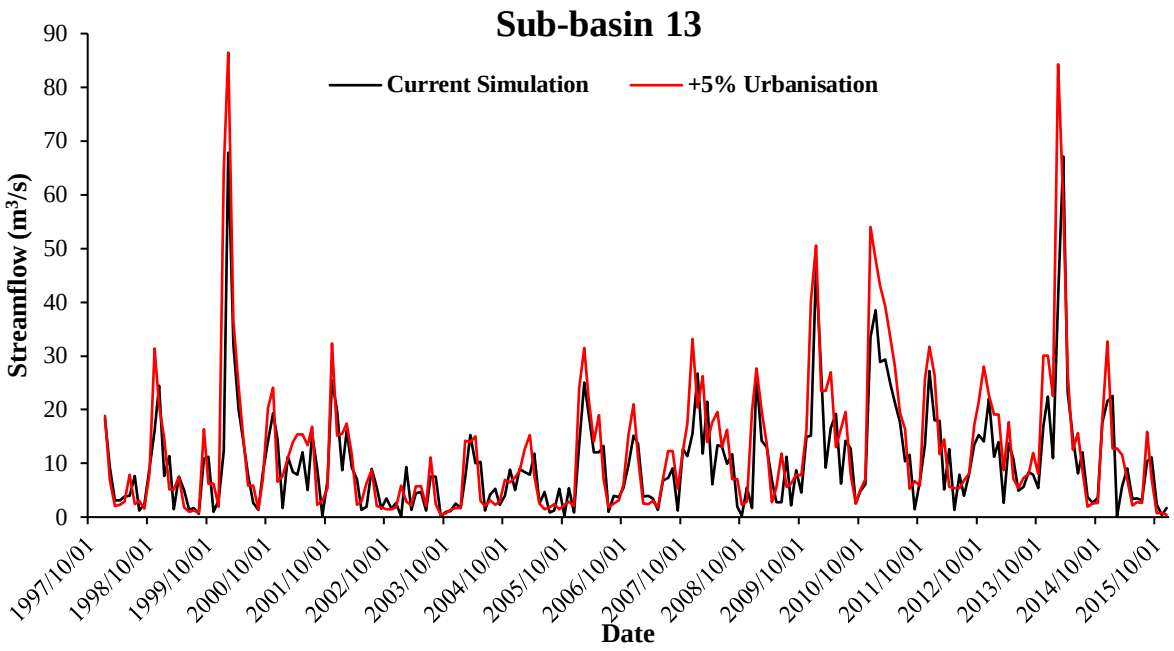


Figure 4.32: Hydrograph showing the effects of a 5% increase in urbanisation on streamflow in sub-basin 13 from 1998 to 2016

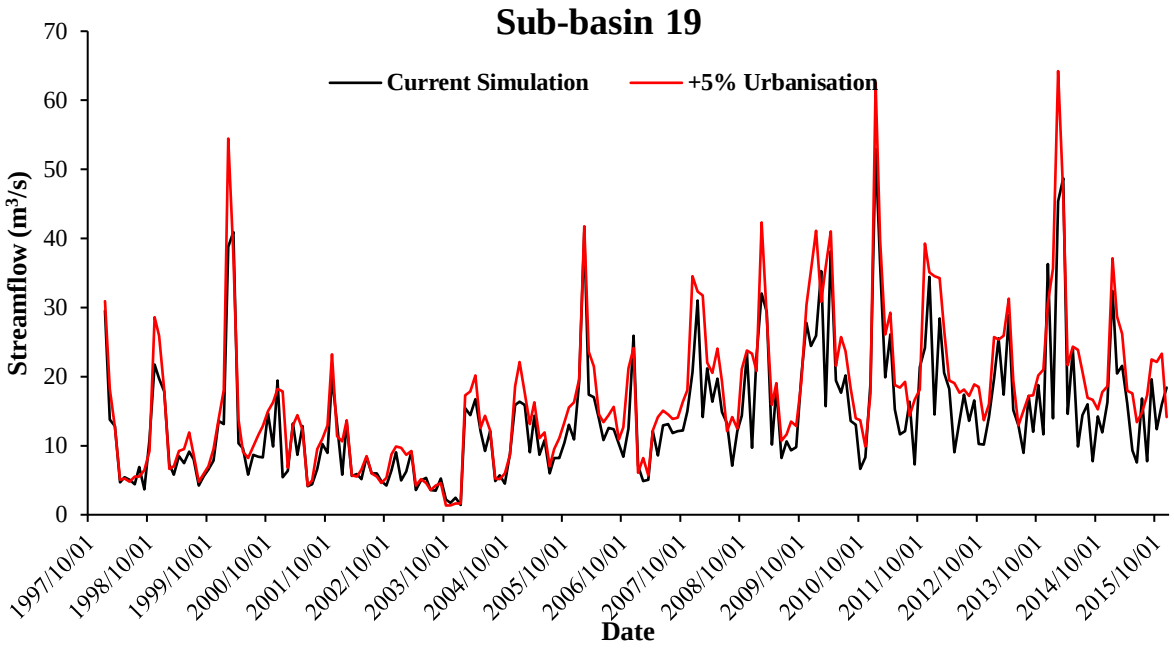


Figure 4.33: Streamflow hydrograph indicating the influence of the urbanisation land-use scenario on UCRB streamflow in sub-basin 19 (1998-2016)

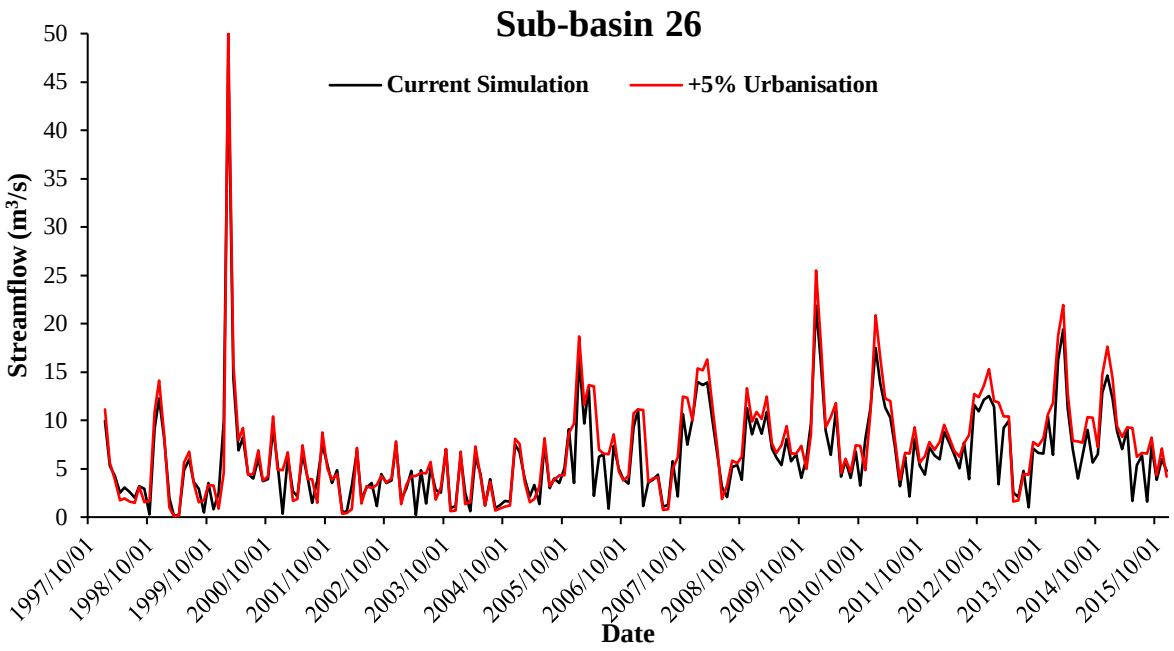


Figure 4.34: Streamflow hydrograph showing the response of sub-basin 26 to a 5% increase in urbanisation (1998-2016)

The land-use change hydrographs showed that a 5% increase in urbanisation in the UCRB inflated streamflow compared to the current simulation in each sub-basin; however, these enhancements were not as great as the 20% rainfall increase simulation. Moreover, all sub-basins expressed uniformity that the urbanisation increased the magnitude of peak flows. Hydrographs of sub-basins 3 and 13 illustrated that the increased urbanisation also influenced the timing of peak flows, advancing peak flow simulation in each case. In contrast, sub-basins 19 and 26 showed that urbanisation did not substantially affect peak flow timing.

4.6 Worst-case Scenario

The prevailing trend in the UCRB's climate towards hotter and drier conditions is associated with decreased water availability (Graham *et al., 2011*; Engelbrecht *et al.*, 2015), which influences run-off and infiltration in the basin (Gleick, 1989). In addition, urbanisation enhances run-off (Dey and Mishra, 2017) and considerably alters the quality of natural streamflow (Edokpayi et al., 2017). Subsequently, a worst-case scenario was developed for the UCRB to illustrate the impacts of its envisaged climate and anthropogenic activity changes on run-off and infiltration processes, and therefore, water availability using streamflow hydrographs, shown in Figures 4.35- 4.38. These hydrographs were synthesised using the 5% urbanisation increase land-use update and a WGEN_user table and text files reflecting a 1.5 °C increase in temperature and 20% decrease in precipitation.

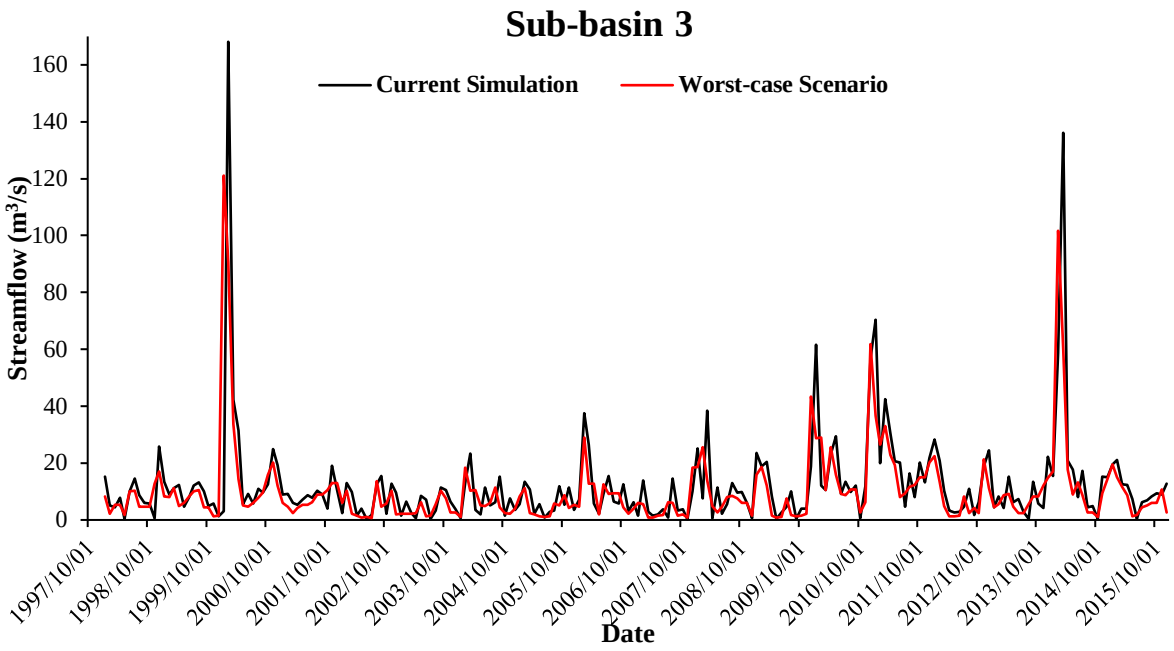


Figure 4.35: The streamflow influence of the worst-case scenario in comparison to the current simulation in sub-basin 3 (1998-2016)

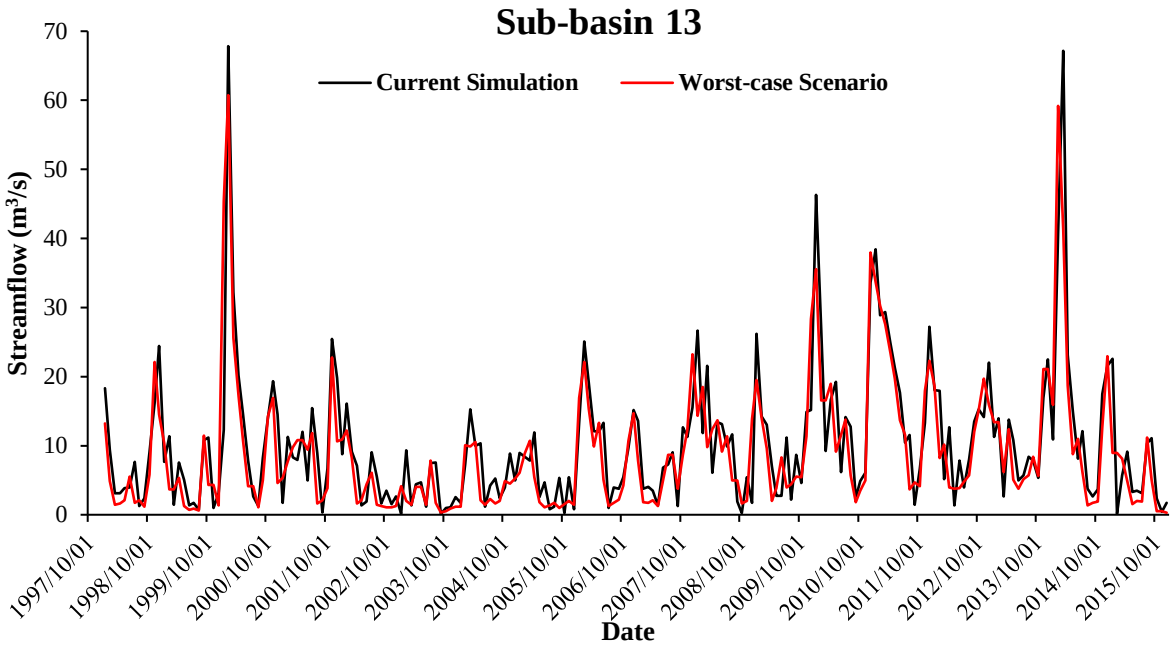


Figure 4.36: Hydrograph of sub-basin 13 indicating the change in streamflow due to the worst-case scenario from 1998 to 2016

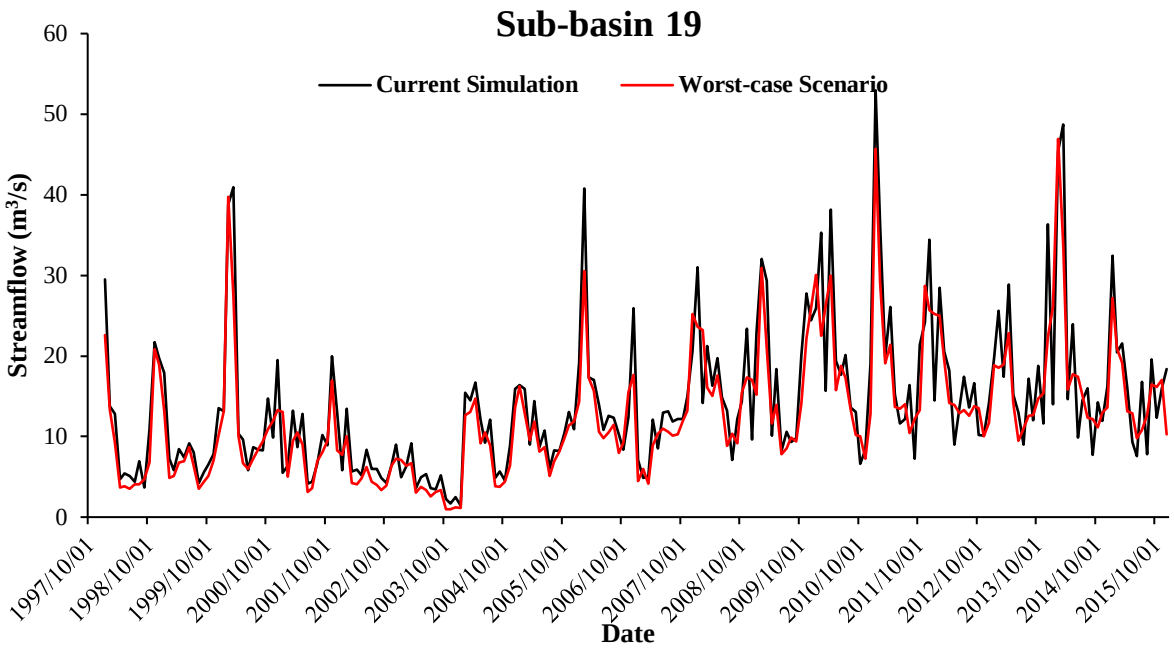


Figure 4.37: Hydrograph showing the change in streamflow in sub-basin 19 due to the worst-case scenario from 1998 to 2016

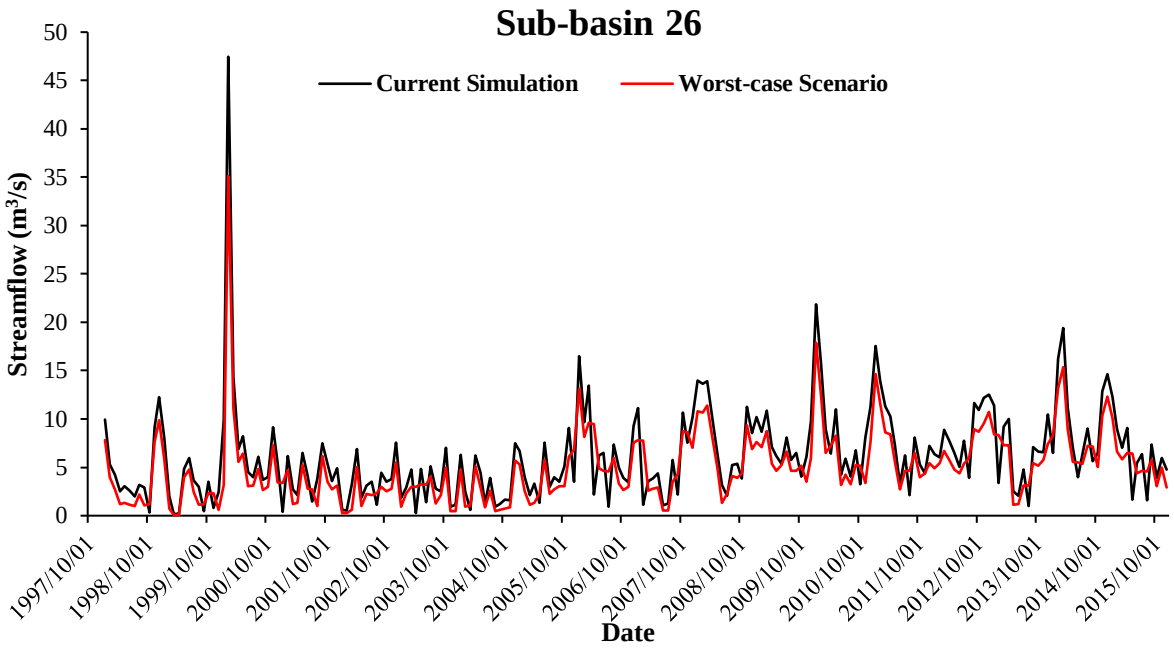


Figure 4.38: Streamflow hydrograph showing the response of sub-basin 26 to the worst-case climate and land-use change scenario (1998-2016)

The worst-case scenario hydrographs show similarities to the urbanisation scenario regarding the advancement of peak flow occurrence in sub-basins 3 and 13, with marginal peak flow progression in sub-basins 19 and 26. In contrast, the worst-case scenario decreased streamflow below the current simulation in each sub-basin, showing substantial reductions in high and low simulation compared to the 5% increase in urbanisation.

4.7 Comparative Analysis

For further characterisation of the relative and combined impacts of land-use and climate changes in the UCRB, a comparative analysis was performed to quantify the streamflow effects of these changes. The assessment expressed the change in streamflow due to the climate and land-use scenarios as a percentage difference compared to the current simulation in each sub-basin, shown in Table 4.7, representing the calibrated model's streamflow response to the realistic climate and human activities occurring over UCRB.

Table 4.7: The change in streamflow due to climate and land-use changes and their combined effects in comparison to the current simulation in each sub-basin

	Climate changes					
Sub-basin	**+ 20% Rainfall**	**-20 % Rainfall**	**-1.5 °C Temperature**	**+1.5 °C Temperature**	**+5% Urbanisation**	**Worst-case scenario**
3	53% ↑	27% ↓	21% ↑	28% ↓	27% ↑	16% ↓
13	45% ↑	21% ↓	20% ↑	26% ↓	25% ↑	12% ↓
19	48% ↑	23% ↓	27% ↑	30% ↓	23% ↑	10% ↓
26	49 % ↑	22% ↓	25% ↑	28% ↓	15% ↑	19% ↓
Average	**48.75% ↑**	**23.25% ↓**	**23.25% ↑**	**28% ↓**	**22.5% ↑**	**14.25% ↓**

These results suggest that streamflow in the UCRB was more sensitive to precipitation increases as opposed to decreases. Increasing rainfall by 20% resulted in an average simulated streamflow increase of 49%, attributed to streamflow increases of 53%, 45%, 48%, and 49% in sub-basins 3, 13, 19, and 26, respectively. Conversely, reducing precipitation by 20% provided an average streamflow decrease of 23% in all sub-basins. Sub-basins 13, 19, and 26 expressed similar streamflow reductions of 21%, 23%, and 22%, respectively, whereas sub-basin 3 showed a more significant streamflow decrease of 27%.

Temperature results revealed a greater influence from the 1.5 °C temperature increase compared to the equivalent decrease. Increasing the temperature in sub-basins 3, 13, 19, and 26 produced streamflow simulation reductions of 26%, 28%, 30%, and 28%, respectively. On

the other hand, decreasing the temperature generated an average streamflow increase of 23% for all sub-basins, which was attributed to streamflow enhancements of 21%, 20%, 27%, and 25% in sub-basin 3, 13, 18, and 26, respectively.

The 5% increase in urbanisation increased streamflow in the UCRB by an average of 22.5%. Sub-basin 26 displayed a minor streamflow increase of 15%, whereas sub-basins 3, 13, and 19 expressed greater streamflow inflations of 27%, 25%, and 23%, respectively. In contrast, the worst-case scenario decreased streamflow in the UCRB by 14% on average, producing streamflow reductions of 16%, 12%, 10%, and 19% in sub-basins 3, 13, 19, and 26, respectively.

CHAPTER5: DISCUSSION

The development of a SWAT model which accurately describes the hydrology of large, dynamic and complex watersheds such as the UCRB is a challenging task due to the nature of data (scale and resolution) required in model synthesis, difficulties associated with the configuration of reservoirs on a stream network, and limitations regarding recorded data used for precision analysis (Kannan *et al.*, 2019). However, numerous studies have proved SWAT's capabilities in accurately predicting streamflow in extensive watersheds using available monitoring data. Fortunately, the UCRB contained six discharge stations with high-quality monthly streamflow data, enabling the successful calibration and validation of the SWAT model to evaluate its streamflow response to changing climate and land-use factors. Moreover, the deterministic nature of SWAT proves beneficial for the assessment under climatic and anthropogenic changes as it produces the same outputs for a given set of inputs. Therefore, the model isolates the hydrological response to changes in a single variable, e.g., climate and land-use (Mwangi *et al.*, 2016), permitting the quantification of the relative and combined impacts of climate and land-use changes on UCRB hydrology.

The attributes of the watershed, stream network, soils, land-uses, climate, reservoirs, and wastewater discharges in the UCRB produced a model that was initially unable to capture river discharge adequately and tended to overestimate streamflow on average. In addition, the initial model's hydrographs showed that simulated streamflow fluctuated markedly and overestimated peak flow magnitude compared to measured data. This was noted as a common occurrence in SWAT streamflow studies (Ghidey *et al.*, 2007; Niraula *et al.*, 2011), owing to the number of parameters influencing streamflow and their interaction affecting various hydrological processes (Arnold *et al.*, 2012). The initial model results suggested that the water balance within the UCRB was erroneous, and therefore, further calibration and validation of the model were necessary to improve its streamflow prediction accuracy.

Sensitivity analysis using SWATCUP identified 13 parameters responsive to streamflow changes in the initial model, from which the soil parameters (SOL_K and SOL_AWC) and run-off parameters (CN2 and OV_N) were the most sensitive to streamflow alterations during calibration. The increased sensitivity of the soil and run-off parameters were common across South African comparative studies (Gyamfi *et al.*, 2016; Ngubane, 2017; Thavhana *et al.*, 2018; Mengistu *et al.*, 2019) used to delineate the most responsive parameters influencing the

UCRB's streamflow. Moreover, all previous South African studies highlighted inaccuracies concerning peak flow simulations from the default SWAT model. The initial model and parameter sensitivity results corroborate these observations and suggests that SWAT failed to characterise run-off and infiltration processes accurately within the UCRB. Additionally, the significant inaccuracies of the initial SWAT South African models are possibly indicating that SWAT has limitations concerning streamflow simulations in the semi-arid conditions of the country.

Calibration of the initial model using SWATCUP's SUFI2 procedure and the multi-site calibration approach against six discharge stations showed that adjusting SWAT parameters within sensible ranges significantly improved the accuracy of streamflow predictions. The p-factor and r-factor results indicated that the calibrated parameter ranges produced a narrow envelope of model uncertainty which encompassed 71% of measured stream discharge, suggestive of good model performance. The calibration results, therefore, supported the perspective of Govender and Everson (2005), who emphasised the importance of parameterising models as precisely and efficiently as possible when applying SWAT to South African catchments. Comparing the calibration results to model performance indices developed by Moriasi *et al.* (2015) proved that the calibration process enhanced streamflow precision and indicated that the model simulated streamflow above a satisfactory standard regarding all objective functions (R^2, PBIAS, and NSE) in sub-basins 3, 13, 19, and 26. However, the calibrated model behaved unsatisfactorily across all performance measures in sub-basin 104 and overestimated streamflow unacceptably in sub-basin 29. The calibration results specified that the multi-site calibration approach successfully produced accurate streamflow simulations for most of the basin, substantiating Piniewski and Okruszko (2011) results using the same method. Moreover, the success of the UCRB model calibration further corroborated the findings of Piniewski and Okruszko (2011) regarding the superior efficacy of multi-site calibration in generating satisfactory stream discharges in large watersheds with substantial spatial heterogeneity as opposed to smaller watersheds.

The validation results expressed that SUFI2's prediction uncertainty produced similar r-factors to calibration, indicative of the limited parameter range used for both calibration and validation processes. Conversely, the p-factor results showed decreases in all sub-basins from calibration to validation, specifying that the uncertainty band enveloped less of the recorded data, and subsequently, the accuracy of validation was determined to be inferior to calibration. The reduced model precision during validation is recurrent in SWAT streamflow studies and was

suggestive that the parameters characterising the UCRB's response to streamflow during calibration did not precisely describe the basin response outside the calibration period (Abbaspour, 2015). Nevertheless, the validation indicated similar results to calibration concerning the superior and adequate streamflow simulations in sub-basins 3, 13, 19, and 26, the overestimation of streamflow in sub-basin 29, and the unsatisfactory discharge predictions in sub-basin 104.

The calibration and validation results indicated that SWAT's streamflow simulations were most accurate in sub-basins 3 and 13, located downstream of the Roodekoppies and Hartbeespoort dams, respectively. The increased precision in the downstream reservoir sub-basins likely indicated that the target release approach to reservoir description successfully predicted dam releases in the UCRB. Furthermore, the efficacy of the target release method was noted by Kim and Parajuli (2012) when assessing the reliability of SWAT's reservoir characterisation methods. The calibration and validation results exhibited a correlation between the mean simulated streamflow and simulation accuracy, possibly suggesting that the validated SWAT model was more proficient in simulating the higher flow conditions in the basin. The average overestimation bias and the inaccurate simulations in the low flow conditions of sub-basins 29 and 104 evidenced this during calibration and validation. In contrast, sub-basin 19 produced the largest average flows yet did not provide the most precise streamflow predictions. The regression graphs and hydrographs observed the discrepancies in the simulation accuracy of sub-basin 19 during calibration and validation, which depicted that SWAT struggled to estimate the low flow or baseflow variability in sub-basin 19. This may be attributed to the insufficient characterisation of the diverse land-use practices in northern Johannesburg, located upstream of sub-basin 19. Moreover, the inadequate description of wastewater discharges from Johannesburg may have contributed to the reduced simulation precision in this sub-basin.

Ultimately, the results for the calibration and validation of the SWAT model indicated that the calibrated parameters reduced the imprecisions between measured and simulated streamflow sufficiently for reliable evaluation under changing climate and land-use scenarios. Nevertheless, during model calibration and validation, inaccurate stream discharge predictions in sub-basins 29 and 104 necessitated their removal from further analyses. As a result, the impacts of climate and land-use changes on the outflow from Roodekoppies Dam (sub-basin 3), the outflow from Hartbeespoort Dam (sub-basin 13), the inflow into Hartbeespoort Dam from the Crocodile River (sub-basin 19), and the flow into the Crocodile River from the Jukskei River (sub-basin 26) were assessed in this study. However, the objective functions observed

that streamflow simulations in these sub-basins were not entirely accurate with measured data. Therefore, the results and interpretations of the effects of climate and land-use changes presented henceforth should be used with caution.

The climatic variables used for evaluation provided a sensible extent to the possible future climatic alterations occurring over the basin this century. In addition, these climate changes enabled a comparison to the results obtained by Leketa and Abiye (2019) when assessing the impacts of climate variability on streamflow in the UCRB. Leketa and Abiye (2019) used PRMS to analyse the effects of increases and decreases in temperature by 1.5 °C and rainfall by 20% with a subsequent worst-case scenario (1.5 °C temperature increase, and 20% precipitation decrease) on streamflow and baseflow in the Crocodile River (sub-basin 19). Therefore, despite their study including baseflow analyses, it did not assess the impact of climate variability on streamflow to the same extent and did not incorporate the influence of land-use changes on stream discharge in the UCRB.

The SWAT results showed that increasing and decreasing rainfall by 20% resulted in the average streamflow enhancements of 49% and reductions of 23%, respectively, compared to the current simulation. Temperature change results indicated that a 1.5 °C rise in average temperature lowered stream discharge by 28% on average, whereas a 1.5 °C decrease in temperature increased streamflow by 23% compared to the current simulation. Therefore, it was determined that stream discharge in the UCRB was more sensitive to precipitation and temperature increases as opposed to decreases. These trends concur with the observations of Leketa and Abiye (2019). Moreover, a comparison of SWAT results to those obtained by Leketa and Abiye (2019) in sub-basin 19 showed a 49% improvement in SWAT streamflow from a 20% precipitation increase, which was similar to the 52% enhancement reported by Leketa and Abiye (2019) through PRMS application. Reducing rainfall by 20% resulted in a 23% decrease in SWAT stream discharge prediction in sub-basin 19, which corroborated the 23% decrease observed by Leketa and Abiye (2019). Temperature increases produced a 30% streamflow decrease in sub-basin 19, similar to the 27% reduction noted by Leketa and Abiye (2019). In contrast, temperature decreases inflated SWAT streamflow in sub-basin 19 by 27%, significantly different from the 18% observed by Leketa and Abiye (2019). Lastly, the temperature and precipitation hydrographs showed that climate change did not influence the simulation of peak and low flows from the current simulation, suggesting that climate changes affected the antecedent moisture conditions in the UCRB and did not influence its basin response (Roberts and Klingeman, 1970).

The land-use scenario reflected a 5% urban expansion in the UCRB as a result of its envisaged population growth due to economic migration into the basin (DWAF, 2008), leading to increased urbanisation (Abiye *et al.*, 2015). These results indicated that urbanisation increased stream discharge by 22.5% on average. However, sub-basin 26 showed a marginal streamflow increase of 15% in comparison to the 27%, 25%, and 23% experienced by sub-basins 3, 13, and 19, respectively. This is possibly attributed to the existence of sub-basin 26 within the confinement of Johannesburg. Therefore, its streamflow is already potentially influenced by urban developments and is less sensitive to urban expansions. Nevertheless, the hydrographs of all evaluated sub-basins showed that urbanisation increased the run-off volume and peak discharge compared to the current simulation. In addition, a 5% urbanisation increase advanced peak flow simulation, and therefore, reduced the lag time between rainfall and run-off in each sub-basin (Moon *et al.*, 2004). These results indicate that the increased urbanisation influenced streamflow similarly to previous urbanisations studies (Cheng and Wang, 2002; Moon *et al.*, 2004), suggesting that a 5% urban expansion increased the imperviousness of the UCRB.

The worst-case scenario developed for the UCRB aimed to illustrate the water availability effects of its perceived changing climate towards hotter and drier conditions in addition to its predicted urbanisation increases. Resultantly, the worst-case scenario evaluated the influence of a 1.5 °C increase in temperature, a 20% decrease in precipitation and a 5% increase in urban expansion on streamflow in the basin. In addition, the relative and combined impacts of climatic and land-use changes on stream discharge could, therefore, be delineated by comparing the worst-case scenario results to those of the increased urbanisation scenario. The worst-case scenario results showed a 14% average streamflow reduction relative to the current simulation. Moreover, comparing these results to the urbanisation scenario indicated that the climatic changes associated with the worst-case scenario subsequently decreased streamflow by 43%, 37%, 33%, and 34% in sub-basins 3, 13, 19, and 26, respectively. Therefore, the results for sub-basin 19 were consistent with the 39% reduction approximated by Leketa and Abiye (2019), with discrepancies likely attributed to alterations in the hydrological processes of the basin due to urban land-use increases. The worst-case scenario hydrographs displayed similarities to the peak flow simulation of the urbanisation hydrographs, indicative of the more impervious nature of the UCRB. In contrast, the hydrographs expressed substantial decreases in the magnitude of peak and low flow simulation relative to the current simulation, suggestive that the temperature and rainfall changes accompanying the worst-case scenario reduced water availability in the basin.

The individual impacts of an increase in temperature and decrease in precipitation and their combined effects, portrayed by the worst-case scenario, were shown to reduce streamflow in each sub-basin drastically. Therefore, it was determined that these climatic changes decreased the antecedent moisture conditions, ultimately reducing water availability for run-off and infiltration. Moreover, the land-use change scenario indicated that increasing urbanisation subsequently strengthened the impervious nature of the basin, thereby enhancing run-off and decreasing infiltration. As a result, both the climate and land-use changes associated with the worst-case scenario depleted the infiltration processes. Decreases in infiltration are related to reduced groundwater recharge (Healy, 2010), and hence, lower baseflow feeding the stream network (Winter, 1998). Consequently, the UCRB's envisaged climate and land-use changes might have devastating consequences for the quality of its surface water resources as reduced baseflow results in less natural water for dilution of lower quality wastewater in the basin (Leketa and Abiye, 2019). In addition, increasing urbanisation is expected to yield larger water surpluses due to inflated return flows in the basin (DWAF, 2004). Therefore, it is predicted to compromise the quality of streams and impoundments in the UCRB, particularly the Hartbeespoort Dam (DWAF, 2008).

Groundwater resources may also be negatively influenced by its projected climate and human activity changes. Groundwater recharge occurs mainly from rainfall before evaporation in the crystalline rocks and Malmani dolomites (Leketa *et al.*, 2019), which are intimately connected with surface water in the area west of Johannesburg (Abiye *et al.*, 2015). In addition, mixing processes of fresh and polluted water occur in the shallow zones of weathered crystalline rocks and the dissolution cavities of the dolomitic aquifers below Johannesburg (Abiye, 2011; Abiye *et al.*, 2011). The predicted change in the UCRB towards decreased infiltration will likely reduce recharge and the availability of groundwater resources. Decreasing infiltration may also reduce the abundance of freshwater below the surface, which will mitigate the dilution between fresh and polluted water, adversely affecting the quality of the basin's groundwater resources. This is particularly concerning, given that the dolomites, which supply water to Tshwane and for irrigation, are already susceptible to pollution from industrial spills and sewerage leaks (DWAF, 2004). Moreover, groundwater in Johannesburg is negatively influenced by acid mine drainage (Abiye, 2011; Abiye *et al.*, 2011; Abiye, 2014) due to water table rises from mine closures resulting in a plume of mine water severely impacting aquifers and freshwater resources (Abiye, 2014). Therefore, groundwater resources in the UCRB are regarded as of

increasing importance, which requires adequate protection from decision-makers and users, given the growing water demand in the basin (Abiye, 2013).

The predicted growth of anthropogenic influences in the UCRB and its accompanying water demand increases were first recognised by the Department of Water Affairs (DWAF, 2004; 2008), who developed water management strategies to limit human activities impacts on the basin. These strategies predominantly concerned water demand management and water re-use in the basin. Water demand management focused on minimising leaks in the urban and industrial sectors, where most of the losses occur, and reducing consumptive use in the basin. Water re-use strategies concerned recycling of the return flows to the UCRB or using return flows in or downstream from the Hartbeespoort Dam for irrigation and mining activities (DWAF, 2008). Water demand management is imperative for establishing a decreased and efficient use of water, and hence, the survival of water resources in the basin. However, the water re-use strategies may be detrimental to the UCRB's water resources sustainability. This study highlights that the envisaged climate and land-use changes in the basin will likely aggravate the availability and quality of surface and groundwater resources. As a result, the return flows entering the Hartbeespoort Dam via run-off or baseflow will probably contain increased pollutant and nutrient loads. As such, re-using water in or downstream from the dam for irrigation and mining, as suggested by the Department of Water Affairs, will only exacerbate the UCRB's water quality condition. In addition, as return flow re-use will increase the salinity of crocodile systems (DWAF, 2004), the re-use strategies will likely negatively impact humans and ecosystems in the basin by compromising water accessibility and availability through water quality reductions. Therefore, improved integrated water resources management is required to ensure efficient and safe water use, which meets growing water demands. This will guarantee water resources sustainability in the basin, even through the decreased surface and groundwater quantity and quality due to the UCRB's predicted climate and human activity changes, as recognised by this study.

CHAPTER 6: CONCLUSION, CHALLENGES, AND RECOMMENDATIONS

6.1 Conclusion

This study was aimed to assess the applicability of the SWAT model in simulating the streamflow response of the Upper Crocodile River Basin to land-use and climate changes. The Upper Crocodile River Basin encompassed part of the major cities of Johannesburg and Pretoria and received effluents from numerous wastewater treatment plants, making water quality of primary concern in the basin. In addition, the UCRB's predicted urbanisation increases and climate change towards decreased water availability might aggravate its water quality concerns. Therefore, it was necessary to model the impacts of climate and human activity changes on streamflow in the UCRB to mitigate their potential influence on water resources in the basin. The deterministic nature of the SWAT model enabled the delineation of the relative and combined streamflow effects of climate and land-use changes in the UCRB.

The description of the catchment characteristics and climate over the UCRB produced an initial SWAT model that could not simulate stream discharge adequately and fluctuated considerably regarding its streamflow predictions. Further evaluation of the initial model using measured streamflow recorded at six discharge stations and the R^2, PBIAS, and NSE objective functions proved that SWAT inaccurately simulated stream discharge in the UCRB and overestimated streamflow on average. Hence, further calibration and validation of the model were required to improve streamflow prediction reliability in response to the basin's climate and human activity changes.

Based on previous studies, the calibration process identified thirteen parameters that were sensitive to streamflow in the UCRB, from which the SOL_K, CN2, SOL_AWC, and OV_N parameters were most sensitive. Constraining the calibration parameter ranges resulted in SWATCUP's SUFI2 procedure producing a narrow uncertainty band that enveloped 71% of observed streamflow, signifying that the calibrated parameter ranges successfully predicted streamflow in the UCRB. Analysis of the calibration accuracy using the R^2, PBIAS, and NSE performance measures showed that SWAT precisely simulated stream discharge with recorded data in sub-basins 3, 13, 19, and 26 and inaccurately simulated streamflow in sub-basins 29 and 104. Similar results were obtained for the validation process, and therefore, it was

concluded that the calibrated model satisfactorily predicted streamflow in sub-basins 3, 13, 19, and 26 for evaluation under climate and land-use scenarios.

The climate changes towards a 1.5 °C decrease in temperature and a 20% increase in precipitation inflated streamflow in the UCRB. However, the UCRB's envisaged climate change towards hotter and drier conditions, reflected by a 1.5 °C increase in temperature and a 20% reduction in rainfall, decreased the low and peak flow simulation, suggesting a decrease in the antecedent moisture condition in the UCRB. The 5% urbanisation increase enhanced run-off and peak flow magnitude and reduced the lag time between precipitation and run-off, indicative of a more impervious UCRB. Therefore, the UCRB's predicted climate and land-use changes ultimately reflect lower baseflow contribution to streamflow. Hence, effluent loadings from wastewater treatment plants will likely constitute a more significant portion of stream discharge, reducing water quality in the basin. Moreover, the connection between surface and groundwater in the basin suggests that groundwater resources will also be adversely affected by the UCRB's predicted climate and human activity changes. Consistency between the climate and land-use change results in sub-basins 3, 13, 19, and 26 indicate that decreased water quality and availability will affect the entire UCRB, from the streams draining Johannesburg to the Crocodile River draining the basin through the Hartbeespoort and Roodekoppies dams. Therefore, improved integrated water resources management, beyond the current developed scope, is necessary to ensure water sustainability in the UCRB.

6.2 Challenges

The synthesis of a SWAT model for a large and complex watershed such as the UCRB required extensive data acquisition and refinement, resulting in several issues incurred:

- The soil data from FAO contained vital soil properties necessary for the development of the usersoil table. However, the soil properties requiring calculation were based on soil composition, and therefore, may not have provided the realistic soil characteristics affecting UCRB hydrology, leading to streamflow simulation discrepancies.
- Associating the land-uses of the SANLC 2018 to SWAT was difficult as categorising the 73 SANLC 18 classes often resulted in different land-uses being incorporated in the same SWAT category, which reduced land-use variability in the UCRB, and hence, increased the uncertainty of streamflow predictions.

- Characterising the reservoirs of the UCRB resulted in challenges regarding the estimation of the emergency spillway volume and surface area and the number of days required to reach target storage, owing to a lack of reservoir data availability.
- Delineating the parameters influencing streamflow in the UCRB during the calibration process was arduous due to the number of parameters affecting streamflow in SWAT and their interaction affecting other SWAT parameters.

6.3 Recommendations

The successful calibration and validation of the SWAT model in the UCRB delineated numerous factors which may improve future SWAT streamflow studies:

- The target release approach to reservoir description proved beneficial in simulating reservoir releases in response to changing water availability in the UCRB. Therefore, it is suggested that the target release method be used when monthly or daily reservoir outflow data is insufficient.
- Developing a SWAT model that initially simulates stream discharge adequately is inherently difficult due to the numerous data requirements. However, this study notes the advantage of confirming that the initial model simulates a positive NSE prior to calibration and validation of the model, as an adequate NSE performance indicates a good hydrograph shape, which can be altered via calibration to agree with observed data.
- This study highlights the vital resource that is daily streamflow data. Five discharge stations within the UCRB contained high-quality daily streamflow data, which was paralleled with monthly stream discharges during the calibration process to certify that the calibrated parameters accurately reflected the UCRB's response on a daily and monthly basis.
- Improved monitoring data is required in the UCRB, particularly concerning its reservoirs, as the lack of available reservoir data necessitated the use of the target release approach during model synthesis, which increased the uncertainties surrounding model predictions.
- The SWAT model exhibited numerous discrepancies with measured data post-calibration, which indicated that its streamflow predictions were not entirely precise. Therefore, SWAT should be used in conjunction with other hydrological models to improve streamflow simulation reliability. In addition, SWAT streamflow studies

should be coupled with water quality studies such as sediment and nutrient loads to ensure that streamflow simulation represents the actual processes occurring in a watershed.

- The results of this study indicate that the developing change in UCRB's and South Africa's climate toward increased temperatures and reduced rainfalls have negative impacts for streamflow and water resources. Therefore, it is imperative that greenhouse gas emissions are reduced at the national and global scales to avoid or mitigate these climate changes and ensure water resources sustainability.
- Decreases in rainfall within southern Africa are also attributed to the El Niño event, which requires attention from authorities and decision-makers regarding the water policies considered to ensure adequate water accessibility in South Africa during rainfall abundant and deficient periods.

REFERENCES

Abbaspour K.C., 2015. SWAT-CUP 2012: SWAT calibration and uncertainty programs - A user manual, Switzerland: Eawag Aquatic Research.

Abbaspour, K.C., Rouholahnejad, E., Vaghefi, S.R.I.N.I.V.A.S.A.N.B., Srinivasan, R., Yang, H. and Kløve, B., 2015. A continental-scale hydrology and water quality model for Europe: Calibration and uncertainty of a high-resolution large-scale SWAT model. *Journal of hydrology*, *524*, pp.733-752.

Abiye, T.A., 2011. Provenance of groundwater in the crystalline aquifer of Johannesburg area, South Africa. *International Journal of Physical Sciences*, *6*(1), pp.98-111.

Abiye, T.A., Mengistu, H. and Demlie, M.B., 2011. Groundwater resource in the crystalline rocks of the Johannesburg area, South Africa. *J. Water Resour. Protection*, *3*(4), pp.199-212.

Abiye, T.A., 2013. Surface water and groundwater interaction in the upper Crocodile River basin. *The use of isotope hydrology to characterize and assess water resources in South (ern) Africa*, pp.141-163.

Abiye, T.A., 2014. Mine water footprint in the Johannesburg area, South Africa: analysis based on existing and measured data. *South African Journal of Geology*, *117*(1), pp.87-96.

Abiye, T.A., Mengistu, H., Masindi, K. and Demlie, M., 2015. Surface water and groundwater interaction in the upper Crocodile River Basin, Johannesburg, South Africa: Environmental isotope approach. *South African Journal of Geology*, *118*(2), pp.109-118.

Ahn, K.H. and Merwade, V., 2014. Quantifying the relative impact of climate and human activities on streamflow. *Journal of Hydrology*, *515*, pp.257-266.

Anhaeusser, C.R., 1971. *The Geology and Geochemistry of the Archaen Granites and Gneisses of the Johannesburg-Pretoria Dome* (No. 62). University of the Witwatersrand, Economic Geology Research Unit.

Arnell, N.W. and Liv, C., 2001. Hydrology and water resources.

Arnold J.G., Moriasi D.N., Gassman P.W., Abbaspour K.C., White M.J., Srinivasan R., Santhi C., Harmel R.D., van Griensven A., Van Liew M.W., Kannan N., Jha M.K. 2012. SWAT:

Model use, calibration and validation. *American Society of Agricultural and Biological Engineers 55*: 1491-1508.

ASSAf (2017) First biennial report to cabinet on the state of climate change science technology in South Africa. South Africa (ASSAf).

Baker, T.J. and Miller, S.N., 2013. Using the Soil and Water Assessment Tool (SWAT) to assess land use impact on water resources in an East African watershed. *Journal of hydrology*, *486*, pp.100-111.

Barnard H.C., 2000. An explanation of the 1:500 000 general hydrogeological map. Pretoria, South Africa.

Bouraoui, F., Benabdallah, S., Jrad, A. and Bidoglio, G., 2005. Application of the SWAT model on the Medjerda river basin (Tunisia). *Physics and Chemistry of the Earth, Parts A/B/C*, *30*(8-10), pp.497-507.

Bosch, N.S., 2008. The influence of impoundments on riverine nutrient transport: An evaluation using the Soil and Water Assessment Tool. *Journal of Hydrology*, *355*(1-4), pp.131-147.

Bosch, J.M. and Hewlett, J.D., 1982. A review of catchment experiments to determine the effect of vegetation changes on water yield and evapotranspiration. *Journal of hydrology*, *55*(1-4), pp.3-23.

Brath, A., Montanari, A. and Moretti, G., 2006. Assessing the effect on flood frequency of land use change via hydrological simulation (with uncertainty). *Journal of Hydrology*, *324*(1-4), pp.141-153.

Brock, B. B., and Pretorius, D. A., 1964. The geology of the Central Rand Goldfield. In Haughton, S. H., Ed., The Geology of Some Ore Deposits in Southern Africa. *Geol. Soc. S. Afr., vol. I*, 63-108.

Brown, A.E., Zhang, L., McMahon, T.A., Western, A.W. and Vertessy, R.A., 2005. A review of paired catchment studies for determining changes in water yield resulting from alterations in vegetation. *Journal of hydrology*, *310*(1-4), pp.28-61.

Budyko, M.I., 1974. *Climate and life*. Academic press.

Callaway, J.M., 2004. Adaptation benefits and costs: how important are they in the global policy picture and how can we estimate them? *Global environmental change. 14,* 273-284.

Cao, W., Bowden, W.B., Davie, T. and Fenemor, A., 2006. Multi-variable and multi-site calibration and validation of SWAT in a large mountainous catchment with high spatial variability. *Hydrological Processes: An International Journal*, *20*(5), pp.1057-1073.

Cawthorn, R.G., 2006. Centenary of the Discovery of Platinum in the Bushveld Complex. *Platinum Metals Review*, *50*(3), pp.130-133.

Che, Z., 1995. Discussing the empirical formula and graph of soil permeability coefficient. *Water Resour. Hydropower Northeast China*, *9*, pp.17-19.

Cheng, S.J. and Wang, R.Y., 2002. An approach for evaluating the hydrological effects of urbanization and its application. *Hydrological Processes*, *16*(7), pp.1403-1418.

Choi, W. and Deal, B.M., 2008. Assessing hydrological impact of potential land use change through hydrological and land use change modeling for the Kishwaukee River basin (USA). *Journal of Environmental Management*, *88*(4), pp.1119-1130.

Chow, V. T., Maidment, D. R. & Mavs, L. W. (1988) *Applied Hydrology*, McGraw-Hill, New York,

Cotter, A.S., Chaubey, I., Costello, T.A., Soerens, T.S. and Nelson, M.A., 2003. Water quality model output uncertainty as affected by spatial resolution of input data 1. *JAWRA Journal of the American Water Resources Association*, *39*(4), pp.977-986.

Cukic, E.Z. and Venter, P., 2012. Sediment removal and management: Hartbeespoort Dam remediation. *Civil Engineering= Siviele Ingenieurswese*, *2012*(7), pp.42-47.

Dale, V.H., 1997. The relationship between land-use change and climate change. *Ecological applications, 7(3)*, pp.753-769.

Department of Water Affairs and Forestry (2004) Crocodile River (West) and Marico water management area: Internal strategic perspective of the Crocodile River (West) catchment. Department of Water Affairs and Forestry, Pretoria, South Africa.

Department of Water Affairs and Forestry (2008) The development of a reconciliation strategy for the Crocodile (West) water supply system: Summary of previous and current studies. Department of Water Affairs, Pretoria, South Africa.

Dey, P. and Mishra, A., 2017. Separating the impacts of climate change and human activities on streamflow: A review of methodologies and critical assumptions. *Journal of Hydrology*, *548*, pp.278-290.

Devia, G.K., Ganasri, B.P. and Dwarakish, G.S., 2015. A review on hydrological models. *Aquatic procedia*, *4*, pp.1001-1007.

Dile Y, Srinivasan R, George C. 2015. QGIS interface for SWAT (QSWAT): User manual for QSWAT version 1.4.

Dooge, J.C.I., 1992. Hydrologic models and climate change. *Journal of Geophysical Research: Atmospheres*, *97*(D3), pp.2677-2686.

Dudula, M.Z., 2007. *A situation analysis of the water quality in the Hartbeespoort dam catchment: nutrients and other pollutants' assessment on rivers entering the dam* (Doctoral dissertation).

Edokpayi, J.N., Odiyo, J.O., Msagati, T.A. and Popoola, E.O., 2015. A Novel Approach for the removal of lead (II) ion from wastewater using mucilaginous leaves of diceriocaryum eriocarpum plant. *Sustainability*, *7*(10), pp.14026-14041.

Edokpayi, J.N., Odiyo, J.O. and Durowoju, O.S., 2017. Impact of wastewater on surface water quality in developing countries: a case study of South Africa. *Water quality*, pp.401-416.

Engel, B., D. Storm, M. White, J. Arnold, and M. Arabi. 2007. A hydrologic/water quality model application protocol. *J. American Water Resour. Assoc. 43(5)*: 1223-1236

Engelbrecht, F., Adegoke, J., Bopape, M.J., Naidoo, M., Garland, R., Thatcher, M., McGregor, J., Katzfey, J., Werner, M., Ichoku, C. and Gatebe, C., 2015. Projections of rapidly rising surface temperatures over Africa under low mitigation. *Environmental Research Letters*, *10*(8), p.085004.

Eriksson, P.G., Altermann, W., Hartzer, F.J., Johnson, M.R., Anhaeusser, C.R. and Thomas, R.J., 2006. The Transvaal Supergroup and its precursors. *The Geology of South Africa*, pp.237-260.

Fadil, A., Rhinane, H., Kaoukaya, A., Kharchaf, Y. and Bachir, O.A., 2011. Hydrologic modeling of the Bouregreg watershed (Morocco) using GIS and SWAT model. *Journal of Geographic Information System*, *3*(04), p.279.

Feyen, L., Vázquez, R., Christiaens, K., Sels, O. and Feyen, J., 2000. Application of a distributed physically-based hydrological model to a medium size catchment. *Hydrology and Earth System Sciences*, *4*(1), pp.47-63.

Fisher, J.I. and Mustard, J.F., 2004. High spatial resolution sea surface climatology from Landsat thermal infrared data. *Remote Sensing of Environment*, *90*(3), pp.293-307.

Fu, G., Charles, S.P. and Chiew, F.H., 2007. A two-parameter climate elasticity of streamflow index to assess climate change effects on annual streamflow. *Water Resources Research*, *43*(11).

Fukunaga, D.C., Cecílio, R.A., Zanetti, S.S., Oliveira, L.T. and Caiado, M.A.C., 2015. Application of the SWAT hydrologic model to a tropical watershed at Brazil. *Catena*, *125*, pp.206-213.

Gallego-Ayala, J. and Juízo, D., 2011. Strategic implementation of integrated water resources management in Mozambique: An A'WOT analysis. *Physics and Chemistry of the Earth, Parts A/B/C*, *36*(14-15), pp.1103-1111.

Ghaffari, G., Keesstra, S., Ghodousi, J. and Ahmadi, H., 2010. SWAT-simulated hydrological impact of land-use change in the Zanjanrood basin, Northwest Iran. *Hydrological Processes: An International Journal*, *24*(7), pp.892-903.

Ghidey, F., Sadler, E.J., Lerch, R.N. and Baffaut, C., 2007. Scaling up the SWAT model from goodwater creek experimental watershed to the long branch watershed. In *2007 ASAE Annual Meeting* (p. 1). American Society of Agricultural and Biological Engineers.

Glavan, M., White, S. and Holman, I.P., 2011. Evaluation of river water quality simulations at a daily time step–Experience with SWAT in the Axe Catchment, UK. *CLEAN–Soil, Air, Water*, *39*(1), pp.43-54.

Gleick, P.H., 1989. Climate change, hydrology, and water resources. *Reviews of Geophysics*, *27*(3), pp.329-344.

Govender, M. and Everson, C.S., 2005. Modelling streamflow from two small South African experimental catchments using the SWAT model. *Hydrological Processes: An International Journal*, *19*(3), pp.683-692.

Graham, L.P., Andersson, L., Horan, M., Kunz, R., Lumsden, T., Schulze, R., Warburton, M., Wilk, J. and Yang, W., 2011. Using multiple climate projections for assessing hydrological

response to climate change in the Thukela River Basin, South Africa. *Physics and Chemistry of the Earth, Parts A/B/C*, *36*(14-15), pp.727-735.

Gupta, H.V., Sorooshian, S. and Yapo, P.O., 1999. Status of automatic calibration for hydrologic models: Comparison with multilevel expert calibration. *Journal of hydrologic engineering*, *4*(2), pp.135-143.

Gyamfi, C., Ndambuki, J.M. and Salim, R.W., 2016. Application of SWAT model to the Olifants Basin: calibration, validation and uncertainty analysis. *Journal of Water Resource and Protection*, *8*(03), p.397.

Healy, R.W., 2010. *Estimating groundwater recharge*. Cambridge university press.

Himanshu, S.K., Pandey, A., Yadav, B. and Gupta, A., 2019. Evaluation of best management practices for sediment and nutrient loss control using SWAT model. *Soil and Tillage Research*, *192*, pp.42-58.

IPCC, 2001: *Climate Change 2001: The Scientific Basis. Contribution of Working Group I to the Third Assessment Report of the Intergovernmental Panel on Climate Change* [Houghton, J.T., Y. Ding, D.J. Griggs, M. Noguer, P.J. van der Linden, X. Dai, K. Maskell, and C.A. Johnson (eds.)]. Cambridge University Press, Cambridge, United Kingdom and New York, NY, USA, 881pp.

IPCC, 2007: *Climate Change 2007: Synthesis Report. Contribution of Working Groups I, II and III to the Fourth Assessment Report of the Intergovernmental Panel on Climate Change* [Core Writing Team, Pachauri, R.K and Reisinger, A. (eds.)]. IPCC, Geneva, Switzerland, 104 pp.

IPCC, 2013: *Summary for Policymakers. In: Climate Change 2013: The Physical Science Basis. Contribution of Working Group I to the Fifth Assessment Report of the Intergovernmental Panel on Climate Change* [Stocker, T.F., D. Qin, G.-K. Plattner, M. Tignor, S.K. Allen, J. Boschung, A. Nauels, Y. Xia, V. Bex and P.M. Midgley (eds.)]. Cambridge University Press, Cambridge, United Kingdom and New York, NY, USA

IPCC, 2021: Summary for Policymakers. In: *Climate Change 2021: The Physical Science Basis. Contribution of Working Group I to the Sixth Assessment Report of the Intergovernmental Panel on Climate Change* [Masson-Delmotte, V., P. Zhai, A. Pirani, S. L. Connors, C. Péan, S. Berger, N. Caud, Y. Chen, L. Goldfarb, M. I. Gomis, M. Huang, K.

Leitzell, E. Lonnoy, J.B.R. Matthews, T. K. Maycock, T. Waterfield, O. Yelekçi, R. Yu and B. Zhou (eds.)]. Cambridge University Press. In Press.

Jayakrishnan, R.S.R.S., Srinivasan, R., Santhi, C. and Arnold, J.G., 2005. Advances in the application of the SWAT model for water resources management. *Hydrological Processes: An International Journal*, *19*(3), pp.749-762.

Kannan, N., Santhi, C., White, M.J., Mehan, S., Arnold, J.G. and Gassman, P.W., 2019. Some challenges in hydrologic model calibration for large-scale studies: a case study of SWAT model application to Mississippi-Atchafalaya River Basin. *Hydrology*, *6*(1), p.17.

Kim, H. and Parajuli, P.B., 2012. Impacts of Reservoir Operation in the SWAT Model Calibration. In *2012 Dallas, Texas, July 29-August 1, 2012* (p. 1). American Society of Agricultural and Biological Engineers.

Krause, P., Boyle, D.P. and Bäse, F., 2005. Comparison of different efficiency criteria for hydrological model assessment. *Advances in geosciences*, *5*, pp.89-97.

Krysanova, V. and Srinivasan, R., 2015. Assessment of climate and land use change impacts with SWAT.

Kuchment, L.S., 2004. The hydrological cycle and human impact on it. *Water Resources Management, p.40.* Available at: https://d1wqtxts1xzle7.cloudfront.net/33519959/ (Accessed: 21 May 2020).

Kundzewicz, Z.W., Mata, L.J., Arnell, N.W., Döll, P., Jimenez, B., Miller, K., Oki, T., Şen, Z. and Shiklomanov, I., 2008. The implications of projected climate change for freshwater resources and their management. *Hydrological sciences journal*, *53(1)*, pp.3-10.

Kusangaya, S., Warburton, M.L., Van Garderen, E.A. and Jewitt, G.P., 2014. Impacts of climate change on water resources in southern Africa: A review. *Physics and Chemistry of the Earth, Parts A/B/C*, *67*, pp.47-54.

Legates, D.R. and McCabe Jr, G.J., 1999. Evaluating the use of "goodness-of-fit" measures in hydrologic and hydroclimatic model validation. *Water resources research*, *35*(1), pp.233-241.

Legesse, D., Abiye, T.A., Vallet-Coulomb, C. and Abate, H., 2010. Streamflow sensitivity to climate and land cover changes: Meki River, Ethiopia. *Hydrology and Earth System Sciences*, *14*(11), pp.2277-2287.

Leketa, K., Abiye, T. and Butler, M., 2018. Characterisation of groundwater recharge conditions and flow mechanisms in bedrock aquifers of the Johannesburg area, South Africa. *Environmental Earth Sciences*, *77*(21), pp.1-11.

Leketa, K.C., 2019. *Holistic approach to groundwater recharge assessment in the Upper Crocodile River Basin, Johannesburg, South Africa* (Doctoral dissertation).

Leketa, K. and Abiye, T., 2019. Modelling the impacts of climatic variables on the hydrology of the Upper Crocodile River Basin, Johannesburg, South Africa. *Environmental Earth Sciences*, *78*(12), pp.1-16.

Leketa, K., Abiye, T., Zondi, S. and Butler, M., 2019. Assessing groundwater recharge in crystalline and karstic aquifers of the Upper Crocodile River Basin, Johannesburg, South Africa. *Groundwater for Sustainable Development*, *8*, pp.31-40.

Li, Z., Liu, W.Z., Zhang, X.C. and Zheng, F.L., 2009. Impacts of land use change and climate variability on hydrology in an agricultural catchment on the Loess Plateau of China. *Journal of hydrology*, *377*(1-2), pp.35-42.

Mango, L.M., Melesse, A.M., McClain, M.E., Gann, D. and Setegn, S., 2011. Land use and climate change impacts on the hydrology of the upper Mara River Basin, Kenya: results of a modeling study to support better resource management. *Hydrology and Earth System Sciences*, *15*(7), pp.2245-2258.

Matalas, N.C., Winter, T.C., Harvey, J.W., Franke, O.L. and Alley, W.M., 1998. *Ground water and surface water: a single resource* (Vol. 1139). DIANE Publishing Inc.

McCarthy, T. S., and Rubidge, B., 2005. The story of earth & life. A Southern African perspective. Cape Town: Struik Nature, Random House Struik (Pty) Ltd. 333p.

Me, W., Abell, J.M. and Hamilton, D.P., 2015. Effects of hydrologic conditions on SWAT model performance and parameter sensitivity for a small, mixed land use catchment in New Zealand. *Hydrology and Earth System Sciences*, *19*(10), pp.4127-4147.

Mengistu, A.G., van Rensburg, L.D. and Woyessa, Y.E., 2019. Techniques for calibration and validation of SWAT model in data scarce arid and semi-arid catchments in South Africa. *Journal of Hydrology: Regional Studies*, *25*, p.100621.

Moon J, Kim J-H, Yoo C. 2004. Storm-coverage effect on dynamic flood frequency analysis: empirical data analysis. *Hydrological Processes 18: 159–178.*

Moriasi, D.N., Arnold, J.G., Van Liew, M.W., Bingner, R.L., Harmel, R.D. and Veith, T.L., 2007. Model evaluation guidelines for systematic quantification of accuracy in watershed simulations. *Transactions of the ASABE*, *50*(3), pp.885-900.

Moriasi, D.N., Gitau, M.W., Pai, N. and Daggupati, P., 2015. Hydrologic and water quality models: Performance measures and evaluation criteria. *Transactions of the ASABE*, *58*(6), pp.1763-1785.

Motsinger, J., Kalita, P. and Bhattarai, R., 2016. Analysis of best management practices implementation on water quality using the soil and water assessment tool. *Water*, *8*(4), p.145.

Mwangi, H.M., Julich, S., Patil, S.D., McDonald, M.A. and Feger, K.H., 2016. Modelling the impact of agroforestry on hydrology of Mara River Basin in East Africa. *Hydrological Processes*, *30*(18), pp.3139-3155.

Narsimlu, B., Gosain, A.K. and Chahar, B.R., 2013. Assessment of future climate change impacts on water resources of Upper Sind River Basin, India using SWAT model. *Water resources management*, *27*(10), pp.3647-3662.

Nash, J.E. and Sutcliffe, J.V., 1970. River flow forecasting through conceptual models part I—A discussion of principles. *Journal of hydrology*, *10*(3), pp.282-290.

Nazari-Sharabian, M., Taheriyoun, M. and Karakouzian, M., 2020. Sensitivity analysis of the DEM resolution and effective parameters of runoff yield in the SWAT model: a case study. *Journal of Water Supply: Research and Technology-Aqua*, *69*(1), pp.39-54.

Neitsch, S.L., Arnold, J.G., Kiniry, J.R. and Williams, J.R. (2011) Soil and Water Assessment Tool Theoretical Documentation Version 2009. Texas Water Resources Institute Technical Report No. 406.

Ngubane, Z., 2017. *Catchment Hydrological Modelling Using ArcSWAT: A study of the Ingula Pumped Storage Scheme (IPSS) Catchments, South Africa.* Unpublished.

Niel, H., Paturel, J.E. and Servat, E., 2003. Study of parameter stability of a lumped hydrologic model in a context of climatic variability. *Journal of Hydrology*, *278*(1-4), pp.213-230.

Niraula, R., Kalin, L., Wang, R. and Srivastava, P., 2011. Determining nutrient and sediment critical source areas with SWAT: effect of lumped calibration. *Transactions of the ASABE*, *55*(1), pp.137-147.

Piniewski, M. and Okruszko, T., 2011. Multi-site calibration and validation of the hydrological component of SWAT in a large lowland catchment. In *Modelling of hydrological processes in the narew catchment* (pp. 15-41). Springer, Berlin, Heidelberg.

Pohlert, T., Huisman, J.A., Breuer, L. and Frede, H.G., 2005. Modelling of point and non-point source pollution of nitrate with SWAT in the river Dill, Germany. *Advances in Geosciences*, *5*, pp.7-12.

Pretorius, D.A., 1976. The nature of the Witwatersrand gold-uranium deposits, ch. 2. In *Handbook of strata-bound and stratiform ore deposits; section 2., regional studies and specific deposits*.

Prowse, T.D., Wrona, F.J., Reist, J.D., Gibson, J.J., Hobbie, J.E., Lévesque, L.M. and Vincent, W.F., 2006. Climate change effects on hydroecology of Arctic freshwater ecosystems. *AMBIO: A Journal of the Human Environment*, *35(7)*, pp.347-358.

Querner, E.P. and Zanen, M.V., 2013. *Modelling water quantity and quality using SWAT: A case study in the Limpopo River basin, South Africa* (No. 2405). Wageningen.

Refsgaard, J.C., 1997. Parameterisation, calibration and validation of distributed hydrological models. *Journal of hydrology*, *198*(1-4), pp.69-97.

Robb, L.J. and Meyer, F.M., 1995. The Witwatersrand Basin, South Africa: geological framework and mineralization processes. *Ore Geology Reviews*, *10*(2), pp.67-94.

Roberts, M.C. and Klingeman, P.C., 1970. The influence of landform and precipitation parameters on flood hydrographs. *Journal of Hydrology*, *11*(4), pp.393-411.

Romagnoli, M., Portapila, M., Rigalli, A., Maydana, G., Burgués, M. and García, C.M., 2017. Assessment of the SWAT model to simulate a watershed with limited available data in the Pampas region, Argentina. *Science Of The Total Environment*, *596*, pp.437-450.

Romanowicz, A.A., Vanclooster, M., Rounsevell, M. and La Junesse, I., 2005. Sensitivity of the SWAT model to the soil and land use data parametrisation: a case study in the Thyle catchment, Belgium. *Ecological modelling*, *187*(1), pp.27-39.

Rose, S. and Peters, N.E., 2001. Effects of urbanization on streamflow in the Atlanta area (Georgia, USA): a comparative hydrological approach. *Hydrological Processes*, *15*(8), pp.1441-1457.

Saha, P.P., Zeleke, K. and Hafeez, M., 2014. Streamflow modeling in a fluctuant climate using SWAT: Yass River catchment in south eastern Australia. *Environmental earth sciences*, *71*(12), pp.5241-5254.

Santhi, C., Arnold, J.G., Williams, J.R., Dugas, W.A., Srinivasan, R. and Hauck, L.M., 2001. Validation of the swat model on a large rwer basin with point and nonpoint sources 1. *JAWRA Journal of the American Water Resources Association*, *37*(5), pp.1169-1188.

Schaake, J.C., 1990. From climate to flow. *Climate change and US water resources.*, pp.177-206.

Schuol, J. and Abbaspour, K.C., 2006. Calibration and uncertainty issues of a hydrological model (SWAT) applied to West Africa. *Advances in geosciences*, *9*, pp.137-143.

Schuol, J., Abbaspour, K.C., Srinivasan, R. and Yang, H., 2008. Estimation of freshwater availability in the West African sub-continent using the SWAT hydrologic model. *Journal of hydrology*, *352*(1-2), pp.30-49.

Serpa, D., Nunes, J.P., Santos, J., Sampaio, E., Jacinto, R., Veiga, S., Lima, J.C., Moreira, M., Corte-Real, J., Keizer, J.J. and Abrantes, N., 2015. Impacts of climate and land use changes on the hydrological and erosion processes of two contrasting Mediterranean catchments. *Science of the Total Environment*, *538*, pp.64-77.

Servat, E. and Dezetter, A., 1991. Selection of calibration objective fonctions in the context of rainfall-ronoff modelling in a Sudanese savannah area. *Hydrological Sciences Journal*, *36*(4), pp.307-330.

Sood A. and Ritter W.F. 2010. Evaluation of best management practices in Millsboro pond watershed using soil and water assessment tool (SWAT) model. *J. Water Resour. Protect. 2(5)*: 403–412.

Sorooshian, S. and Gupta, V.K., 1983. Automatic calibration of conceptual rainfall-runoff models: The question of parameter observability and uniqueness. *Water Resources Research*, *19*(1), pp.260-268.

Srinivasan, R., Zhang, X. and Arnold, J., 2010. SWAT ungauged: hydrological budget and crop yield predictions in the Upper Mississippi River Basin. *Transactions of the ASABE*, *53*(5), pp.1533-1546.

Stehr, A., Debels, P., Romero, F. and Alcayaga, H., 2008. Hydrological modelling with SWAT under conditions of limited data availability: evaluation of results from a Chilean case study. *Hydrological sciences journal*, *53*(3), pp.588-601.

Tessema, S.M., 2011. *Hydrological modeling as a tool for sustainable water resources management: a case study of the Awash River Basin* (Doctoral dissertation, KTH Royal Institute of Technology).

Thavhana, M.P., Savage, M.J. and Moeletsi, M.E., 2018. SWAT model uncertainty analysis, calibration and validation for runoff simulation in the Luvuvhu River catchment, South Africa. *Physics and Chemistry of the Earth, Parts A/B/C*, *105*, pp.115-124.

Tomer, M.D. and Schilling, K.E., 2009. A simple approach to distinguish land-use and climate-change effects on watershed hydrology. *Journal of hydrology*, *376*(1-2), pp.24-33.

Tong, S.T., Liu, A.J. and Goodrich, J.A., 2009. Assessing the water quality impacts of future land-use changes in an urbanising watershed. *Civil Engineering and Environmental Systems*, *26*(1), pp.3-18.

Trenberth, K.E., 1999. Conceptual framework for changes of extremes of the hydrological cycle with climate change. In *Weather and climate extremes* (pp. 327-339). Springer, Dordrecht.

Vaghefi, S.A., Mousavi, S.J., Abbaspour, K.C., Srinivasan, R. and Arnold, J.R., 2015. Integration of hydrologic and water allocation models in basin-scale water resources management considering crop pattern and climate change: Karkheh River Basin in Iran. *Regional environmental change*, *15*(3), pp.475-484.

Van der Westhuizen, W.A., De Bruiyn, H. and Meintjes, P.G., 1991. The Ventersdorp supergroup: an overview. *Journal of African Earth Sciences (and the Middle East)*, *13*(1), pp.83-105.

Van Liew, M.W., Arnold, J.G. and Garbrecht, J.D., 2003. Hydrologic simulation on agricultural watersheds: Choosing between two models. *Transactions of the ASAE*, *46*(6), p.1539.

Wagner, P.D., Kumar, S. and Schneider, K., 2013. An assessment of land use change impacts on the water resources of the Mula and Mutha Rivers catchment upstream of Pune, India. *Hydrology and Earth System Sciences*, *17*(6), pp.2233-2246.

Watson, B., Ghafouri, M. and Selvalingam, S., 2003, January. Application of SWAT to model the water balance of the Woady Yaloak River catchment, Australia. In *SWAT 2003: 2nd International SWAT Conference* (pp. 94-110). USDA-ARS Research Lab.

Welderufael, W.A., Tetsoane, S.T. and Woyessa, Y.E., 2013. Evaluation of the SWAT model in simulating catchment hydrology: case study of the Modder River Basin.

Williams, J.R., 1995. The EPIC model. In: Computer Models of Watershed Hydrology. Water Resources Publications, pp. 909–1000.

Winter T.C., 1998. Ground water and surface water: a single resource. US Geological Survey circular. US Geological Survey, Denver

WWF-SA 2016, Water: Facts & Futures. Available at: http://awsassets.wwf.org.za/downloads/

Yang, S., Dong, G., Zheng, D., Xiao, H., Gao, Y. and Lang, Y., 2011. Coupling Xinanjiang model and SWAT to simulate agricultural non-point source pollution in Songtao watershed of Hainan, China. *Ecological Modelling*, *222*(20-22), pp.3701-3717.

Ye, X., Zhang, Q., Liu, J., Li, X. and Xu, C.Y., 2013. Distinguishing the relative impacts of climate change and human activities on variation of streamflow in the Poyang Lake catchment, China. *Journal of Hydrology*, *494*, pp.83-95.

Zeckoski, R.W., Smolen, M.D., Moriasi, D.N., Frankenberger, J.R. and Feyereisen, G.W., 2015. Hydrologic and water quality terminology as applied to modeling. *Transactions of the ASABE*, *58*(6), pp.1619-1635.

Zettam, A., Taleb, A., Sauvage, S., Boithias, L., Belaidi, N. and Sánchez-Pérez, J.M., 2017. Modelling hydrology and sediment transport in a semi-arid and anthropized catchment using the SWAT model: The case of the Tafna river (northwest Algeria). *Water*, *9*(3), p.216.

Zhang, Y., Guan, D., Jin, C., Wang, A., Wu, J. and Yuan, F., 2011. Analysis of impacts of climate variability and human activity on streamflow for a river basin in northeast China. *Journal of Hydrology*, *410*(3-4), pp.239-247.

Zhao, F.F., Zhang, L. and Xu, Z.X., 2009, July. Estimating the effects of vegetation cover change on streamflow at different spatial scales. In *18th World IMACS Congress and MODSIM09 International Congress on Modelling and Simulation* (pp. 3591-3597). Modelling

and Simulation Society of Australia and New Zealand and International Association for Mathematics and Computers in Simulation Canberra, ACT Australia.

Zhao, F., Zhang, L., Xu, Z. and Scott, D.F., 2010. Evaluation of methods for estimating the effects of vegetation change and climate variability on streamflow. *Water Resources Research*, *46*(3).

Zheng, C., Hill, M. C., Cao, G., and Ma, R., 2012. MT3DMS: Model use, calibration, and validation. *Trans. ASABE, 55(4)*, 1549-1559.

Ziervogel, G., New, M., Archer van Garderen, E., Midgley, G., Taylor, A., Hamann, R., Stuart-Hill, S., Myers, J. and Warburton, M., 2014. Climate change impacts and adaptation in South Africa. *Wiley Interdisciplinary Reviews: Climate Change*, *5*(5), pp.605-620.

Zondi, S.N., 2017. *Recharge rates and processes in the upper Crocodile catchment* (Doctoral dissertation).

Zuo, D., Xu, Z., Wu, W., Zhao, J. and Zhao, F., 2014. Identification of streamflow response to climate change and human activities in the Wei River Basin, China. *Water Resources Management*, *28*(3), pp.833-851.

APPENDIX A: METHODOLOGY

Table A.1: The Land-use lookup table showing the 73 SANLC 2018 land-use classes associated using SWAT codes

LAND-USE ID	SANLC 2018 Description	SWAT CODE	LAND-USE ID	SANLC 2018 Description	SWAT CODE
1	Contiguous Forest	FRSD	**38**	Irrigated Land	AGRL
2	Contiguous Low Forest and Thicket	FRST	**39**	Irrigated Land	AGRL
3	Dense Forest & Woodland	FRSE	**40**	Commercial Crops	AGRL
4	Open Woodland	FRST	**41**	Subsistence Crops	AGRC
5	Contiguous and Dense Planted Forest	FRSE	**42**	Trees	FRSD
6	Open and Sparse Planted Forest	FRST	**43**	Bush	FRST
7	Temporary Unplanted Forest	FRST	**44**	Grass	RNGE
8	Low Shrubland	RNGB	**45**	Bare	SWRN
9	Fynbos	RNGE	**46**	Low Shrubland	RNGB
10	Succulent Karoo	RNGE	**47**	Residential Trees	FRSD
11	Nama Karoo	RNGB	**48**	Residential Bush	FRST
12	Sparsely Wooded Grassland	FRST	**49**	Residential Grass	RNGE
13	Natural Grassland	RNGE	**50**	Residential Bare	URML
14	Rivers	WATR	**51**	Residential Informal Trees	FRSD
15	Estuaries and Lagoons	WATR	**52**	Residential Informal Bush	FRST
16	Ocean	WATR	**53**	Residential Informal Grass	RNGE
17	Lakes	WATR	**54**	Residential informal Bare	URML
18	Pans	WATR	**55**	Village Bare	URML
19	Dams	WATR	**56**	Village Dense Bare	URHD
20	Sewage Ponds	WATR	**57**	Smallholdings Trees	FRSD
21	Flooded Mine Pits	WATR	**58**	Smallholdings Bush	FRST
22	Herbaceous Wetlands	WETN	**59**	Smallholdings Grass	RNGE
23	Herbaceous Wetlands	WETN	**60**	Smallholdings Bare	SWRN
24	Mangrove Wetlands	WETF	**61**	Field Trees	FRSD
25	Natural Rock Surfaces	SWRN	**62**	Field Bush	FRST
26	Dry Pans	SWRN	**63**	Field Grass	RNGE
27	Eroded Lands	SWRN	**64**	Field Bare	SWRN
28	Sand Dunes	SWRN	**65**	Commercial Crops	UCOM
29	Beach Sand	SWRN	**66**	Industrial	UIDU
30	Bare Riverbed Material	SWRN	**67**	Roads and Railways	UTRN
31	Other Bare	SWRN	**68**	Mines	UIDU
32	Orchards	ORCD	**69**	Open cast and Quarries	SWRN
33	Vineyards	ORCD	**70**	Salt Mines	SWRN
34	Sugarcane	AGRR	**71**	Tailing Dumps	SWRN
35	Pineapples	ORCD	**72**	Landfills	SWRN
36	Sugarcane	AGRR	**73**	Wetlands	WETN
37	Sugarcane	AGRR			

Table A.2: The soil look-up table used in SWAT HRU creation where SOIL_ID is the raster image shape identifier and SNAM is the soil name located in the usersoil table

SOIL_ID	SNAM	SOIL_ID	SNAM
30914	ZA802	**30793**	ZA686
30908	ZA797	**30790**	ZA683
30906	ZA794	**30789**	ZA682
30905	ZA793	**30778**	ZA671
30900	ZA788	**30773**	ZA666
30889	ZA778	**30770**	ZA663
30885	ZA773	**30769**	ZA662
30882	ZA770	**30761**	ZA655
30880	ZA769	**30752**	ZA647
30877	ZA766	**30750**	ZA645
30873	ZA761	**30749**	ZA644
30869	ZA756	**30748**	ZA643
30867	ZA754	**30742**	ZA637
30864	ZA750	**30736**	ZA631
30862	ZA749	**30722**	ZA617
30860	ZA747	**30720**	ZA614
30857	ZA744	**30712**	ZA607
30856	ZA743	**30710**	ZA605
30847	ZA735	**30708**	ZA602
30846	ZA734	**30703**	ZA599
30832	ZA720	**30700**	ZA596
30827	ZA716	**30699**	ZA595
30825	ZA714	**30690**	ZA587
30824	ZA713	**30681**	ZA578
30822	ZA711	**30674**	ZA571
30817	ZA707	**30668**	ZA566
30815	ZA705	**30658**	ZA556
30814	ZA704	**30648**	ZA547
30812	ZA702	**30629**	ZA527
30811	ZA701	**30624**	ZA522
30802	ZA694	**30608**	ZA507
30796	ZA689	**30505**	ZA407
30794	ZA687		

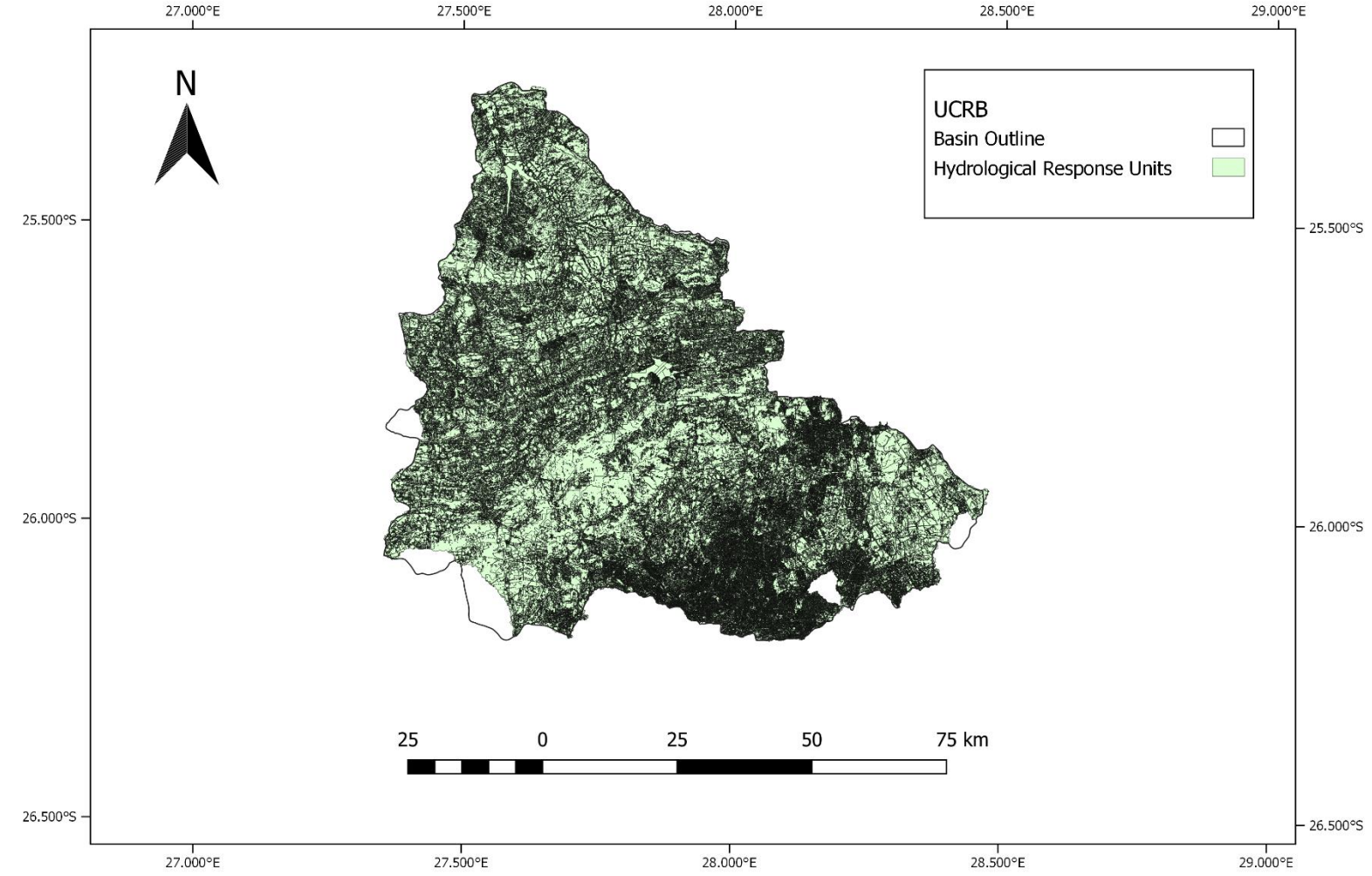


Figure A.1: The 8863 HRUs generated for the UCRB during the Create HRUs stage of model development

APPENDIX B: RESULTS

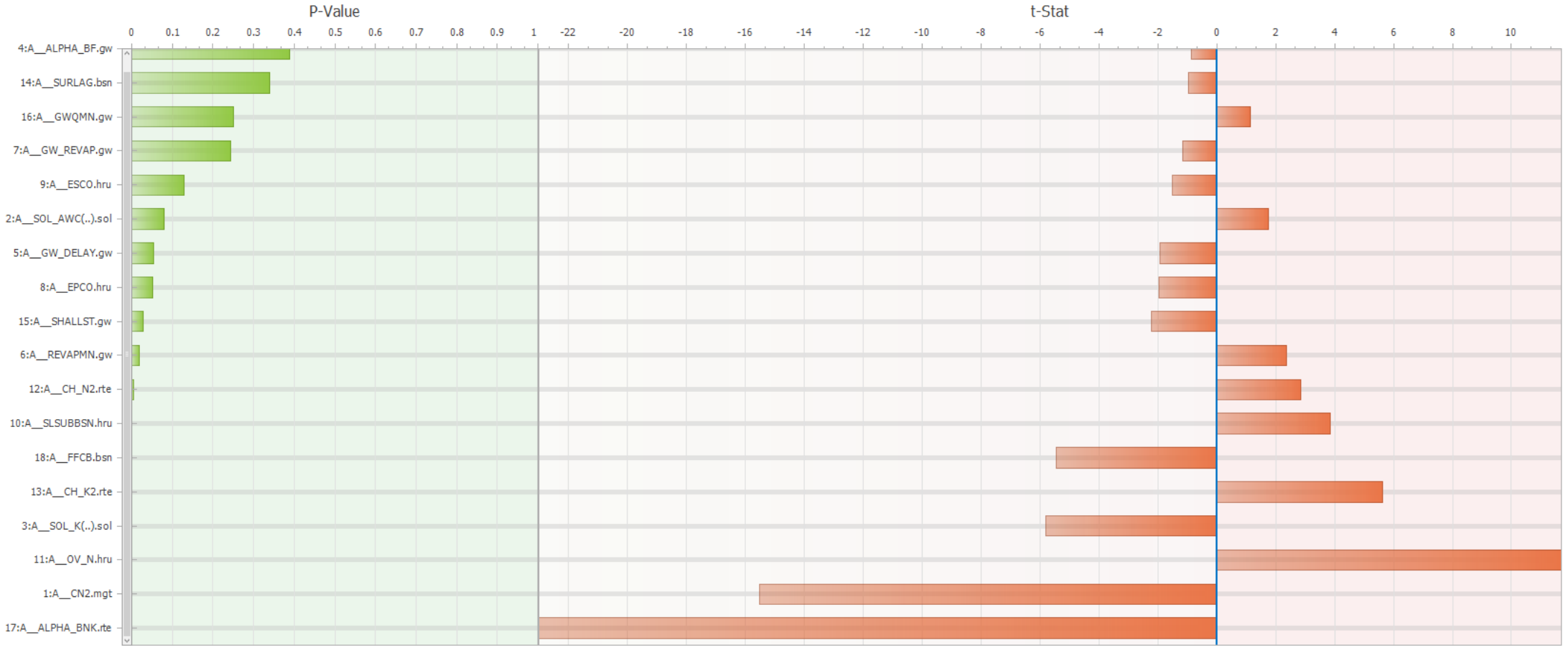


Figure B.1: The sensitivity analysis graph showing the sensitivities of the different parameters considered for SWATCUP calibration

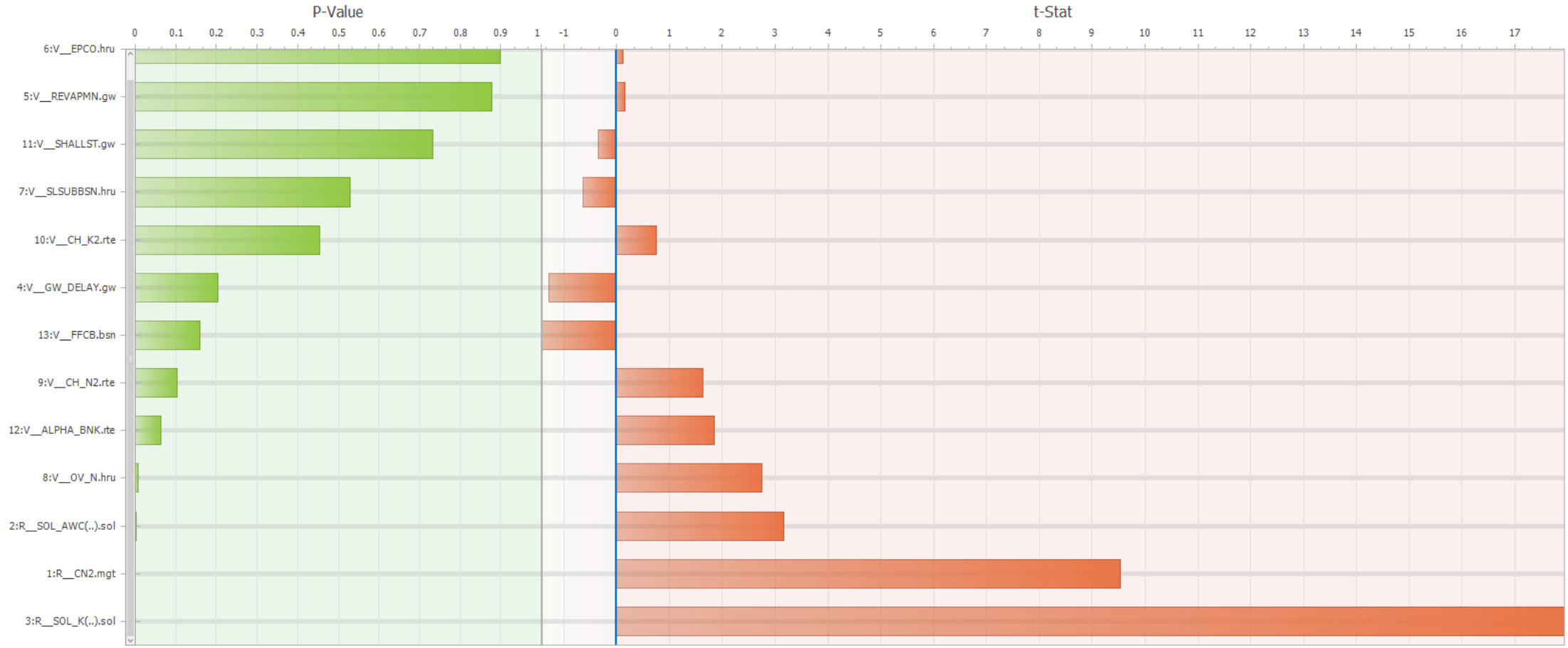


Figure B.2: The sensitivity analysis graph of the 13 parameters used to achieve the best results during model calibration

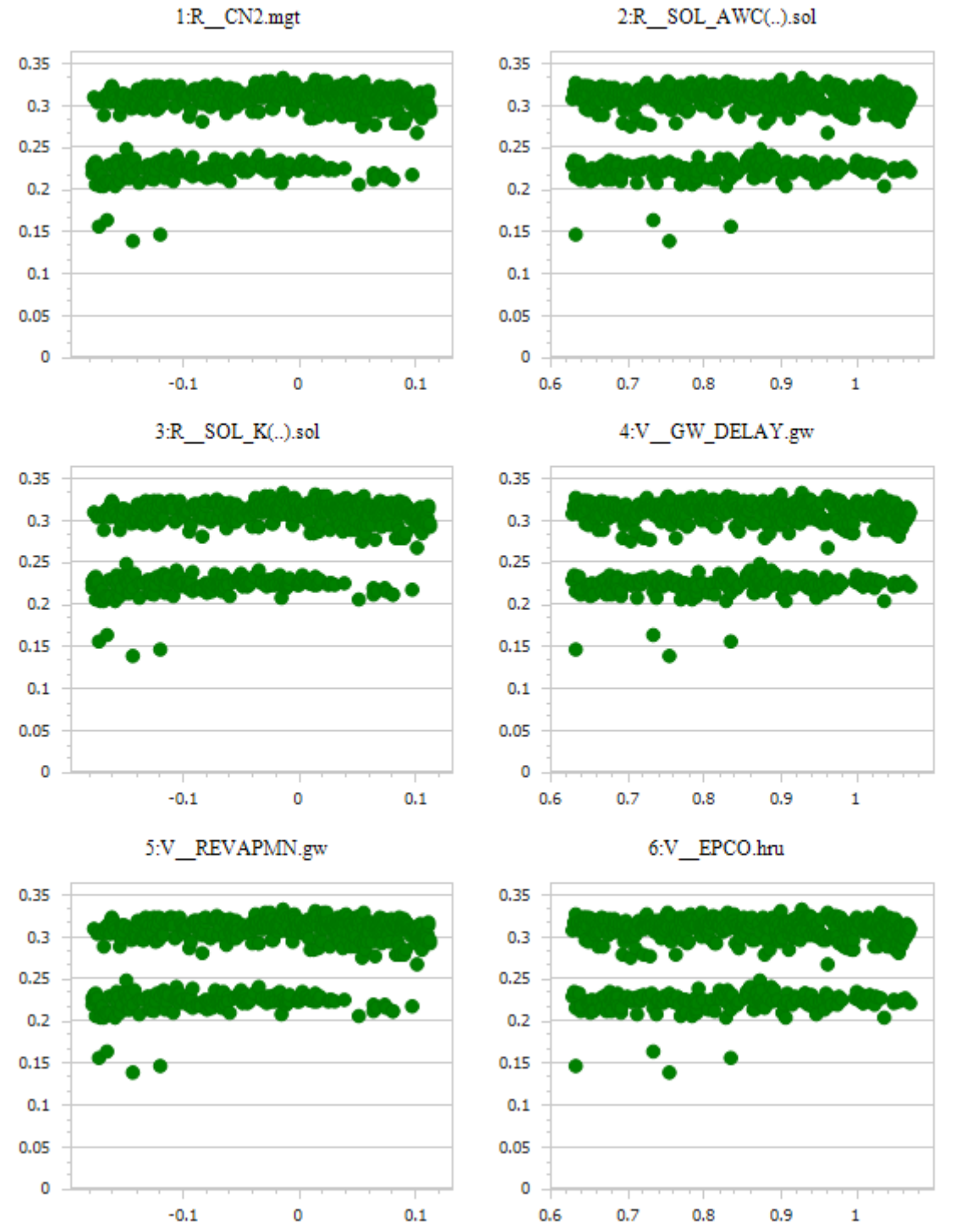


Figure B.3: Scatter plots showing the parameter values used for calibration versus the NSE result obtained

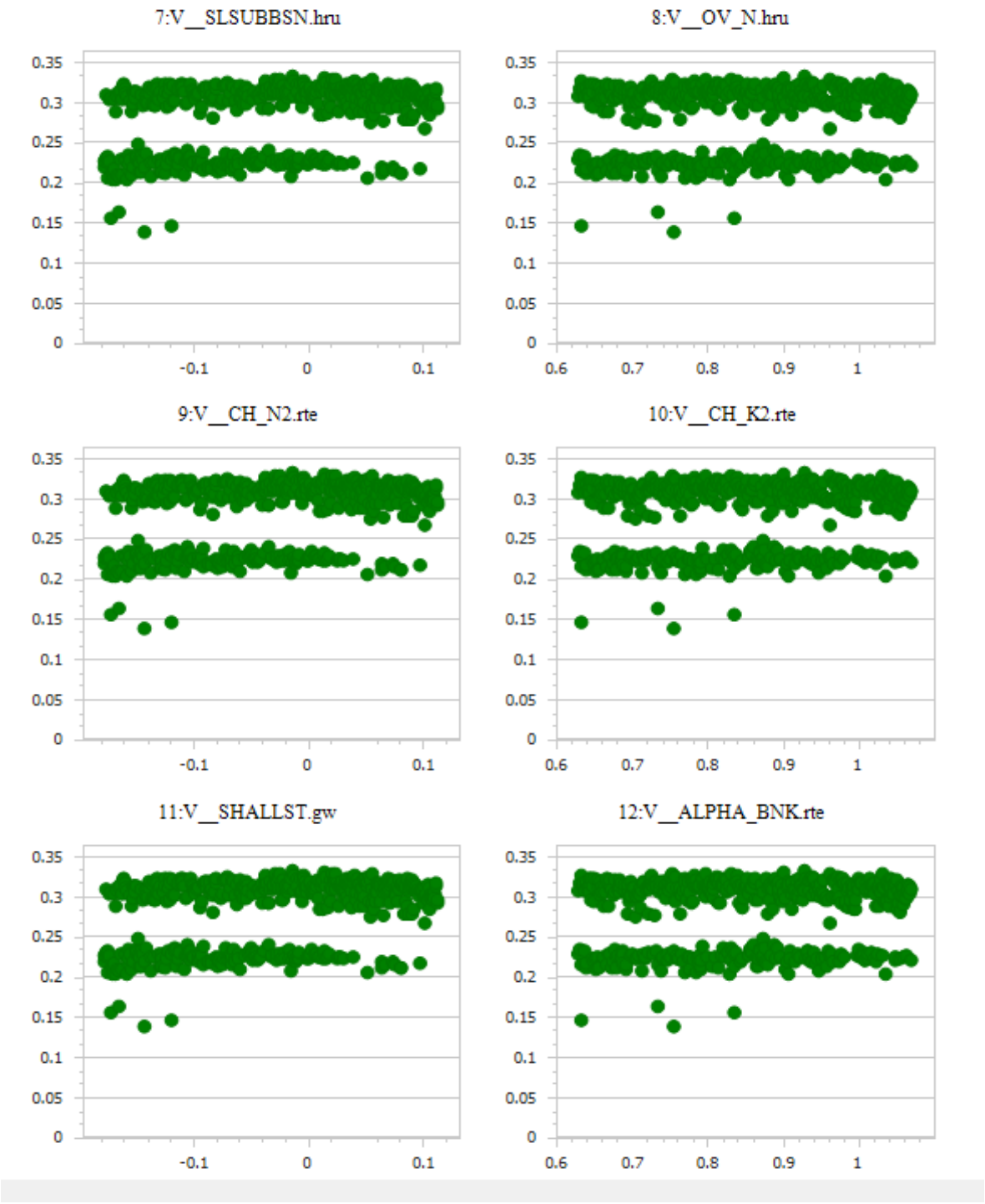


Figure B.3 (continued): Scatter plots showing the parameter values used for calibration versus the NSE result obtained

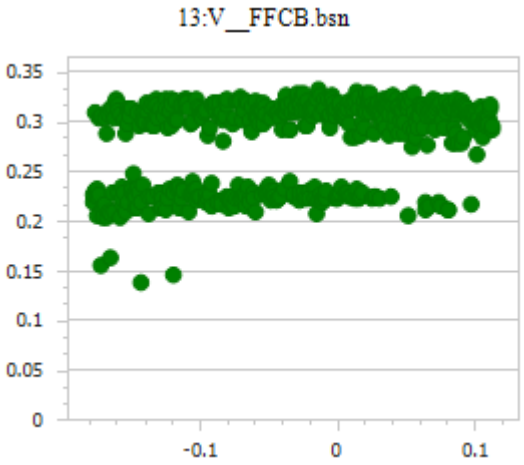


Figure B.3 (continued): Scatter plots showing the parameter values used for calibration versus the NSE result obtained

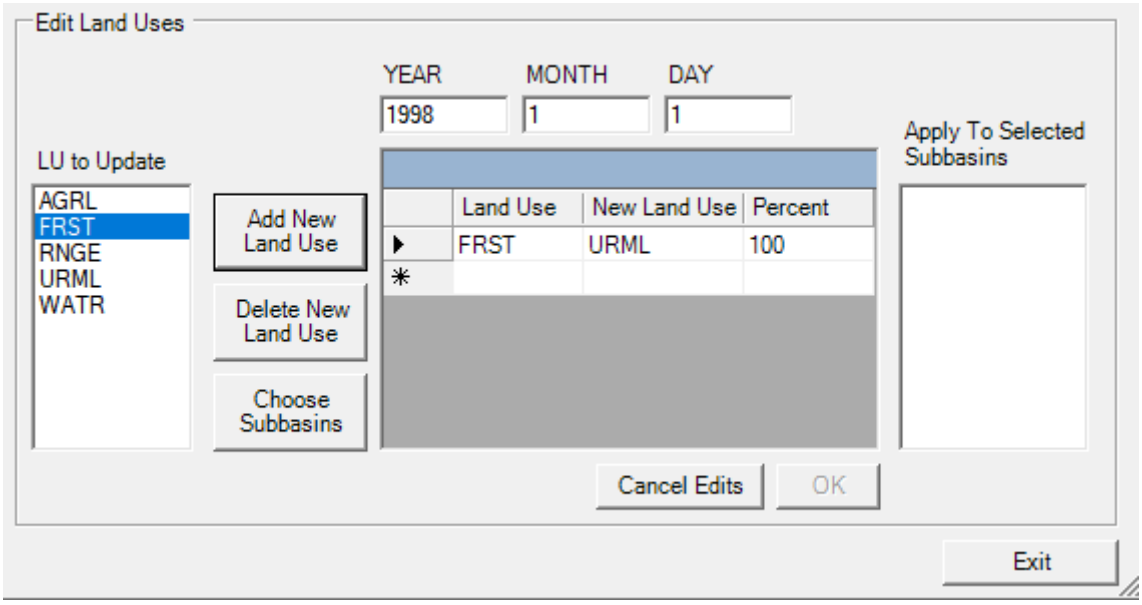


Figure B.4: The land-use update table used to define the land-use scenario implemented for analysis

Watershed	Area [ha] 616263.57	
Landuse	Area [ha]	%Watershed
FRST	136247.22	22.11
URML	23673.87	3.84
RNGE	261509.40	42.43
FRSE	29659.23	4.81
AGRL	82032.75	13.31
UTRN	1521.45	0.25
WATR	5372.19	0.87
FRSD	15198.84	2.47
SWRN	22527.81	3.66
WETN	11216.97	1.82
URHD	3420.90	0.56
ORCD	3935.25	0.64
UIDU	6153.39	1.00
AGRC	4500.27	0.73
UCOM	7542.81	1.22
RNGB	1751.22	0.28

Watershed	Area [ha] 616263.57	
Landuse	Area [ha]	%Watershed
FRST	125594.52	20.38
URML	54477.70	8.84
RNGE	241328.81	39.16
FRSE	29659.23	4.81
AGRL	82032.75	13.31
UTRN	1521.45	0.25
WATR	5372.19	0.87
FRSD	15198.84	2.47
SWRN	22527.81	3.66
WETN	11216.97	1.82
URHD	3420.90	0.56
ORCD	3935.25	0.64
UIDU	6153.39	1.00
AGRC	4500.27	0.73
UCOM	7542.81	1.22
RNGB	1751.22	0.28

Figure B.5: The change in the land-uses of the UCRB showing the land-uses before (left) and after (right) scenario development